RF Project 760719/784771
Interim Report

LEVEL II

the ohio state university
research foundation
1314 kinnear road
columbus, ohio
43212

COLORIMETRIC TOPOGRAPHY OF ATHEROSCLEROTIC LESIONS BY TELEVISION IMAGE PROCESSING

Daniel R. Shook
Bio-Medical Engineering Center

J. Fredrick Cornhill
Department of Surgery

Robert M. Nerem
Department of Aeronautical and Astronautical Engineering

For the Period
1 July 1977 - 31 May 1979

U.S. AIR FORCE
Air Force Office of Scientific Research
Bolling Air Force Base, D.C. 20332

Grant No. AFOSR 77-3411

15 June 1979

Approved for public release;
distribution unlimited.

The experiments reported herein were conducted in accordance with the principles in the Guide for the Care and Use of Laboratory Animals [DHEW Publication No. (NIH) 78-23].

The views and conclusions contained in this document are those of the authors and should not be interpreted as necessarily representing the official policies or endorsements, either expressed or implied, of the Air Force Office of Scientific Research or the U.S. Government.

Unclassified

SECURITY CLASSIFICATION OF THIS PAGE (When Data Entered)

REPORT DOCUMENTATION PAGE	READ INSTRUCTIONS BEFORE COMPLETING FORM
1. REPORT NUMBER: AFOSR-TR-79-0918	2. GOVT ACCESSION NO.
3. RECIPIENT'S CATALOG NUMBER	
4. TITLE (and Subtitle): COLORIMETRIC TOPOGRAPHY OF ATHEROSCLEROTIC LESIONS BY TELEVISION IMAGE PROCESSING	5. TYPE OF REPORT & PERIOD COVERED: Interim 1 Jul 1977-31 May 1979
	6. PERFORMING ORG. REPORT NUMBER: OSURF-760719/784771
7. AUTHOR(s): Daniel R. Shook, J. Fredrick Cornhill, and Robert M. Nerem	8. CONTRACT OR GRANT NUMBER(s): AFOSR-77-3411
9. PERFORMING ORGANIZATION NAME AND ADDRESS: The Ohio State Univereity Research Foundation, 1314 Kinnear Rd., Columbus, Ohio 43212	10. PROGRAM ELEMENT, PROJECT, TASK AREA & WORK UNIT NUMBERS: 61102F, 2312/A2
11. CONTROLLING OFFICE NAME AND ADDRESS: Air Force Office of Scientific Research (NL), Air Force Systems Command, Bolling AFB, D.C. 20332	12. REPORT DATE: 15 Jun 1979
	13. NUMBER OF PAGES: 192
14. MONITORING AGENCY NAME & ADDRESS (if different from Controlling Office)	15. SECURITY CLASS. (of this report): Unclassified
	15a. DECLASSIFICATION/DOWNGRADING SCHEDULE

16. DISTRIBUTION STATEMENT (of this Report)

Approved for public release; distribution unlimited.

17. DISTRIBUTION STATEMENT (of the abstract entered in Block 20, if different from Report)

18. SUPPLEMENTARY NOTES

19. KEY WORDS (Continue on reverse side if necessary and identify by block number)

Image Processing
Atherosclerosis
Arterial Wall

20. ABSTRACT (Continue on reverse side if necessary and identify by block number)

A measurement technique has been developed to quantify the degree and location of sudanophilic lesions in necropsy specimens. Transparencies of longitudinally opened arterial specimens are digitized by television image processing to discrete values of location and luminance. The image is photographically partitioned to increase location information. Binary maps are produced by thresholding the image at several luminance levels of a preprocessed hue. Thus, only the preprocessed hue is available for luminance

DD FORM 1 JAN 73 1473

Approved for public release; distribution unlimited.

Unclassified

SECURITY CLASSIFICATION OF THIS PAGE (When Data Entered)

Abstract-continued

thresholding. By means of a standard transformation to suppress biological variation, the binary maps of numerous specimen images are overlaid to produce statistical contour maps whose topography represents the level of Sudan IV stain saturation. The accuracy and precision of this technique are far superior to previous methods.

CONTENTS

LIST OF FIGURES

LIST OF TABLES

CHAPTER I

1.0 Introduction

Assessing the degree of atherosclerosis and identifying the dynamic behavior of the characteristic lesion is of primary importance in the prognostic management of the disease. However, little is known of its pathogenesis due, in part, to the lack of an accurate and precise technique for the quanititative assessment of the extent and location of gross lesions. In this chapter, the problem of assessment is described in detail and shown to be a viable one despite numerous existing techniques. Finally, the solution which this thesis proposes is outlined.

1.1 Problem Statement

Atherosclerosis is a pathological condition characterized morphologically by localized accumulations of lipid-containing material within or beneath arterial intima. These dense lipid deposits cause local discoloration of the luminal surface. In addition, coloration may be enhanced by lipophilic stains. This visual characteristic is a highly evident indicator of pathology (1,2). It is, therefore, expedient that a method be developed by which to assess this indicator. Herein lies the problem.

Numerous techniques have been devised to assess the atherosclerotic lesion (2-26). The most significant techniques are described in detail in Section 2.1. Basically, two forms of assessment exist. The first is qualitative assessment which attempts to categorize the degree of atherosclerosis by class, such as intimal thickening, fatty streak,

fibrous plaque, and calcified or ulcerated lesion. Qualification employs gross examination of necropsy specimens for visual and tactile evidence of class characteristics (3-8). The second form is quantitative assessment, placing a numerical measurement on the atherosclerotic state. Quantification may employ any of several techniques, some manual and tedious (2,9-19), and others implementing advanced image processing technology (20-26). Though both method types are sufficiently accurate and precise when properly used, image processing with the aid of electronic digital computers permits automatic statistical analyses of measurement data as well. It should be noted that quantitative assessments in some cases, those involving surface optical contrast (26) for example, are limited to one of the universally recognized lesion classes. However, other quantitative methods, such as measuring tissue dimensions (12,25), disregard the confines of recognized classes and, therefore, obscure the individual etiology of each class.

The problem addressed by this thesis research is one of measurement, specifically, assessment of the atherosclerotic lesion, so as to determine, in part, the atherosclerotic state. In general, the problem requires a solution technique which embodies the following characteristics. It should be quantitative. It should provide measurement data rapidly with, at least, the accuracy and precision of existing methods and be capable of defining the recognized classes. Finally, this information should be presented in a form acceptable to the clinical and basic research scientists. The viability of this problem must be questioned, given the numerous existing solution techniques. Furthermore, the characteristics of the solution techniques, as stated, must be justified.

It is the purpose of the next section, first to describe the limitations of existing techniques and, thereby, the need to develop a more accurate and precise quantitative technique, and second, to justify the aforementioned solution characteristics.

1.2. Justification for the Present Work

This section first describes the accuracy and precision of qualitative and then quantitative methods. That there is a need for a quantitative technique is universally recognized and echoed throughout the literature. Prognosis and ultimate treatment demands a knowledge of the course of the disease. In its simplest form, this course is a sequence of known atherosclerotic states. Differentiation of atherosclerotic states requires multiple assessments to determine the static or dynamic behavior of the disease. Though qualitative assessments can detect gross progression or regression into adjacent classes, they are useless for detection of dynamic conditions within an arbitrarily assigned class. Quantitative assessments, however, by definition, place numerical measurements on the atherosclerotic states, thereby determining dynamics. Furthermore, the resolution to which a change can be detected defines the static state as well as the maximum error in a static determination. Of those methods based upon the classing (grading) methods of the International Atherosclerosis Project (IAP) (4,6), some are purely qualitative, identifying by visual examination the lesion grades visible on the specimen, and others are "pseudo-quantitative", subjectively estimating the relative area of surface involvement for each grade (11,13,17).

Since reference standards are usually unavailable, the accuracy of these methods is difficult to interpret, and seldom reported (13). Several studies of precision, or repeatability, have shown a range of intra-laboratory peak reliabilities of 80 to 90% and of inter-laboratory peak reliabilities of 65 to 75% (11,13,27). Tests confirm that experience and training are essential for the successful application of visual assessment techniques (11,18). While errors are very large, they represent state of the art for many laboratories. To take advantage of the significantly higher intra-laboratory reliabilities and to economize data storage and assessment time, a common plea among investigators of atherosclerosis is the establishment of a central service for the quantitization of lesion development (10,12,13,18,27).

Strictly quantitative assessments do not use the IAP grading method, though some techniques are limited to one or two of the universally recognized classes. Arterial casting and angiographic techniques expose lumenal stenosis and intimal thickening, which are common to all classes (20-25). Implementing quantitative techniques has required advanced technology and computing facilities, whose high initial cost forces the use of these methods to a central service, which, as mentioned, is advantageous for the working pathologist. The actual assessment procedure is very rapid and permits statistical analysis by computer. All of these techniques are still in developmental stages. Each has been shown, however, to equal or surpass any subjective human grading method in accuracy and more so in precision. Whether advanced methods can maintain their superiority in mass usage has yet to be shown (22).

The quantitization, speed, accuracy, and precision requirements of the solution to the assessment problem have been briefly discussed. The remaining requirements are not strictly hardware oriented, but deal with the clinical and research scientists' ability to interface with the technique, that is, to understand its use and to interpret its findings.

Although the IAP grading method is qualitative, the classes themselves are important in quantitative assessment and should not be obscured. Not only are these classes an assessment of the disease course, but they may also represent etiologically different processes (1). Indeed, early intimal thickening may be independent of the pathogenesis of clinically significant lesions. Furthermore, the fatty streak may be a very dynamic, and reversible, precurser to the clinical lesion (1,8). Until these basic questions are resolved, the results of assessment techniques which eliminate these classes (12,20-25), should be viewed with extreme caution in pathological studies, since the apparent disease course may not be clinically significant. Furthermore, the tools and processes, particularly those applied to the specimen, must be acceptable to the pathologist. If these treatments unfavorably alter the histochemical manifestations of atherosclerosis, interpretation of these studies may be impossible.

Finally, prognosis requires a knowledge of dynamic behavior, which can be detected and measured only by multiple assessments. This requirement is satisfied, though in varying degrees, by all techniques employed.

Since the method proposed in this thesis overcomes them, a number of difficulties in the existing quantitative techniques should be discussed. The xerographic technique (26), which senses surface optical contrast, does not employ stain enhancement. Though this procedure permits subsequent histochemical studies on the specimen, surface optical contrast has not been shown to correlate with any underlying pathology. This characteristic may produce artifacts on the "xerox copy," due to surface reflections, ostia, or otherwise discolored tissue. Furthermore, it has been observed that data from stained specimens are not comparable with that from unstained. The quantitative change upon staining in the fatty streak was an increase in apparent pathologic area, while staining the calcified plaque appeared to decrease the pathologic area (10,13). Since the IAP Standard Operating Protocol (6), defines the fatty streak in terms of Sudan IV staining, the acceptability of a xerographic delineation of the fatty streak is questionable.

Angiographic densitometry (22,23,25) has the great advantage of assessing the artery in vivo. Output from the densitometry of cineartériographic frames is analyzed through various computer algorithms to determine lumenal narrowing. Not only is this technique plagued by artifact sensitive image analysis, but it also produces a view of only a single longitudinal plane section. Also, since only lumenal outline irregularities are detected, diffuse fibrous intimal thickening, characteristic of advanced disease, can not be determined. Even if these and the mechanistic difficulties of multiplane (rotated) viewing are overcome, a formidable task in itself, the technique nevertheless does not differentiate major lesion classes, as the assessment problem requires.

Television analysis of vascular permeability to colloidal carbon tracers is not a macroscopic technique (28). The exact relationship of endothelial permeability to atherosclerosis has yet to be determined. This technique is mentioned here due to its similarity to the television application proposed in this thesis.

Arterial casting is a very promising method to map the location and degree of stenotic lesions (21,24). This technique is also quite acceptable to the pathologist since geometrical alteration of the arterial lumen, and subsequent histochemical changes are minimal. However, an automated system which scans the cast surface to form a topographical map has yet to be developed. The method, in addition, does not differentiate lesion classes, and, therefore, sheds no new light on the dynamics of the fatty streak in contrast to the fibrous plaque.

In Section 2.1.1., a method developed in 1962, which is very similar to that proposed in this thesis is described in detail (20). A flying spot scanner and photomultiplier tube determine the optical density of black and white transparencies of Sudan IV stained necropsy specimens. The technique had accuracy and precision far above any obtained by visual examination, the only well-developed alternative method available at that time. However, the system suffered from several technical problems, the greatest of which was a lack of digital image processing capability. The apparent demise of this technique is perhaps due to lack of appropriate data handling and misinterpretation of artifacts.

Several quantitative methods employ a manual and tedious counting or measuring procedure to assess lesion geometry. In essence the procedures are similar to an advanced image processing method, but lack automation. The polar coordinate method (19), for example, which measures strictly periorificial sudanophilia, could be automated through spiral field television processing. As mentioned, since automation is usually expensive, a central service would facilitate wide spread use of this and other automated methods.

In summary, it is clear that the problem of quantitative assessment is still viable, despite numerous existing techniques. The next section briefly outlines the technique proposed in this thesis, with justification in light of the problem statement, and defines the technique's scope of applicability.

1.3. Proposed Solution Technique

The proposed technique has evolved from the use of a television image processing system developed recently at The Ohio State University, Department of Electrical Engineering, as the doctoral dissertation of J. M. Jagadeesh (29). An example of the hue-luminance processing scheme, this system is described in detail in Chapter III. Other systems are sold in the United States which are somewhat simpler than the Jagadeesh system. The potential of these systems is discussed in Chapter VI. The theory described in Chapter III is the basis for all these systems, however. The proposed technique also employs mapping procedures to statistically represent location and degree of sudanophilia in necropsy specimens. In implementing the method, utmost consideration was given

to the fact that the pathologist should remain responsible for preparation of specimens and interpretation of processed data. It is the pathologist who will use the data in final form to illucidate mechanism and predict the course the disease will follow.

The specimen data, presented to a central service by pathologists throughout the world, must travel great distances, under extreme environmental conditions, and be handled by many people. When that data has been the specimen itself, it was "inevitably damaged by this treatment."* It was decided, therefore, that data resistant to harm and produced conveniently by the pathologist be collected. Conventional photographic color transparencies in the 35 mm format, taken under controlled conditions fulfill this requirement and satisfy the analytical implements at hand. Preparation of the specimen, performed by the experienced pathologist according to standard protocol, must be compatible with the assessment technique and produce minimal alteration. "The majority of investigators have preferred to examine the intimal surface of the longitudinally opened, flattened artery because the early and intermediate stages of the disease process -- fatty streak and fibrous plaques -- can be best seen and measured in this manner."** This limits the assessment to early lesions. However, the importance of this dynamic period, for gaining true insight into the mechanism of athersclerosis, was understood as early as 1911 (3) and has been reiterated often since (2).

---

*Kagan, A.; Uemura, K. 1962. Grading Atherosclerosis in Aorta and Coronary Arteries Obtained at Autopsy. B WHO 27:672

**Eggen, D. A.; Strong, J. P.; McGill, H. D. 1962. An Objective Method for Grading Atherosclerotic Lesions. Lab Inv 11(9):732.

The proposed image processing system functions on color, or hue, and image brightness, or luminance. It can assess the image for any desired value of the parameters. Note that the uncertain correlation between lipid deposition and the yellow colored streak qualifies the use of yellow hue as an indicator (2,10,13). As mentioned in Section 1.2., the early lesion is defined in terms of sudanophilia (2,6). Therefore, major emphasis is placed on lipid enhancement by Sudan IV staining and processing the photographic image on this basis.

The staining and photographic procedures are standardized to avoid inter-laboratory error; however, the system is insensitive to small variations of photographic parameters and stain color. The photographic protocol provides for the inclusion of "landmarks" on the specimen, which allow its image to be subdivided and later restored to increase processing accuracy. The image of the entire specimen is divided into parts for processing so that extreme resolution can be attained. Determination of the smallest change in lesion dynamics is directly proportional to the resolution of the image. Indeed, the system is capable of detecting such fine dynamics that epidemiologic factors effecting those changes can not be measured practically. Registration of the landmarks facilitates restoration of the segments. The mathematical transforms, by which a statistical number of specimens of common epidemiology, species, and age, are grouped to overcome biological variability, employ the landmarks in a coordinate mapping scheme. All specimens are mapped into the same geometry, called the "standard specimen." Chapter VI details this procedure. The standard specimen forms the graphical and numerical output of the processing system which is available

to the pathologist for interpretation. In this way, comparisons within and among arbitrarily chosen groups are made with quantitative data.

Before these statistical analyses and mappings can be performed, the specimen's photographic image must be digitized. This is the function of the television image processor. Its complex theory is detailed in Chapter III. In short, the specimen's image, projected onto the vidicons of a color television camera, is converted to electrical signals which are processed on the hue and luminance they represent. The image processor operates on a preprogrammed hue range by means of luminance thresholding, producing numerous binary mappings which retain accurate and precise information on location and degree of sudanophilia.

Isolated communities throughout the world have very different occurance patterns and development of clinical atherosclerosis (30). Numerous risk factors have been determined by group comparison and some etiology and mechanism has been illucidated (1). A central service for quantitative assessment and data storage would facilitate worldwide comparisons of grossly differing atherosclerotic patterns. Only when all investigators have access to this data can efficient research continue. The ultimate goal of this central service assessment technique will be the establishment of a computer data base which will allow pathologists to draw upon a huge international statistical library quantifying the progression and regression of sudanophilia. It is hoped that an in-depth understanding of atherogenesis may thereby come one step closer to reality.

CHAPTER II

2.0 Introduction: Background

Much effort has been expended in developing assessment techniques to quantify atherosclerosis. Each laboratory has developed or altered a method which its facilities can accomodate. The facilities vary widely from laboratory to laboratory and thus so do the methods. Much controversy also exists on some aspects of atherogenesis, so that the opinion of each investigator adds to the variety of methods. However, the validity of some techniques has been demonstrated through their acceptance and use by other laboratories. This chapter d ibes the most significant methods in view of that proposed in this thesis. Therefore, it is restricted to techniques which view and assess lumenal atherosclerotic lesions on opened and flattened necropsy specimens. Special emphasis is placed on the flying spot scanner due to its similarity to colorimetric topography. The latter parts of the chapter outline the applicable theoretical apsects of digital image processing and, briefly, overlaid binary mappings.

2.1. Previous Methods

Section 1.2. justified the need for further development by showing some deficiencies of methods currently in use. Several of these methods are similar to colorimetric topography, in that they examine the longitudinally opened, flattened artery, some through unaided and others through mechanized viewing.

Years of unaided visual examination of necropsy specimens inated in the Protocol designed by the International Committee and used by the Central Processing Laboratory of the International Atherosclerosis Project.(6). The time period over which necropsy specimens were collected for the Project was 1962 through 1965. A similar project was undertaken in 1962 by the World Health Organization in Europe (13). The use of autopsy specimens was justified by the committee since viewing of autopsy materials was a well-established practice; the arteries could be opened so that lesions could be easily detected visually; Sudan IV, a lipid dye, could be used to advantage; important aspects of case histories were available; and the tissues could be retained for repeated grading. The Protocol standardized the procedure for viewing and applying a grade and relative surface involvement estimate. Terminology relating to anatomy, dissection procedure, and grades was explicitly defined. Pilot studies confirmed the applicability of the protocol, which was then distributed freely to all participants. The results of the Project were copious, and in general, supported widely held ideas, though much new controversy now surrounds some of the findings (31). Many problems with the method were recognized, the greatest of which was the lack of accuracy in the area estimate and, therefore, poor differentiation of similar lesions. Further investigation into the dynamics of the Sudan IV stained fatty streak, or sudanophilia, is needed to determine its relation to the advanced lesion and clinical atherosclerosis. Problems of the protocol with respect to colorimetric topography were discussed in Chapter I and have also been extensively

reviewed in the literature, and so will not be described further here.*

The vast majority of method development since the IAP involves (1) modification of that protocol by statistical analyses of intra- and interlaboratory comparisons, and lesion grade redefinition and weighting; (2) changes in anatomic region under study, dissection or staining procedures, autopsy case history and geographic distribution requirements, and central service laboratory; or (3) introduction of progression/regression studies and associated statistics, and subsequent histological studies. However, the basic viewing method, grading concept, and involved surface area estimation remains unaltered. The two techniques described next show the steps recently taken to overcome the crudeness and subjectivity of the IAP and modified methods.

The morphometric method permits an accurate, but still quite subjective, means for placing a numerical measurement on the area of the atherosclerotic lesion (14,15,17). In the present stage of development, only the aorta has been adapted to the technique. The entire aorta is segmented, or sectioned transversely, to produce four segments: mid-thoracic, diaphragmatic, mid-abdominal, and terminal abdominal. Each segment, unstained, is placed on a tray and covered by a transparent 1 cm x 1 cm ruled graticule. Viewing this composite tray, by eye, one estimates and sums those areas, or fractions of unit area, under which is seen each class of lesion: normal, fatty streak, fibrous plaque, calcification, complicated plaques, and ulceration.

*The entire issue of Laboratory Investigation 18(5):462-654, 1968 was dedicated to R. L. Holman and Geographic Pathology, and forms an extensive review and bibliography of the IAP.

This method is obviously subjective in its qualitative assessment, though once lesion quality has been determined the area can be tediously estimated. Note that the graticule is ruled by major division lines at 1 cm and minor lines at 0.5 cm so that the smallest area resolution is 0.25 cm^2. The authors of the technique state that estimates down to one-eighth of this minimal area must be made visually. For all but the largest arteries, this resolution is far from sufficient. No location information is provided. Precision was measured at 90%, also low for a "quantitative" technique.

The xerographic method uses the Xerox Copier to reproduce the specimen image for further processing (26). Here the entire unstained aorta is placed in a thin transparent bag and laid lumenal-surface downward on the glass of the copier. This is one of the few techniques using flattened, opened aortae, in which the sensing transducer is not the eye. This is a positive step toward the elimination of subjectivity in "quantitative" analyses. The copier, as most of us have experienced, senses surface optical contrast, and reproduction density is accumulated electrostatically. Greys levels are poorly reproduced since the electrostatic fields are not continuously variable. As mentioned in Section 1.2., surface optical contrast has not been shown to correlate with underlying pathology. The resolution of the equipment is not stated by the authors. Common experience suggests that it is sufficient for the aorta in life size magnifications, however. Numerous artifacts are produced by the copier, since it detects and enhances all contrast gradients. For example, "folds and overlapping tissue were distinguished

from lesion boundaries by coloring with a pen."* At this point, the quantitization was made by manually tracing the boundaries, made visible on the copy, onto thin transparent 1 mm x 1 mm graph paper and the unit areas, or fractions of unit areas (down to 0.25 cm^2), within lesion boundaries, were counted visually.

To compute accuracy, the method was compared to another technique very similar to the mophometric method, except that the aorta was stained by Oil-Red 0. That is, a specimen, previously xeroxed, was stained, overlaid by a transparent grid, and lesion areas counted. The correlation coefficient between these two subjective methods was high, $r = 0.998$ ($p < 0.01$), which is questionable since the precision of each is low. Mechanical distortion by the copying process was stated as about 3%, and precision of the counting procedure as 93%. The increase in precision over the morphometric method is probably due to the higher resolution of the xerographic counting method. The method, again, gives no statistical lesion location information, though a "hard copy" of each aorta exists.

That a technique implementing advanced technology has not been developed, previous to this thesis, is surprising. Basic research in academic settings is traditionally advanced, and electronic computing facilities are common. Yet a lack of biomedical engineering is quite evident, especially in routine applications. The xerographic method employs technology to "image" the aortic lesions, but stops short of the

*Hata, Y.; et al 1978. A Xerographic Method for the Quantitative Assessment of Atherosclerotic Lesions. Atheroscler 29:252.

most advantageous application of technology, routine counting for data acquisition. Digital processing permits the retention of differential information which is necessary for the development of mapping procedures.

2.1.1. Flying Spot Scanner

This strictly quantitative, objective technique for assessment of atherosclerotic involvement employs a photographic negative to measure reflectivity of sudanophilic lesions and a radiograph to measure thickness of the specimen wall. Both images are made of the opened, flattened, and stained artery. The image density on the radiograph is inversely proportional to the thickness of the specimen at that point, and the density on the photographic negative is directly proportional to the reflectivity of the stained specimen.

Both films are operated upon by the flying spot scanner. A scan is made by deflecting the electron beam, or "flying spot," repeatedly across the phosphore screen of a cathode ray tube. The device is completely analogous to a television reception tube where the beam is not modulated. First the spot must be focused upon the tube's phosphore screen. This is done conventionally with electrostic controls on the scanner regulator. This spot image is projected through an objective lens which focuses it on the negative or radiograph to be scanned. One fixed lens is sufficient to focus the entire phosphore screen on the film plane. Diverging lenses, immediately below the film plane, spread the spot image, regardless of its location in the deflecting field, over the same area of the photomultiplier end-window. Note that

now the spot image need not be defined by both its location and intensity. Immediately after passing through the negative or radiograph, the spot image location is known explicitly and its intensity is modulated by the film's density distribution. After impinging upon the photomultiplier, the spot image location is known only implicitly, this information being carried now in a time modulated signal. Spot image intensity is converted from an explicit function of location to a function of time.

To produce a measurement of area, the signal is applied to a comparator that produces a gating pulse which opens a gate between a constant frequency oscillator and a counter, whenever the video signal is greater than a reference voltage. For the photographic negative, this reference voltage is produced by that portion of the specimen image chosen to represent a normal, non-sudanophilic, area of the artery. For the radiograph, the reference corresponds to the densest portion, that chosen to represent the normal thinner areas of the arterial wall. The authors point out that, since arterial wall thickness gradually changes with lumenal taper along the length of the artery, the reference must be changed frequently to avoid the error introduced by averaging the wall thickness over a longer length. The total count for one complete scan of either film is then proportional to the area producing a voltage above reference.

The flying spot method and that proposed in this thesis both produce, though by different means, video signals basically similar to that of a conventional television camera (the thesis method requires a color camera signal for preprocessing on hue, Section 2.2.1.). However, the condi-

tioning and analysis of the signals from this point onward differ conceptually in the two methods. The flying spot method electronically integrates its video signal to produce a quantity proportional to the mean of the reciprocal of the film density, which in ratio with the total arterial area, gives a proposed measure of severity. The colorimetric topographical technique of this thesis allocates digital computer memory to store the original differential data in two dimensional addressable arrays, which permits numerical integration or any other mathematical or statistical manipulation, without loss of explicit geographic mapping capability.

The accuracy of the flying spot method is not stated by the authors; however, the photographic illumination varied by a maximum of 4% over the field, and spot intensity variation over the phosphore screen was at most 10%. Though the errors reported in this study are large, illumination techniques and scanners today are much more uniform, and these errors are no longer limiting factors. Since the films were "black and white," and scanned as such, absolute contrast had to be maintained to permit comparisons with different specimens. The uniformity of contrast was held within ± 0.04 units of 1.00, a negligible error. Precision test results were shown on scatter diagrams (not reproduced here) but values of correlation coefficients were not computed.

Note that the grey level reproduction of red stain is not unique. The entire gamut of red saturation levels and numerous artifacts, such as ostia, gross discoloration of the specimen, folds, specular reflectances, and careless dissection can produce equivalent grey levels.

Thus a black and white reproduction and processing on that basis cannot separate sudanophilia distinctly from these artifacts, even with the use of highly refined densitometric techniques. To overcome this obstacle, the method of colorimetric topography employs the concepts of preprocessing on hue followed by thresholding on luminance. The next section discusses these techniques.

2.2. Digital Image Processing

Image processing by digital computer is a very rapidly expanding field today. Though the majority of the literature is application oriented, a considerable body of processing theory and techniques has evolved to guide and define further development. Since this thesis itself is application oriented, the mathematical tools of the theory will be presented only parenthetically.* Of the several aspects of image processing, descriptions of those employed by colorimetric topography are included here.

Image processing developed naturally from an analysis of human visual perception. Many aspects of image processing were designed to overcome the eye's limitations, while others were developed to simulate useful characteristics of vision. The latter aspects are necessarily compromises due to our poor understanding of the mechanism of Weber's Law, color perception, and especially the Gestalt Laws of Organization, and also due to the imperfections of electronic signal conditioning. These problems are discussed in detail in Chapter III. Though no

*Readers interested in mathematical image processing theory are referred to Reference (32).

computer scene analysis can equal the analytical capability of the human brain, it can overcome certain shortcomings of human visual perception, yielding stark objectivity and untiring precision. Furthermore, digital electronics permits distortionless manipulation of image data.

In general, a color image of a real scene, or the scene itself, is characterized by its physical propoerties and by human perception of those properties. Physically, each picture element, or "pixel," radiates energy at a certain rate. This energy is completely specified by the quantity radiated per unit area per unit time for each part of the radiant-energy spectrum. The time rate of radiation of energy is called radiant flux. Radiant flux measured at a certain point of the spectrum is termed spectral radiant flux. Finally, describing the absolute distribution of this radiant flux per unit area over the entire spectrum completely specifies the energy radiated from the scene or its image. Since the theory of image processing seeks, in part, to represent a visual image for the human observer in some prespecified manner, spectral distribution of radiant flux for the wavelength range of about 380 nm to about 780 nm is usually sufficient specification.

The eye as transducer for radiant energy specification does not permit the measurement of these physical properties. Not only does the eye approximate the trichromatic model of color perception, but it also utilizes several forms of adaptation in its presentation of information to the brain.* Thus, through human perception, the scene or its image, is characterized by so called psychological properties. Several sets of

*More information is available on this subject in References (33-36).

properties have been proposed to account for the variation in perception among different observers. Specification of psychological properties is relative rather than absolute, the result of adaptation often being a tremendous handicap. The fundamental measurement is in terms of color difference, since all experiments involve color comparisons. The vocabulary that has evolved over the last few centuries of investigation into color phenomena can be differentiated by color appearance models. Common to all models are: light-source mode, object-color mode, luminance, lightness, and hue. Two of the several models explain the vast majority of perception types. In the luminance-hue-saturation model, the vocabulary differs in the concept of saturation and in the luminance-hue-chroma model, in the concept of chroma. These terms are defined as follows, and a geometrical representation of the models is given in Figure 2.1.

Light-source mode: appearance of an area which is self-luminous, that is, a light-source, such as the slide-filtered light emitted from a slide projector.

Object-color mode: appearance of an area which is nonself-luminous, that is, a solely reflecting surface, such as the screen from which the slide image from the slide proejctor is reflected.

Luminance: attribute of a visual sensation by which an area appears to emit more or less light; for stimuli perceived as self-luminous only. Luminance may range from dim to dazzling. (Synonomous with brightness.)

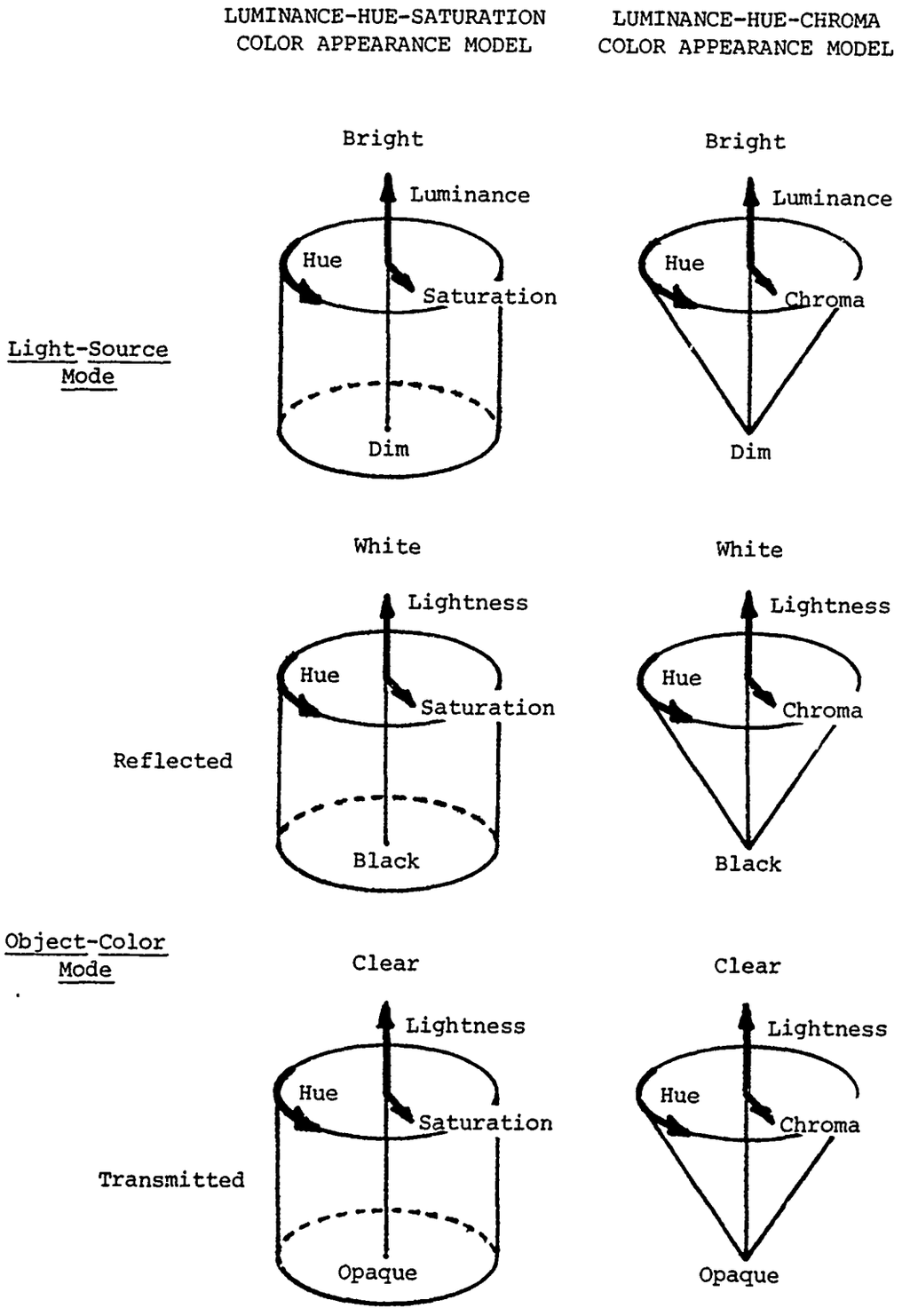

Figure 2.1. The two Color Appearance Models occurring most frequently in human color perception.

Lightness: attribute of a visual sensation by which a surface appears to reflect or diffusely transmit a larger or smaller fraction of the incident light; for stimuli perceived as nonself-luminous only. Lightness, for reflecting surfaces, ranges from black to white, and for transmitting surfaces, from opaque to clear.

Hue: attribute of a visual sensation by which an area or surface appears to match a remembered spectral sensation or a combination of spectral sensations. The names of spectral colors, such as red, blue, and green, and nonspectral colors, such as brown (yellow-red), purple (red-blue), and aqua (blue-green), arise from this sensation.

Saturation: attribute of a visual sensation by which a hue is judge to be more or less pure, that is less or more mixed with white. A very desaturated hue is often called pale.

Chroma: attribute of a visual sensation by which amounts of pure chromatic color are judged to be present, irrespective of the amount of achromatic color. For a given luminance and hue, equal sensation intervals of saturation and chroma are identical. However, for a given saturation, chroma increases with luminance.

For an excellent treatment of the complex interaction between the physical properties of color and human perception, emphasizing the development of standards in colorimetry, color matching theory, and the chromaticity diagram (Maxwell's Triangle) and its use in standards for color television, the reader is referred to reference (37).

It should be noted that a scene, or its image, may be characterized by a third set of properties, known as psychophysical properties. These form the bridge between the physical and psychological properties. Every attempt has been made by the color industry to maintain a quantitative theory to describe them. The result of this theory is the 1931 (x,y)-Chromaticity Diagram, which will be introduced in Chapter III. It is the psychophysical analysis of color that permits the construction of a model on which electronic hardware can be designed.

The color image of a real scene may be represented mathematically by a two-dimensional tensor-valued function. (Note that, of the two color appearance models discussed, only the luminance-hue-chroma model satisfies the requirements of a tensor space rigorously; luminance-hue-saturation does not, since saturation is a function of luminance, as shown in Figure 2.1. However, all existing models are three dimensional, and since luminance-hue-saturation models are the most commonly occuring perception types, this model is used in the remaining discussion of image processing. Furthermore, colorimetric topography eventually reduces the order of the tensor from two to zero, where the interdependence of the tensoral values is suppressed.) The values of this function are luminance, hue, and saturation, and the dimensional components are the spatial coordinates, here taken as x and y. If the image is a photograph, this function F(x,y), is usually taken as non-negative and bounded, that is,

$$0 \leq F(x,y) \leq M,$$

where M is the maximum value of luminance, hue, or saturation. To be handled by computer, F(x,y) must be digitized, at a frequency appropriate

to retain adequate image detail, and each resulting picture element, or "pixel," quantitized at an appropriate level. The choice of frequency and quantitization level is dictated by the character of the original image and the image process desired, such as compression, enhancement, or segmentation. Not only is the pixel location defined by discrete variables, but the functional values, luminance, hue, and saturation, also assume discrete levels within the range [O,M]. For example, a television image may be sampled to high resolution by a 500 x 500 pixel array, each pixel capable of assuming 50 discrete levels.

Digitization is of prime importance in the application of this thesis. The binary arrays produced may be manipulated mathematically for statistical analyses. A large digital computer can store and operate upon the overwhelming 1.5 megabit information complex inherent in the detailed television image just described, and do so in a realistic time frame. The more modest and economical minicomputer, with typically less than 100K of central memory, has also been adapted to image processing. This is made possible through the use of various schemes developed in image processing theory to further reduce memory requirements and processing times. The most improtant scheme proposed in colorimetric topography is segmentation. Segmentation refers to analysis, the input to which is pictoral, but whose output is a description of the original image. This is in contrast to an approximation to, or an improved version of, the input image which requires compression, enhancement, or restoration schemes.

The character of segmentation is differential, that is identification of parts of the scene. These parts, regions, or objects, may be defined in terms of size, shape, texture, color, contrast, luminance, and so on. (Image processing should be distinguished from pattern recognition, in which the description generated is compared to a reference in an attempt to recognize the parts by similarity.) Segmentation is, therefore, a technique by which parts of a scene can be extracted, by means of their unique character, from the remainder of the scene, the background. The two forms of segmentation used in colorimetric topography are preprocessing and thresholding. Note that these lead to a reduction in order of the representative function from tensor to scalar valued. The ramifications of this reduction are discussed in the next two sections.

2.2.1. Preprocessing on Hue

Preprocessing on image, sometimes called semi-thresholding, is useful when only certain parts of the image are to be segmented further. Preprocessing is required when the character of those parts of interest cannot be differentiated from uninteresting parts by the primary segmentation scheme. This is the case in colorimetric topography. Luminance thresholding, the primary segmentation scheme, discussed in the next section, cannot distinguish the reflected brightness levels within the red, Sudan IV stained lesion areas from those of ostia, ostial shadow, and the other grey level artifacts discussed earlier. Therefore, sudanophilia must be extracted from the image by a scheme which processes on their unique characteristic, red hue. The sudanophilic fatty streak

is thereby differentiated from the remaining surface area.

In this example, the red pixels in the image have been differentiated by their red hue and set apart from the image background. The process can be considered a transformation, by which certain pixels have been earmarked for further processing. As defined, saturation is a property of hue. However, the segmentation scheme of thresholding on luminance is not a function of hue, since it processes variations only in luminance. Therefore, a polychromatic image has been transformed to a monochromatic one, all image pixels of hue other than the preprocessed hue having been nullified. (The meaning of "nullified" will become evident in the next section.) An image no longer characterized by hue contains redundant information in saturation and luminance. It is for this reason that the second and primary segmentation scheme applied in colorimetric topography is thresholding on luminance, which retains saturation information in terms of luminance.

Mathematically, the tensor-valued function, $F(x,y)$, has been reduced in order by two, eliminating hue and saturation, and producing the scalar function of luminance $f(x,y)$. In colorimetric theory, as applied to television image reproduction, this reduction is manifest by reference to the unpreprocessed image function as valued by luminance and chromaticity, seemingly a vector function. Chromaticity, however, encompasses both hue and saturation in its colorimetric definition. Chromaticity is further discussed in Chapter III. Preprocessing on hue, then eliminates chromaticity variations and produces an image function whose only remaining value is luminance.

2.2.2. Thresholding on Luminance

Thresholding techniques are numerous, since this segmentation scheme is widely used to reduce binary memory requirements. In general, thresholding establishes a central value on the function being processed, identifies those pixels whose values are above and below that central value, or threshold, and expresses that information as a binary function of location. This can be stored in central memory by encoding, for example, pixel values below threshold as 0, and those above threshold as 1. Of course, this information is dichotomous about a single threshold and may not be representative of a continuous image occupying numerous functional vluaes. Therefore, the threshold may be incremented between an arbitrary minimum and maximum by an amount sufficient to describe the image appropriately but minimize memory requirements. Then each of these binary mappings of the thresholded image location function can be overlaid to produce a contour map at prescribed levels of the function. For the 500 x 500 pixel location array of the television example cited in the previous section, the maximum number of discrete levels chosen was 50. Each television image would require, therefore, 250,000 (= 500 x 500) addressable locations of 6 ($50 \leq 2^6$) bit word length, a total of 1500K of central memory. This is far beyond the memory capabilities of a minicomputer to which any image processor used in colorimetric topography may be interfaced. Indeed, this requirement exceeds the memory of the Digital Equipment Corporation PDP series computers which are used in the Jagadeesh System mentioned previously. The requirement is reduced, therefore, by two separate means: (1) thresholding on the luminance function, so that it becomes dichotomous rather

than stepwise continous to 2^6 levels, allowing a total luminance range of 255 discrete levels; and (2) reducing the sampling frequency applied to the location function, but partitioning and magnifying the image presented to the television camera, simultaneously, to maintain high resolution and accuracy.

The result of preprocessing on hue is a monochrome image which may vary from a completely saturated hue, for example a deepest red, to a completely desaturated hue, that is, white. The image no longer varies on hue. All hues, other that the preprocessed hue, are nullified, that is, reduced to zero luminance, and are seen (on a telelvision image monitor) as completely black. Only the single, monochromatic multisaturated hue chosen is available for thresholding. The variation in saturation of this image is inversely proportional to the variation in luminance of that image. Thresholding, then, on incremented values of luminance, produces dichotomous, or binary, images, one binary image for each luminance value..

Mathematically, after thresholding on luminance, f(x,y) becomes a binary function as previously explained. It is this function on which graphical and statistical analyses are made. See Chapter V.

2.2.3. Overlay of Binary Mappings

The binary images produced by these segmentation schemes can be overlaid with precise registration to produce a three-dimensional representation of the image of interest. The dimensions are image width and image height, in the horizontal plane, and image luminance in the

normal direction. The vertical contours represent changes in luminance and, thus, also in saturation of the preprocessed hue. Collapsing the levels in the normal direction onto the plane of the origin, and outlining the areas representing planes of constant luminance, a two-dimensional topographic mapping results. In colorimetric topography applied to images of sudanophilia, these "contour lines" delineate surface areas of constant saturation; the origin, or "lower elevation" on the map being completely desaturated, or white healthy tissue, and the "high elevations" representing greater saturations of stain color.

Precise registration is assured by inclusion of landmarks in the original scene. These landmarks are the ostia on the biological specimen. They maintain absolute locations throughout processing, and thereby form registration indices to permit coincidence of numerous binary mappings. Exact pixel location information is thus maintained. Manipulations of this information, in the form of the binary function, $f(x,y)$, permit calculation of areas and locations. How these quantities are generated, and how numerous values from different biological specimens are statistically compared, are the subject of Chapter V. The chapter that follows now describes the colorimetric theory through which the color television signals implement the image processing scheme discussed here.

CHAPTER III

3.0 Introduction: The Image Processor

The image processor is a device that produces a digitized representation of the specimen image. The system hardware consists of an image projector, a color television camera, and the image processor. These three components together permit the implementation of the processing schemes developed in the previous chapter. An example of the equipment required is the Jagadeesh System, an experimental system available on the University campus (29).

The purpose of this chapter is to explain how the image is "segmented" with respect to hue and luminance by a generalized television image processing system (not necessarily the Jagadeesh System). To understand the transition from psychological color properties to color television signals, the Commission International d'Eclairage (CIE) 1931 (x,y)-Chromaticity Diagram is developed from fundamentals. The Jagadeesh System is then presented, describing first the practical constraints leading to this unique design, and finally, the design model. The circuit designs and diagrams are not discussed except where necessary; they are available in Reference (29).

3.1. Luminance, Chromaticity, and Color Television

The sections which follow relate luminance, hue, and saturation to the standardized quantities of luminance and chromaticity. Luminance is described in photometric terms, and chromaticity in colorimetric terms, in an effort to bridge the gap between psychological and physical prop-

erties. The Chromaticity Diagram simplifies the understanding of color television signals and how they link the eye to the original scene. A highly detailed discussion of these concepts is presented in References (37-41).

3.1.1. Luminance

The perception of luminance does not result solely from scotopic vision. Luminance derives from the action of radiant energy on a selective receptor. Only the sensitivity of that receptor dictates the perceived luminance of a given radiant source. Scotopic vision allows the brain to differentiate one wavelength from another solely in terms of relative luminance, Figure 3.1.1.A. Photopic vision on the other hand, permits the brain to differentiate spectral wavelengths in terms of hue and relative luminance, Figure 3.1.1.B., although the insensitivity of photopic receptors requires high absolute luminance levels for activation. Both forms of vision exhibit sensitivities varying with wavelength. Figures 3.1.1. plot the sensitivities of both receptors for monochromatic stimuli of constant radiance. The difference between luminosity and radiance, photometric and physical terms, respectively, is apparent from these figures. Sensitivity is called luminous efficiency, the scotopic curve is called the standard scotopic relative luminous efficiency function, and the photopic curve is called the standard photopic relative luminous efficiency function, denoted by V. The functions are relative since they are normalized to a peak efficiency of 1.0.

It will be seen in the next section that luminance may be derived from a knowledge of the spectral mixtrue of any real color.

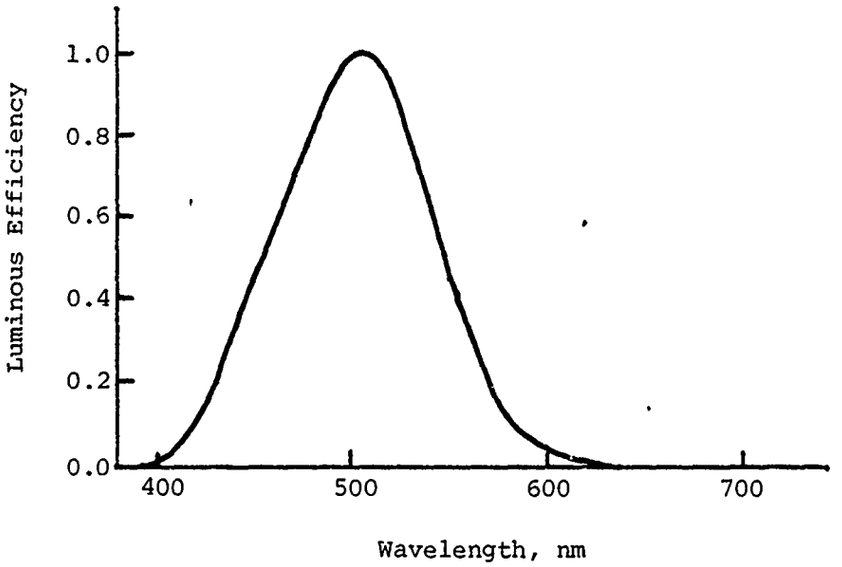

Figure 3.1.1.A. Standard scotopic relative luminous efficiency function. This curve depicts the relative spectral sensitivities of the rods. (Both figures from Judd, D.B.; Wyszecki, G. 1975. Color in Business, Science, and Industry. New York: Wiley-Interscience.)

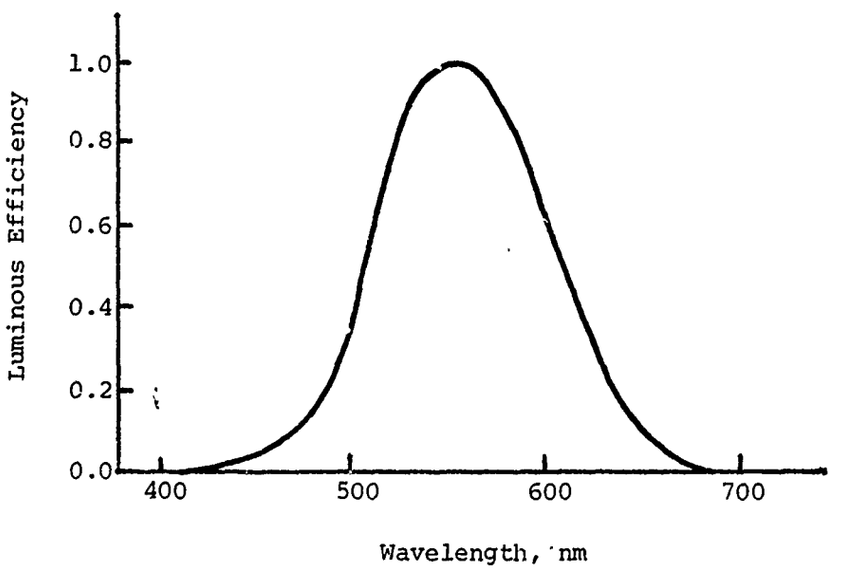

Figure 3.1.1.B. Standard photopic relative luminous efficiency function. This curve depicts the relative spectral sensitivities of the cones.

3.1.2. The Chromaticity Diagram

The eye is trichromatic, in that the entire gamut of color sensation is derived from three largely independent signals (Young-Helmholtz Theory). These signals are generally taken to be those produced through activation of three photopigments sensitive to what is commonly perceived as red (R), green (G), and blue (B) light. It has been shown, and is easily confirmed that a combination of R, G, and B, in proper proportions, can reproduce, or match nearly all visible colors. However, those colors which cannot be matched by any combination of R, G, and B are commonly perceived as "too saturated." The usual interpretation of this finding is that the spectral sensitivities of the cones' photopigments overlap, Figure 3.1.2., which is known to be true from spectrochemical studies. In other words, if there existed spectral energies that excite any given receptor to the exclusion of the other two, it would only then be possible to reproduce all visible colors by combination of these three spectral stimuli. The ramifications of overlap are tremendous. They form the limit on the accuracy with which a television camera can reproduce a visual scene.

It is the object of this section to motivate the Chromaticity Diagram and explain how it was used to develop workable television signals. The trichromatic model of human vision can be represented mathematically by the three dimensional tristimulus vector space, Figure 3.1.3. Note that the axes, representing primary colors, need not be orthonormal. The relative orientation and unit lengths of the primary axes are arbitrarily chosen by practical considerations so that equal amounts of

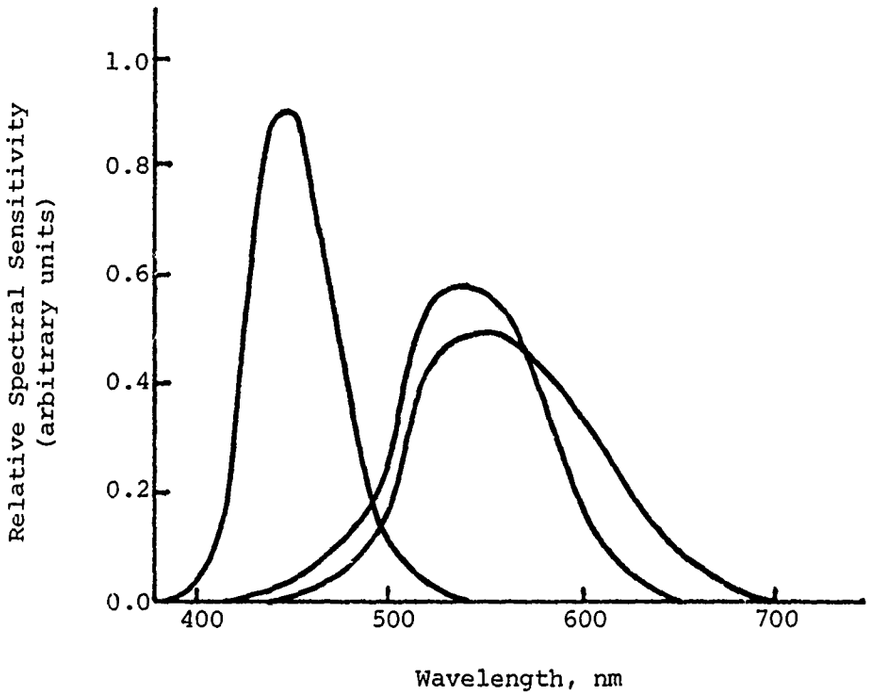

Figure 3.1.2. Relative spectral sensitivity functions of the photopigments postulated by the Young-Helmholtz Theory.

R, G, and B result in a neutral, or achromatic, grey of varying luminance. The locus of all achromatic points defined in this way is the neutral vector $\bar{N}$. Any color $\bar{S}$ has functional components, $\bar{R}$, $\bar{G}$, and $\bar{B}$, such that

$$\bar{S} = R\bar{R} + G\bar{G} + B\bar{B}$$

where R, G, and B denote the amounts of the three primary unit vectors $\bar{R}$, $\bar{G}$, and $\bar{B}$, respectively. All operations in the tristimulus vector space obey the laws of vector algebra. A unit plane can be defined by

$$R + G + B = 1.$$

Any color vector $\bar{S}$, or its length, $|\bar{S}|$, extended, intersects this unit plan at S, Figure 3.1.4. Although S is not unique, its specification does require two dimensions of color vector $\bar{S}$ in terms of unit planar

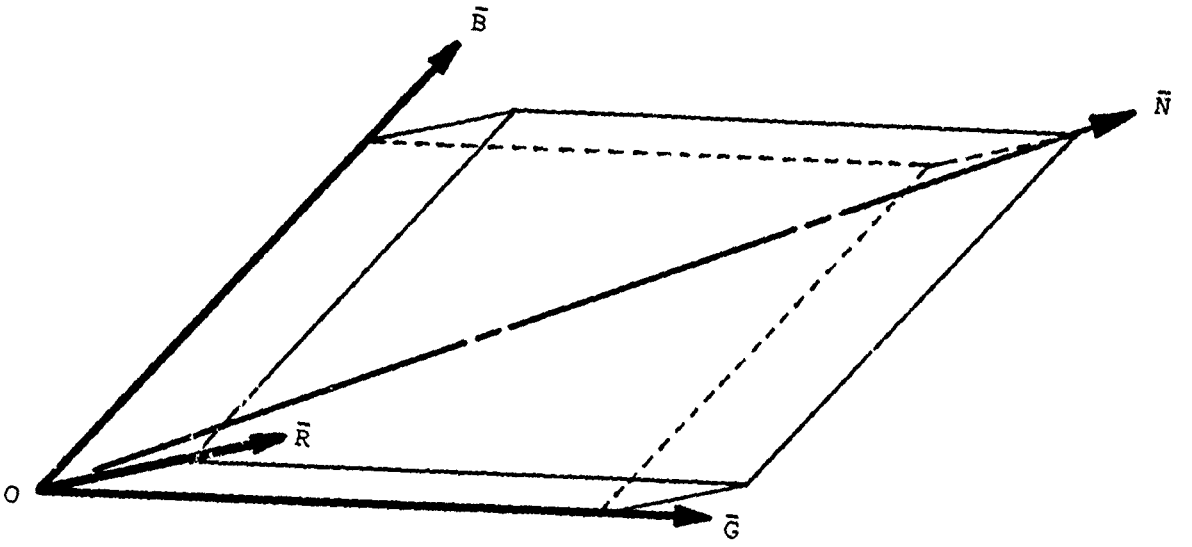

Figure 3.1.3. The three dimensional RGB tristimulus vector space showing the neutral vector $\bar{N}$, the locus of all achromatic colors.

coordinates. Thus, S is referred to as the chromaticity of $\bar{S}$. A chromaticity diagram, then, lies in the unit plane R + G + B = 1. The remaining dimension required to completely specify the color vector is in terms of $|\bar{S}|$. It is obvious that this dimension is not directly available from the unit plane chromaticity diagram.

The correlation between the psychological properties of color and the tristimulus vector space, mediated by color appearance models, is an extremely complex one. Ideally, the psychologically tensor-valued function, F(x,y), should be quantitized to the form of a psychophysically tensor-valued function by comparison to the quantitative RGB space. However, a rigorous definition of F(x,y) depends upon the color appearance model employed (see Section 2.2.1.). Refer to Figure 3.1.5. At

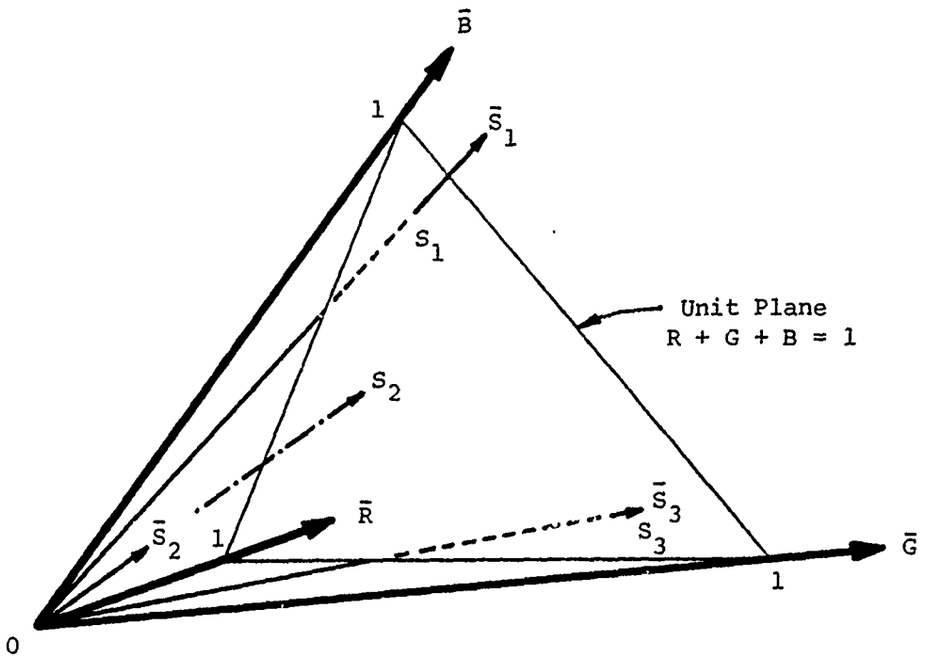

Figure 3.1.4. The RGB space showing the points S_1, S_2, and S_3, in the unit plane R + G + B = 1.

this point in the discussion, the color-matching functions having not yet been derived, it is sufficient to say that $|\bar{S}|$, the distance from the origin to any spatial point, is associated with luminance, and that S is associated with hue and saturation. However, since luminance cannot be defined without specification of a specific receptor, a detailed graphical representation of luminance must await the derivation of color-matching functions for the observer with normal color vision. To continue, the two dimensions which specify chromaticity, S, together represent hue and saturation. As the angle between $\bar{S}$ and $\bar{N}$ increases, S moves away from N to a higher saturation level; N represents an achromatic RGB mixture. If $\bar{S}$ moves strictly radially from $\bar{N}$, saturation of S increases, but S maintains a constant hue. And, of course, if $\bar{S}$ moves other than

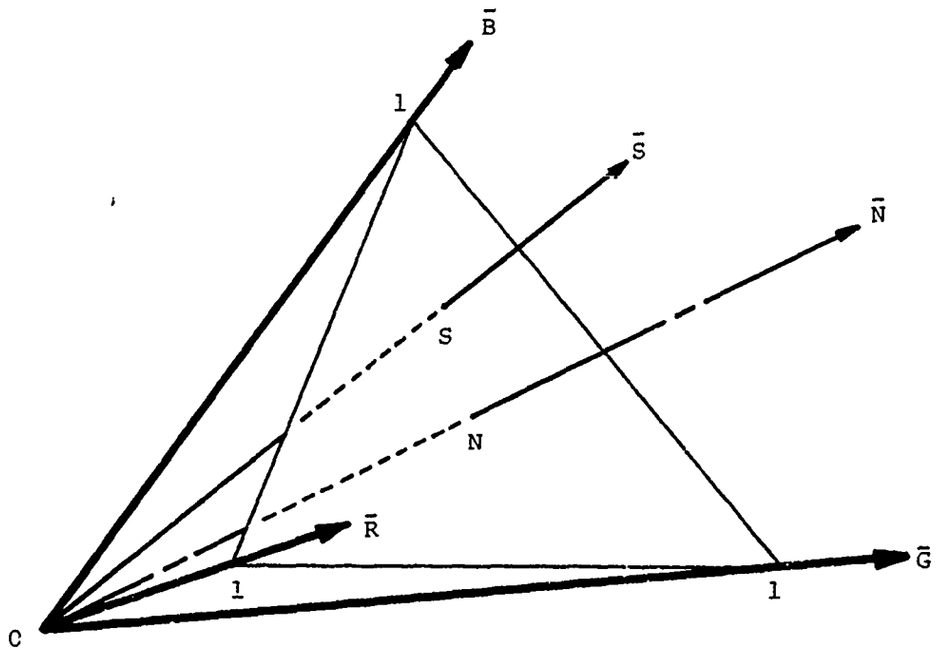

Figure 3.1.5. The RGB space showing a color vector $\bar{S}$ and the neutral vector $\bar{N}$.

strictly radially from N, both hue and saturation of S change.

Note that a color vector moving strictly radially from N generates a plane of constant hue. Through a transformation applied to RGB space outlined later in this section, these isohue planes become isohue surfaces of a given curvature. However, to a first approximation the surfaces may be described by planes (42). The concept of isohue planes is used in the development of the hue processor design in Section 3.2.3.

Note also the possibility of a color $\bar{S}$ outside the first (positive) quadrant of the RGB space. It requires at least one negative tristimulus value for specification. It will be shown later that this fact requires a transformation to positive values be performed on the RGB space so that

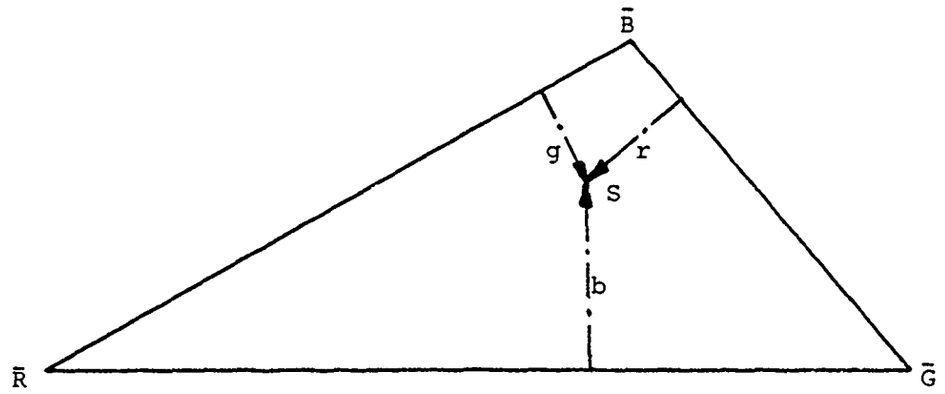

Figure 3.1.6. The RGB space unit plane in true normal view showing the chromaticity coordinates, r, g, and b, of point S.

colorimetric specifications can be practically applied. A gamut of colors is one for which all tristimulus values are positive. Those colors requiring negative specification are said to be outside the gamut.

The location of S in the unit plane, that is the chromaticity of $\bar{S}$, can be specified by the chromaticity coordinates, r, g, and b, as shown in Figure 3.1.6., which is the RGB unit plane shown in true normal view. Note that the tristimulus axes intersect the unit plane chromaticity diagram at chromaticity coordinates (r,g,b) of (1,0,0), (0,1,0) and (0,0,1) for R, G, and B, respectively. These coordinates are the normal distances from S to the corresponding sides of the triangle, and are related to the primary tristimulus values of $\bar{S}$ by

$$r = \frac{R}{R + G + B}, \quad g = \frac{G}{R + G + B}, \quad b = \frac{B}{R + G + B} \qquad 3.1.1.$$

A point specified in a plane by three coordinates carries redundant information; therefore,

$$r + g + b = 1, \qquad 3.1.2.$$

and two chromaticity coordinates are sufficient to completely specify S.

A tristimulus colorimeter is an instrument used in matching a tristimulus mixture of primary lights to an unknown test stimulus by human judgment. Two different colorimeters set to match the same test stimulus may register different sets of tristimulus values. Also, the instruments may employ altogether different tristimulus primaries. Given two colorimeters, one with a triad at primaries producing tristimulus values R, G, and B, and the other with a different triad of primaries producing tristimulus values X, Y, and Z, for the same test stimulus, a relation can be formed as follows:

$$\begin{aligned} X &= X_R R + X_G G + X_B B \\ Y &= Y_R R + Y_G G + Y_B B \\ Z &= Z_R R + Z_G G + Z_B B \end{aligned} \qquad 3.1.3.$$

where X_R, Y_R, and Z_R are the amounts of the second triad required to match the color (R = 1, G = 0, B = 0), X_G, Y_G, Z_G to match (R = 0, G = 1, B = 0), and X_B, Y_B, Z_B to match (R = 0, G = 0, B = 1). Simple substitution of the (R,G,B) specified colors into the given relations shows the latter to be correct. This transformation matrix, in which the subscripted constants are the transformation coefficients, most importantly implies that a sum of stimuli can be treated as a separate stimulus.

Similarly, the chromaticity coordinates are related to the tristimulus values in the second triad system by:

$$x = \frac{X}{X + Y + Z}, \quad y = \frac{Y}{X + Y + Z}, \quad z = \frac{Z}{X + Y + Z} \qquad 3.1.4.$$

Just as the tristimulus values matching a given test stimulus can be

transformed from one triad of primaries to another, respective chromaticity coordinates can be transformed as follows:

$$x = \frac{X_R r + X_G g + X_B b}{(X_R + Y_R + Z_R)r + (X_G + Y_G + Z_G)g + (X_B + Y_B + Z_B)b}$$

$$y = \frac{Y_R r + Y_G g + Y_B b}{(X_R + Y_R + Z_R)r + (X_G + Y_G + Z_G)g + (X_B + Y_B + Z_B)b} \qquad 3.1.5.$$

$$z = \frac{Z_R r + Z_G g + Z_B b}{(X_R + Y_R + Z_R)r + (X_G + Y_G + Z_G)g + (X_B + Y_B + Z_B)b}$$

Again, any two coordinates are sufficient to specify the chromaticity S of $\bar{S}$, since x + y + z = 1. (Equations 3.1.5. are a projective transformation of the chromaticity diagram. This type of ratio transformation permits the controlled distortion of a plane, such as the chromaticity diagram, which is the basis of advanced application of colorimetry.)

To generate the Standard Chromaticity Diagram, it is necessary to define that portion of the RGB (or XYZ) space which represents physically realizable colors. This requires the use of color-matching functions for an observer with normal color vision. A color matching experiment is set up where the triad of primaries will be used to match a test stimulus. Each primary, as well as the test stimulus, in this case, is a monochromatic, or spectral, hue of a narrow band of the visible spectrum centered at the chosen wavelength. Each monochromatic primary can be used exclusively to produce either the color-matching light or part of the stimulus. Typically, the three monochromatic primaries will be mixed together to match the test stimulus. However, for certain test stimuli, those which were earlier stated to be "too saturated," one or

two of the primaries must be completely removed from the color-matching light and added to the test stimulus in an appropriate amount to produce a match. The one or two primaries mixed with the test stimulus cause the latter to become less saturated and capable of being matched by the remaining primaries. The one or two primaries added to the test stimulus have the negative tristimulus values discussed earlier. It is obvious that if a color television camera were to match such a test stimulus, the camera would need to employ a vidicon with a negative sensitivity, which is not possible.

Now, the wavelengths about which the monochromatic primaries are centered are, by international agreement, 700 nm for R, 546.1 nm for G, and 435.8 nm for B. The units of these particular primaries are chosen such that their radiances are in the ratios $L_R:L_G:L_B$ = 72.1:1.4:1.0 (approx.). These ratios result from a separate experiment in which a ratio of primaries is found to match a test mixture of all monochromatic stimuli of the visible spectrum (380 nm to 770 nm) where each stimulus has the same radiance. This spectral mixture is called the equal energy stimulus.

The color-matching experiment to determine the color-matching functions is repeated for numerous test stimuli. Each stimulus is a 5 nm band of the equal energy stimulus, that is a 5 nm band of the visible spectrum where each stimulus has the same radiance. Thus the experiment is repeated 79 [= (770 - 380)/5 + 1] times.

The correction to experimental data described next should be fully understood before continuing. To be colorimetrically correct, the

monochromatic test stimuli must all have the same radiance. However, in practice, the radiances of test stimuli near the extremes of the spectrum must be increased to assure activation of relatively insensitive photopic vision, since the normal eye is used to judge the color match. Therefore, each monochromatic primary actually used to make a match must be decreased by a factor equal to the quotient of the equal energy radiance of the test stimulus and the actual radiance of the test stimulus at match. In this way, the actual monochromatic tristimulus values R, G, and B used for the match are reduced to corresponding values which match test stimuli of constant radiance. This new tristimulus set, denoted by $\bar{r}$, $\bar{g}$, and $\bar{b}$, provides true matches for test stimuli of given wavelengths and constant radiance. Note, that if it were not necessary to increase the radiance of certain test stimuli to assure photopic vision, R,G,B and $\bar{r},\bar{g},\bar{b}$ sets would be equivalent. Table 3.1.1. is an abridged list of $\bar{r}$, $\bar{g}$, and $\bar{b}$ values used to match the 79 monochromatic equal radiance, test stimuli. Note that numerous tristimulus values are negative, indicating that a color match was obtained by using one or two of the primaries to desaturate the test stimulus. Figure 3.1.7. illustrates the $\bar{r}$, $\bar{g}$, and $\bar{b}$ values as functions of wavelength of each equal radiance test stimulus. The $\bar{r}$, $\bar{g}$, and $\bar{b}$ functions can be transformed as in Equation 3.1.3. to obtain $\bar{x}$, $\bar{y}$, and $\bar{z}$ functions with respect to any primaries X, Y, and Z. Table 3.1.2. gives the $\bar{x}$, $\bar{y}$, and $\bar{z}$ values resulting from a transformation chosen by the CIE. Figure 3.1.8. illustrates the $\bar{x}$, $\bar{y}$, and $\bar{z}$ values as functions of wavelength of test stimuli. These transformed monochromatic tristimulus values are the required color-matching functions and define the CIE 1931 Standard Colorimetric Observer

Constant Radiance Test Stimulus Wavelength, nm	Color-Matching Functions		
	$\bar{r}$	$\bar{g}$	$\bar{b}$
380	0.00003	-0.00001	0.00117
400	0.00030	-0.00014	0.01214
420	0.00211	-0.00110	0.11541
440	-0.00261	0.00149	0.31228
460	-0.02608	0.01485	0.29821
480	-0.04939	0.03914	0.14494
500	-0.07173	0.08536	0.04776
520	-0.09264	0.17468	0.01221
540	-0.03152	0.21466	0.00146
560	0.09060	0.19702	-0.00130
580	0.24526	0.13610	-0.00108
600	0.34429	0.06246	-0.00049
620	0.29708	0.01828	-0.00015
640	0.15968	0.00334	-0.00003
660	0.05932	0.00037	0.00000
680	0.01687	0.00003	0.00000
700	0.00410	0.00000	0.00000
720	0.00105	0.00000	0.00000
740	0.00025	0.00000	0.00000
760	0.00006	0.00000	0.00000

Table 3.1.1. The $\bar{r}$, $\bar{g}$, and $\bar{b}$ tristimulus values which match spectral test stimuli of constant radiance, for the observer with normal color vision, using spectral primaries at 435.8 nm, 546.1 nm, and 700.0 nm. (From CIE Publication No. 15, Colorimetry, 1971.)

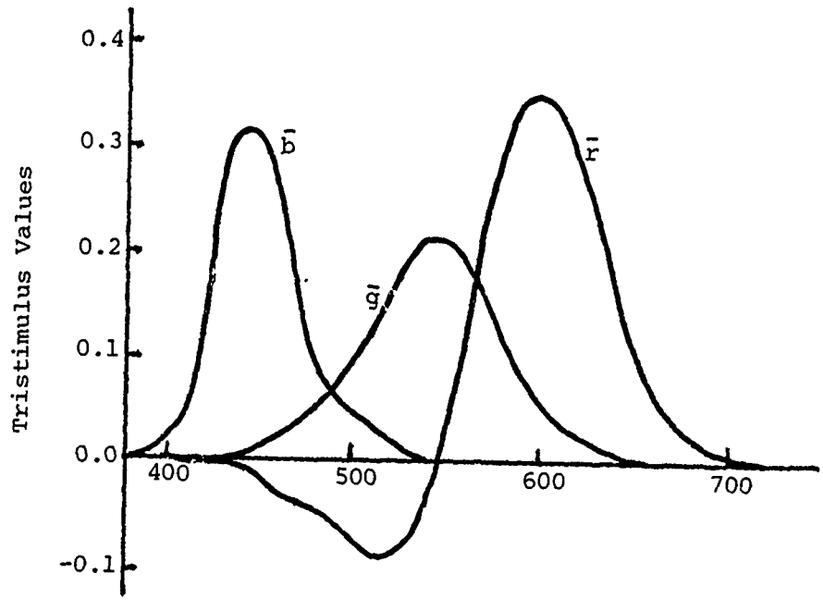

Figure 3.1.7. The $\bar{r}$, $\bar{g}$, and $\bar{b}$ tristimulus values which match spectral test stimuli of constant radiance, for the observer with normal color vision, using spectral primaries at 435.8 nm, 546.1 nm, and 700.0 nm.

Constant Radiance Test Stimulus Wavelength, nm	Color-Matching Functions		
	$\bar{x}$	$\bar{y}$	$\bar{z}$
380	0.0014	0.0000	0.0065
400	0.0143	0.0004	0.0679
420	0.1344	0.0040	0.6456
440	0.3483	0.0230	1.7471
460	0.2908	0.0600	1.6692
480	0.0956	0.1390	0.8130
500	0.0049	0.3230	0.2720
520	0.0633	0.7100	0.0782
540	0.2904	0.9540	0.0203
560	0.5945	0.9950	0.0021
580	0.9163	0.8700	0.0017
600	1.0622	0.6310	0.0008
620	0.8544	0.3810	0.0002
640	0.4479	0.1750	0.0000
660	0.1649	0.0610	0.0000
680	0.0468	0.0170	0.0000
700	0.0114	0.0041	0.0000
720	0.0029	0.0010	0.0000
740	0.0007	0.0002	0.0000
760	0.0002	0.0001	0.0000

Table 3.1.2. The $\bar{x}$, $\bar{y}$, and $\bar{z}$ tristimulus values resulting from the CIE transformation from the $\bar{r}\bar{g}\bar{b}$ values. These color-matching functions define the CIE 1931 Standard Colorimetric Observer. (From Judd, D.B.; Wyszecki, G. 1975. Color in Business, Science, and Industry. New York: Wiley-Interscience.)

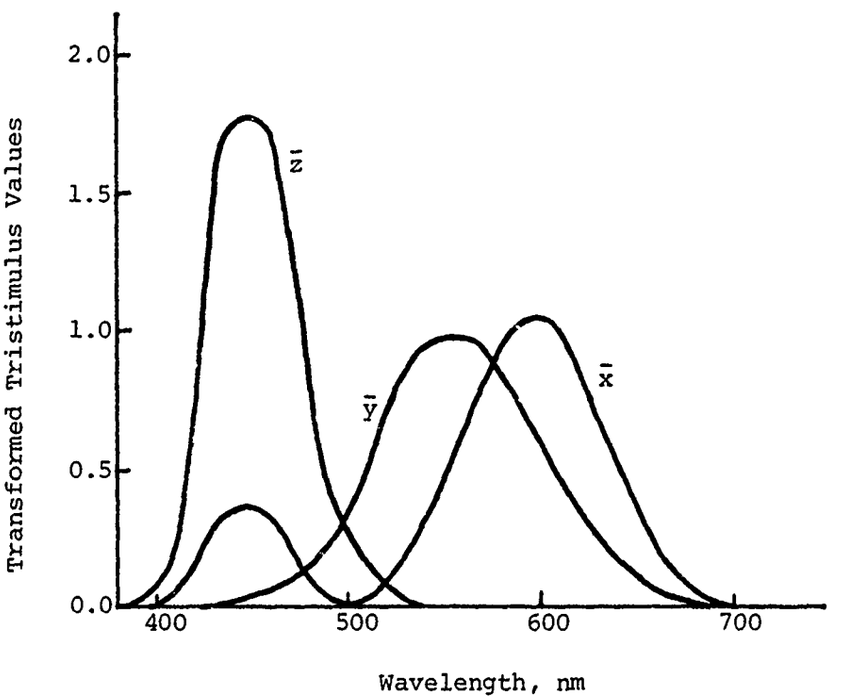

Figure 3.1.8. The $\bar{x}$, $\bar{y}$, and $\bar{z}$ tristimulus values resulting from the CIE transformation from the $\bar{r}\bar{g}\bar{b}$ values. These color-matching functions define the CIE 1931 Standard Colorimetric Observer.

with normal color vision (39). Whereas, the RGB primaries are real, spectral colors, the XYZ primaries may be imaginary, due to the transformation chosen. In the CIE 1931 Standard, the XYZ primaries are, in fact imaginary. This will become evident later. Though there exists, of course, an infinite number of transformations through which $\bar{x}$, $\bar{y}$, and $\bar{z}$ are derived from $\bar{r}$, $\bar{g}$, and $\bar{b}$, the one chosen by the CIE incorporates numerous convenient features. The values of these transformed color-matching functions are positive for all wavelengths of test stimuli, and are thereby easier to manipulate and model mathematically. Also, the $\bar{y}$ function is identical to the standard relative luminous efficienty function, V (see Figures 3.1.1.). Indeed, this fact was insured by the original researchers in colorimetry by reasoning backwards from the desired $\bar{x}\bar{y}\bar{z}$ functions to the experimentally produced $\bar{r}\bar{g}\bar{b}$ functions (43,44). The importance of this fact will become apparent when the television luminance signal is discussed later. There is another important feature of the CIE transformation. Since the X, Y, and Z primaries are imaginary, the experimental correction quotients need not be applied to $\bar{x}$, $\bar{y}$, and $\bar{z}$ to obtain X, Y, and Z, that is, the $\bar{x}$, $\bar{y}$, and $\bar{z}$ functions give, directly, the amounts of the X, Y, and Z primaries, respectively, required to reproduce for the standard observer the equal radiance test stimuli.

Just as the RGB space, the unit plane X + Y + Z = 1 can be constructed in the XYZ space. The orientation of the XYZ coordinate axes is also a useful result of the CIE chosen transformation from R, G, and B to $\bar{x}$, $\bar{y}$, and $\bar{z}$. As shown in Figure 3.1.9., this orientation is such that the unit plane is a right triangle. In this arrangement, the two chromaticity coordinates, x and y, are sufficient to specify any chromaticity, S, in the

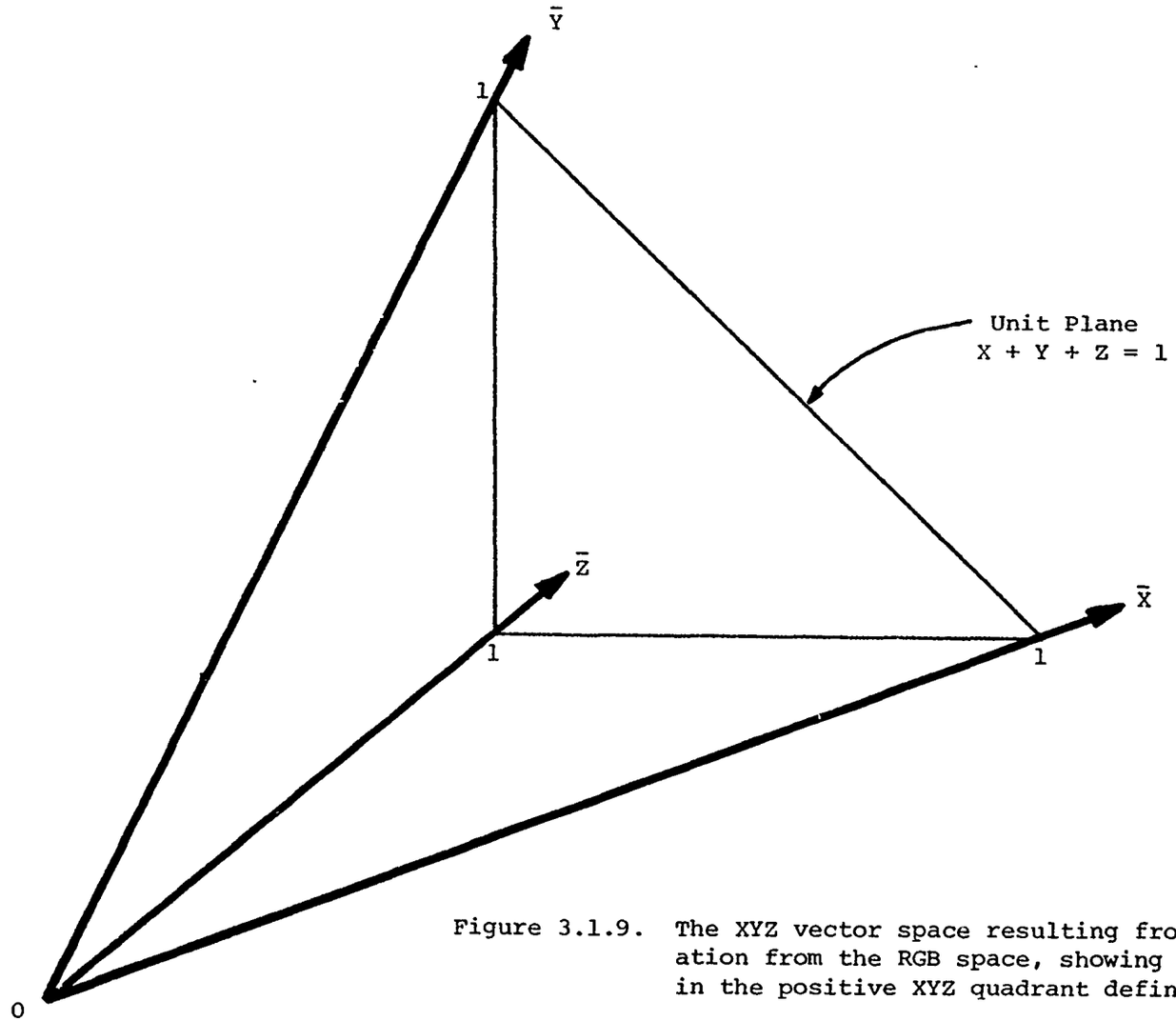

Figure 3.1.9. The XYZ vector space resulting from the CIE transformation from the RGB space, showing the unit plane which in the positive XYZ quadrant defines a right triangle.

unit plane, X + Y + Z = 1. x and y obey the relations of Equations 3.1.4. but were derived from:

$$x = \frac{\bar{x}}{\bar{x} + \bar{y} + \bar{z}}, \quad y = \frac{\bar{y}}{\bar{x} + \bar{y} + \bar{z}}, \quad z = \frac{\bar{z}}{\bar{x} + \bar{y} + \bar{z}} \qquad 3.1.6.$$

Since x, y, and z, are equivalent to X, Y, and Z, Equations 3.1.4. and 3.1.6. are also equivalent. It remains now only to generate the CIE 1931 (x,y)-Chromaticity Diagram from the XYZ space. Figure 3.1.10., first of all, shows the locus of all color vectors, $\bar{s}$, whose components are the transformed monochromatic tristimulus values $\bar{x}$, $\bar{y}$, and $\bar{z}$, of constant radiance. These values are, of course, functions of wavelength. Here, the locus swept out by $\bar{s}$ begins at the origin with a wavelength of 380 nm, proceeds through the XYZ space, and returns to the origin at a wavelength of 780 nm. Note that $|\bar{s}|$, is not constant, so that the luminance of $\bar{s}$ is not constant. This should not be surprising, given the luminous efficiency function of Figures 3.1.1., where luminous efficiency is a function of wavelength. The color vectors, $\bar{S}$, shown in the Figure, are extensions of respective $\bar{s}$ vectors. These extensions intersect the unit plane forming a locus called the spectrum locus. All additive mixtures of the two monochromatic colors, $\bar{S}$ at 380 nm and $\bar{S}$ at 780 nm, form a straight locus called the purple line. The spectrum locus, the purple line, and the triangular area they enclose in the unit plane, define the CIE 1931 (x,y)-Chromaticity Diagram. This is the diagram that this section of Chapter III set out to motivate. Note the vector $\bar{E}$, which represents the equal energy stimulus. The chromaticity, E, of $\bar{E}$, is specified by $x = 1/3$, $y = 1/3$, and since $x + y + z = 1$, $z = 1/3$ These values result from an arbitrary normalization of the unit lengths

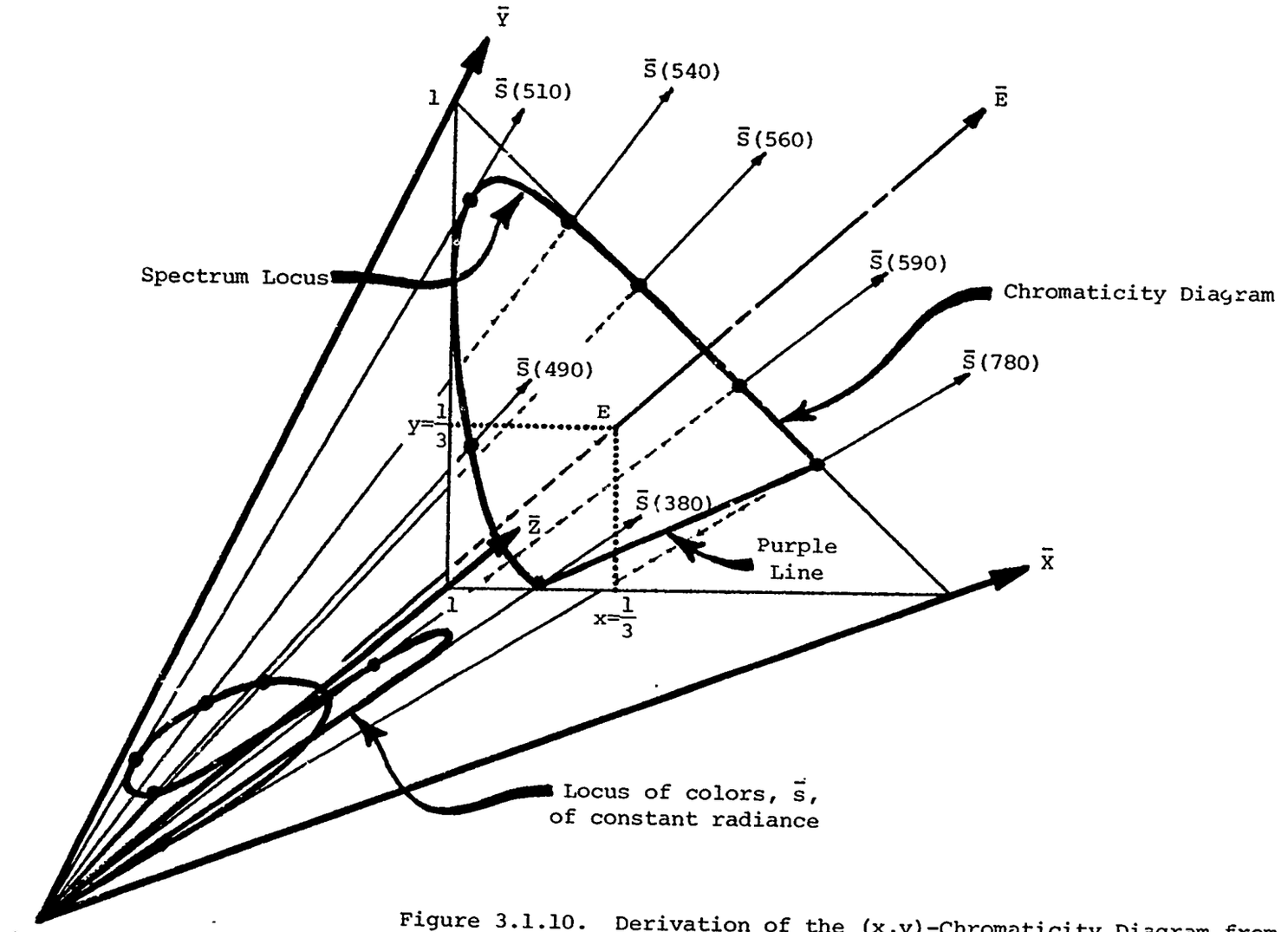

Figure 3.1.10. Derivation of the (x,y)-Chromaticity Diagram from the Standard XYZ vector space. See text for explanation.

of primary axes X, Y, and Z. That the areas under the color-matching functions $\bar{x}$, $\bar{y}$, and $\bar{z}$ are all equal is a consequence of this normalization.

A conical solid is defined by the (x,y)-Chromaticity Diagram, which is the cone's base, and the origin of the XYZ space, the cone's apex. All additive mixtures of the monochromatic color vectors that form the surface of the cone fall within the cone. The cone bounds the gamut of all real colors. All colors whose vectors fall outside this cone are imaginary. Note that any tristimulus value, X, Y, or Z of any real color cannot be negative since the cone of real colors lies wholly in the positive XYZ quadrant. Similarly, all colors whose chromaticities, S, fall on or within the area bounded by the spectrum locus and purple line, are real; all colors whose chromaticities fall outside this area are imaginary.

Figure 3.1.11. shows the full CIE (x,y)-Chromaticity Diagram in true plane view. It has already been shown that the chromaticity coordinates of the equal energy stimulus, E, are ($x = 1/3$, $y = 1/3$). The chromaticity coordinates of all monochromatic stimuli, which, of course, lie on the spectrum locus, are given by Equations 3.1.6. Table 3.1.3. lists these chromaticity coordinates for the values of the color-matching functions given in Table 3.1.2.

The CIE 1931 (x,y)-Chromaticity Diagram, produced by the ingenious transformation of $\bar{r}\bar{g}\bar{b}$ to $\bar{x}\bar{y}\bar{z}$ color-matching functions, neatly embodies several useful chracterıstics. Refer again to Figure 3.1.11. First the right-triangular shape of the unit plane permits color specification by convenient Cartesian coordinates. Second, as already mentioned, the

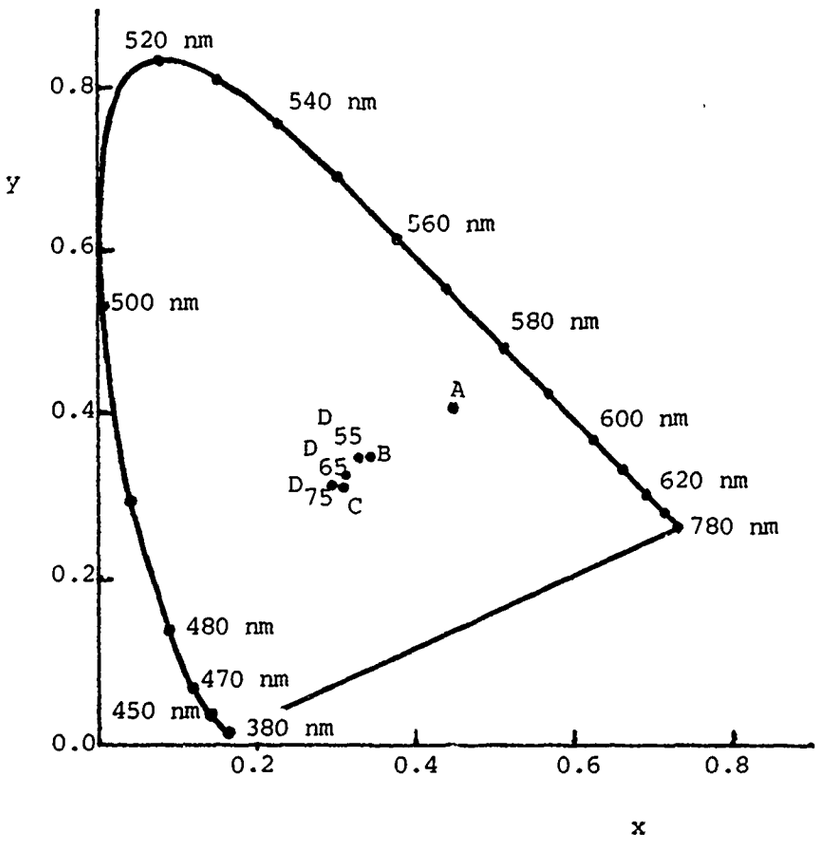

Figure 3.1.11. The CIE 1931 (x,y)-Chromaticity Diagram showing the chromaticity locations of several spectral hues along the spectrum locus and several CIE Standard Illuminants. (From Judd, D.B.; Wyszecki, G. 1975. Color in Business, Science, and Industry. New York: Wiley-Interscience.)

purple line is the locus of all possible additive mixtures of the two monochromatic stimuli forming the termini of the spectrum locus, $\bar{S}$ of 380 nm and $\bar{S}$ of 780 nm. Similar additive mixture loci exist for any two monochromatic stimuli. In other words, a line segment connecting any two monochromatic stimuli contains the chromaticity points of all additive mixtures of the two stimuli. Conversely, the chromaticity of any point within the area bounded by the spectrum locus and purple line can be produced by the appropriate mixture of the two monochromatic stimuli which lie at the intersections of the spectrum locus and any line passing through that chromaticity point. Third, note that the equal energy stimulus, point E, is perceived as achromatic, having no hue. Any two monochromatic stimuli, connected by a line which passes through point E, mix to form an achromatic color, that is, a grey level. These two monochromatic stimuli are called complementary colors. However, those lines passing through point E and any monochromatic stimuli from 494 to 570 nm intersect the purple line. Except for its extremes, 380 nm and 780 nm, the purple line does not represent monochromatic colors, but two-monochromatic-component mixtures. Therefore, the complements of monochromatic stimuli from 494 nm to 570 nm must be comprised of at least two monochromatic stimuli, one at 380 nm and the other at 780 nm. These colors that lie along the purple line are sometimes called nonspectral or purple colors. It is not surprising that any chromaticity point approaching point E is perceived as becoming more achromatic. Since the spectrum locus is always concave outward, it follows also that the chromaticities on any two-monochromatic-component mixture line are approaching point E and are perceived as less saturated than the

monochromatic components themselves. Therefore, perceived saturation decreases as chromaticity approaches the equal energy stimulus, and the monochromatic stimuli are the only completely saturated colors. Fourth, note in Table 3.1.3. that the chromaticity coordinates for monochromatic stimuli beyond about 700 nm are identical. This part of the spectrum has constant chromaticity and is sometimes called the "long-wave end stretch." As are all of the above, this characteristic is a property of normal photopic perception; any spectral stimuli can be matched with any other spectral stimuli in this end stretch by simply equalizing their luminances. Fifth, the area bounded by the spectrum locus and purple line deviates substantially from true triangular shape. For this reason, the area cannot be totally and exclusively enclosed by a triangle. At least two of the vertices of such a triangle must lie outside the area. It is obvious, then, that at least two primaries, of the triad defined by the triangle's vertices, must be imaginary for all colors of the diagram to be formed by additive mixtures of those primaries. The CIE XYZ space employs just such imaginary primaries. This right triangle, which is the unit plane $X + Y + Z = 1$, embodies other interesting characteristics. The hypotenuse is colinear with the spectrum locus from 780 nm to about 560 nm. Also, since y is identical to the standard relative luminous efficiency function, V, and since $\bar{y}$ is equivalent to Y, the Y tristimulus value of any color specified in the XYZ system gives the relative luminous efficiency of that color. The X and Z values of any color, therefore, cannot contribute to the luminous efficiency specification of that color. Note that the x chromaticity axis is defined by the intersections of the X and Z axes with the unit plane $X + Y + Z = 1$. Therefore, the x axis

	Chromaticity Coordinates		
Wavelength, nm	x	y	z
380	0.1741	0.0050	0.8209
400	0.1733	0.0048	0.8219
420	0.1714	0.0051	0.8235
440	0.1644	0.0109	0.8247
460	0.1440	0.0297	0.8263
480	0.0913	0.1327	0.7760
500	0.0082	0.5384	0.4534
520	0.0743	0.8338	0.0919
540	0.2296	0.7543	0.0161
560	0.3731	0.6245	0.0024
580	0.5125	0.4866	0.0009
600	0.6270	0.3725	0.0005
620	0.6915	0.3083	0.0002
640	0.7190	0.2809	0.0001
660	0.7300	0.2700	0.0000
680	0.7334	0.2666	0.0000
700	0.7347	0.2653	0.0000
720	0.7347	0.2653	0.0000
740	0.7347	0.2653	0.0000
760	0.7347	0.2653	0.0000

Table 3.1.3. The CIE 1931 Chromaticity Coordinates of spectral stimuli. (From Judd, D.B.; Wyszecki, G. 1975. Color in Business, Science, and Industry. New York: Wiley-Interscience.)

is the line on which are located the chromaticities of all colors having zero luminance. That this seems physically impossible is reflected by the fact that all x axis colors are imaginary.

Reference has been made often to the equal energy stimulus. This is not the only "achromatic" color defined by the CIE. Standard illumination sources have also been defined. For example, CIE Standard Illuminant A represents light from the ideal black body radiator at 7856 K. The ideal blackbody, of course, obeys Planck's Radiation Law and is often called a Planckian radiator. Illuminants B and C, on the other hand, represent direct sunlight correlated to 4870 K and average daylight correlated to 6770 K respectively. Illuminants D_{55}, D_{65}, and D_{75} representing different phases of daylight correlated to 5500 K, 6500 K, and 7500 K, respectively, are more recent standards than B or C, and may soon supersede them. However, at the time the television luminance signal was standardized, Illuminant C was in accepted usage, and will be used in the discussion of luminance that follows. The positions of these standards on the Chromaticity Diagram are shown in Figure 3.1.11.

Now that the tristimulus matching theory has been explained, the concept of luminance can be further developed. A color $\bar{S}$ may be represented by:

$$\bar{S} = R\bar{R} + G\bar{G} + B\bar{B}$$

in the RGB System. When a single color is specified, its perceived brightness is usually given in a photometric quantity, such as luminance. For the right and left sides of the above equation to be consistent, therefore, the units in which the amounts of R, G, and B are being

measured must be in terms of luminance. It is an experimental fact, and can also be derived from the experimental luminous efficiency function, that the luminances of the three stimuli are not necessarily equal. In fact, they are generally different, for example, when the units are defined such that equal amounts of R, G, and B match the equal energy stimulus. This definition was, of course, established in both the RGB and XYZ spaces. Therefore, the luminance of $\bar{S}$, L_S, can be written:

$$L_S = L_R R + L_G G + L_B B$$

where L_R, L_G, and L_B are the luminance factors for converting the units used for R, G, and B into luminance units. This relationship will be applied in the next section.

3.1.3. Color Television

It should be clear, from the previous section, that color television should mimic the trichromatic model of the human eye, to take maximum advantage of and minimally compromise the eye's characteristics. This, indeed, was the decision reached by the National Television Systems Committee (NTSC) and accepted, along with specific technical recommendations, by the Federal Communications Commission in 1953. It is the purpose of this section to describe these recommendations, which form the principles on which color television operates, so the user of colorimetric topography can understand the function and limitations of his measurement technique.

It has been shown that for all colors to be matched by an additive mixture of three primaries, at least two of those primaries must be imaginary. In the CIE Standard RGB System, three real, monochromatic

primaries were chosen. But to make all color matches one or two of those primaries had to be used in the negative sense, that is added to the test stimulus. The C.I.E. Standard XYZ System, formed by a projective transformation from the Standard RGB System, overcomes the problem of negative tristimulus values, but at the cost of imaginary primaries. Nevertheless, due to numerous computation advantages of the Standard XYZ System, it has been internationally agreed upon as the standard color specification system.

The choice of primaries to be used by color television systems was one of the initial problems facing the NTSC. Consider, as before, R at 700 nm, G at 546.1 nm, and B at 435.8 nm. Whether one thinks in the RGB System, where some colors require negative tristimulus values, or in the XYZ System, where the primaries are imaginary, both systems fall short of a practical specification of primaries. Imaginary primaries cannot be produced. However, the negative tristimulus values of the RGB System may not be an insurmountable problem. If a color television camera is considered the matching system, and the scene being viewed as the test stimulus, it is obvious that adding light of the appropriate primary to the scene in order that it might be matched by the camera, a procedure required by those RGB colors with negative tristimulus values, would result in this new-colored scene being televised. The objective was to televise the original scene. Rather than adding light to the scene, perhaps the camera could produce negative tristimulus values, that is, have negative primary sensitivities. A vidicon tube, of course cannot have negative sensitivities. But seemingly negative sensitivities may be created electronically by matrixing. This technique and its limitations will be discussed later. Though a formidable problem has

thus been partially solved, it remains to produce the RGB System primaries. These primaries are monochromatic, or spectral. As such, they are completely saturated. Highly saturated colors are of low luminance. Therefore, to reproduce a spectral hue, many watts of radiant flux must be emitted by the phosphors, both at the camera and the receiver. This is economically unfeasible, especially at the receiver, where it may also be too hazardous. The question of the existence of phosphors capable of such narrow spectral emission, at any power level, is also raised. It is, then, the physical character of these primaries that causes the problem.

The compromise reached by the NTSC is shown in Figure 3.1.12. The chromaticity coordinates of the compromised primaries are:

$$x_R = 0.67, \quad y_R = 0.33$$
$$x_G = 0.21, \quad y_G = 0.71$$
$$x_B = 0.14, \quad y_B = 0.08$$

These primaries represent the best compromise between the conflicting requirements of a highly multicolored and simultaneously a maximally bright reproduction. Remember, now, that the triangle RGB defines the gamut of the system; color within the triangle can be represented by wholly positive tristimulus values, while those outside, though real, require negative values for specification in terms of the NTSC RGB primaries. Only if matrixing is completely successful can all colors be reproduced by television. The chromaticities of the emittances of the actual phosphors used today are denoted by R*, G*, and B* in Figure 3.1.12.

Before developing the signal forms produced by the color television camera and input to the image processor, it would be consistent and

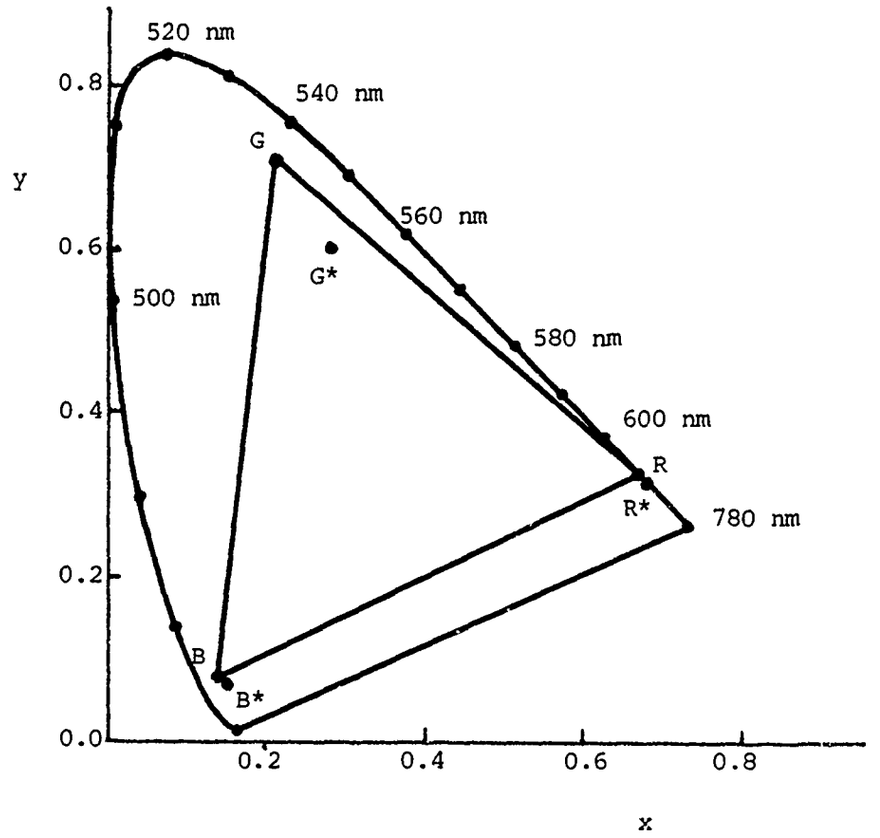

Figure 3.1.12. The CIE 1931 (x,y)-Chromaticity Diagram showing the comprimised NTSC RGB Primaries, R, G, and B, and the chromaticity locations, R*, G*, and B*, of the actual emission phosphors in use today. (From Judd, D.B.; Wyszecki, G. 1975. Color in Business, Science, and Industry. New York: Wiley-Interscience.)

instructional to derive the NTSC $\bar{r}$, $\bar{g}$, and $\bar{b}$ functions. First, solving Equations 3.1.4. for the tristimulus values, X, Y, AND Z, for each NTSC primary, R, G, and B, with respective chromaticity coordinates x_R, y_R, z_R; x_G, y_G, z_G; x_B, y_B, z_B:

$$X_R = k_R x_R, \quad Y_R = k_R y_R, \quad Z_R = k_R z_R,$$
$$X_G = k_G x_G, \quad Y_G = k_G y_G, \quad Z_C = k_G z_G, \qquad 3.1.7.$$
$$X_B = k_B x_B, \quad Y_B = k_B y_B, \quad Z_B = k_B z_B,$$

where $k_R = X_R + Y_R + Z_R$, $k_G = X_G + Y_G + Z_G$, and $k_B = X_B + Y_B + Z_B$ are constants of proportionality yet to be determined. Just as for the CIE RGB System, the unit amounts of the primaries in the NTSC RGB System must be arbitrarily chosen. Thus, k_R, k_G, and k_B must be specified such that a mixture of unit amounts of the NTSC primaries produces a neutral standard. That standard chosen by NTSC for color television is CIE Standard Illuminant C*. Now, k_R, k_G, and k_B can be specified by imposing the condition that the tristimulus values of Illuminant C provide tristimulus values R = G = B = 1. Substituting from Equations 3.1.7. for the transformation coefficients in Equations 3.1.3.:

$$\begin{aligned} X &= k_R x_R R + k_G x_G G + k_B x_B B \\ Y &= k_R y_R R + k_G y_G G + k_B y_B B \\ Z &= k_R z_R R + k_G z_G G + k_B z_B B \end{aligned} \qquad 3.1.8.$$

Solving these equations for k_R, k_G, and k_B:

$$\begin{aligned} k_R &= \frac{(y_G z_B - y_B z_G)X + (x_B z_G - x_G z_B)Y + (x_G y_B - x_B y_G)Z}{Rx_R(y_G z_B - y_B z_G) + Rx_G(y_B z_R - y_R z_B) + Rx_B(y_R z_G - y_G z_R)} \\ k_G &= \frac{(y_B z_R - y_R z_B)X + (x_R z_B - x_B z_R)Y + (x_B y_R - x_R y_B)Z}{Gx_R(y_G z_B - y_B z_G) + Gx_G(y_B z_R - y_R z_B) + Gx_B(y_R z_G - y_G z_R)} \\ k_B &= \frac{(y_R z_G - y_G z_R)X + (x_G z_R - x_R z_G)Y + (x_R y_G - x_G y_R)Z}{Bx_R(y_G z_B - y_B z_G) + Bx_G(y_B z_R - y_R z_B) + Bx_B(y_R z_G - y_G z_R)} \end{aligned} \qquad 3.1.9.$$

Evaluating these equations for the given condition, X = 98.041, Y = 100.000, and Z = 118.103, when R = G = B = 1, and for the NTSC RGB chromaticity coordinates given above:

$$k_R = 90.557,\ k_G = 82.649,\ k_B = 142.937;$$

*From Reference (37), $X_C = 98.041$, $Y_C = 100.000$, $Z_C = 118.103$. Y, for all Standard Illuminants, is normalized to a value of 100.000.

the Transformation Equations 3.1.8. become:

$$X = 60.673R + 17.356G + 20.011B$$
$$Y = 29.884R + 58.681G + 11.435B \qquad 3.1.10.$$
$$Z = 6.612G + 111.491B$$

Equations 3.1.10. are the transformation equations from the NTSC RGB System to the CIE XYZ System. Inverting the coefficient matrix of Equations 3.1.10., the inverse transformation equations become:

$$R = 0.019105X - 0.005326Y - 0.002883Z$$
$$G = -0.009843X + 0.019985Y - 0.000283Z \qquad 3.1.11.$$
$$B = 0.000584X - 0.001185Y + 0.008986Z$$

The NTSC $\bar{r}$, $\bar{g}$, and $\bar{b}$ functions can now be determined. To do this, the values of X, Y, and Z for monochromatic stimuli may be substituted into Euqation 3.1.11. to produce R, G, and B values as functions of wavelength. But $\bar{x}$, $\bar{y}$, and $\bar{z}$ values of monochromatic stimuli may be substituted for X, Y, and Z in Equation 3.1.11, also to produce $\bar{r}$, $\bar{g}$, and $\bar{b}$ values as functions of wavelength. Using $\bar{x}$, $\bar{y}$, and $\bar{z}$ from Table 3.1.2. and representing the results graphically, Figure 3.1.13. is obtained. Note that, as expected, the NTSC $\bar{r}\bar{g}\bar{b}$ functions require negative values to specify the monochromatic stimuli, since those stimuli lie outside the NTSC gamut.

The $\bar{r}\bar{g}\bar{b}$ functions actually represent the camera spectral sensitivities required to reproduce all real colors with perfect fidelity, by means of the NTSC primaries. As mentioned, the "negative sensitivities" are created electronically by matrixing. Matrix circuits receive the signals of anomolous but known spectral sensitivities and cross-mix them in suitable proportions to produce the correct signals of Figure 3.1.13. In the NTSC

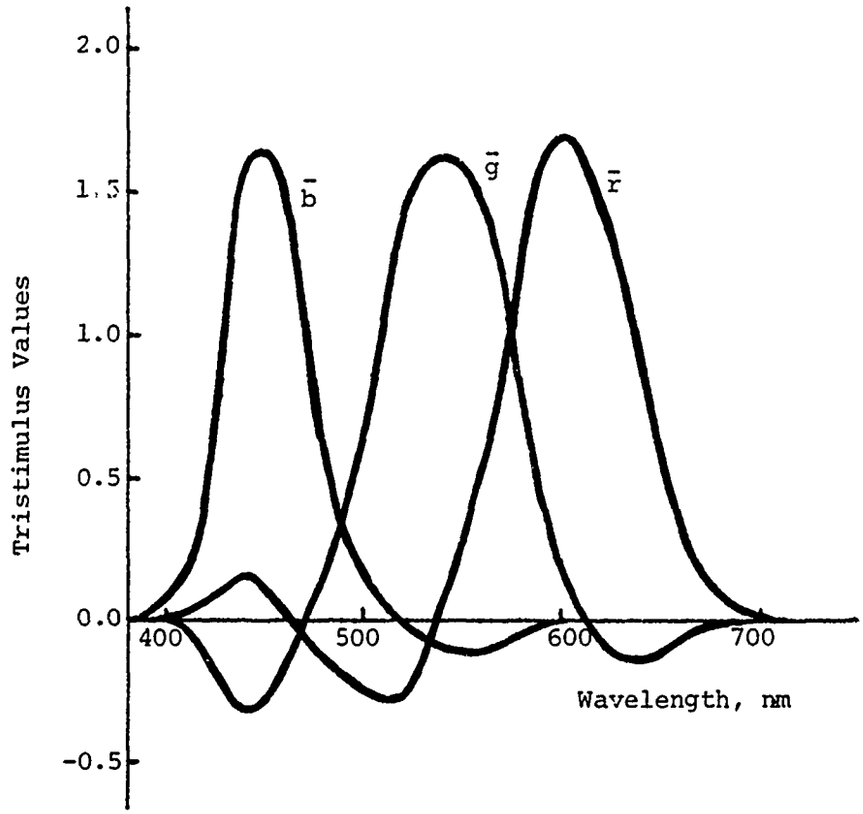

Figure 3.1.13. The $\bar{r}$, $\bar{g}$, and $\bar{b}$ tristimulus values which match spectral test stimuli of constant radiance using the NTSC RGB System Primaries, only one of which is monochromatic. These functions may be derived from Equations 3.1.9. through 3.1.11. Compare this figure with Figure 3.1.7.

Systems, matrixing is performed at the receiver where the introduction of new phosphors can be optimized by readjusting the matrix circuits for that individual receiver. See Reference (40). In inexpensive cameras, matrixing is not used, so that the negative lobes of the $\bar{r}\bar{g}\bar{b}$ functions are simply neglected. The result is reproduction of spectral, and near spectral colors as less saturated.

3.2. The Jagadeesh System

The hue and luminance processors were designed and constructed by J. M. Jagadeesh as part of his doctoral research at The Ohio State University in 1974. The color television camera and its control unit were purchased from Panasonic, Inc. The Digital Equipment Corporation PDP-9 minicomputer and interfacing hardware are of usual design and, therefore, not described here. This system incorporates as input to the image processor a set of signals, basically derived from colorimetric quantities, that have undergone extensive transformation in order that they be capable of transmission by electromagnetic broadcasting. The Jagadeesh System uses these particular signals since they are conveniently available from even the most inexpensive color television camera. However, the quality cameras recommended in this thesis permit the use of the basic colorimetric quantities which are more easily interfaced to processing hardware. The Jagadeesh System was used in the early developmental stages of colorimetric topography to determine the practicality of generating binary maps through television image processing.

3.2.1. Constraints on Transmitted Signals

This section describes the ingenious methods by which the NTSC overcame the limitations of television transmission due to severely restricted bandwidth. The concepts of transmission are not important here, and thus, are not fully explained. The resulting signals, however, produced at the camera, must interface with the image processor, and are, therefore, developed to further understand the unique design and limitations of the Jagadeesh System.

In the camera, an electron beam is modulated by the conductivity variations of the phosphor mosaic as the beam is deflected across the face of the phosphor coated plate. As is commonly known, the beam scans the plate in horizontal lines from top to bottom and then returns to the top of the plate and scans again, this time between the former lines. This is called interlaced scanning. Each complete scan, or field, requires 1/60 second. One complete image, then, is registered in 1/30 second. The flicker produced by 30 pictures per second is unnoticeable by the eye if the luminances of the pictures are moderate. The vertical and horizontal movements of the beam are controlled by separate deflection coils. Since the beam is constantly deflected horizontally, a number of the scan lines are not interlaced properly as the beam returns from bottom to top to begin the second field. The signal modulation is, therefore, "blanked" during this time. A total of 525 lines are scanned in the 1/30 second. At normal viewing distances, these lines are just indistinguishable by the eye. Disregarding the blanking and synchronizing information carried also in 1/30 second, the highest resolution achievable in the vertical direction is 525 lines. At most, one signal modulation occurs at each crossing of the boundary formed by two adjacent lines, that is, 525/2 modulations. Now, if the horizontal resolution is to equal the vertical, the former must be produced by (525/2)4/3 modulations, since the image aspect ratio is 4:3. Therefore, each scanned line requires (525/2)4/3 modulations. The full image requires 525(525/2)4/3 modulations, for all 525 lines. These modulations must occur for each image, that is, for each 1/30 second, or (30)525(525/2)4/3 modulations per second. This would require a bandwidth of

$$(30)525(525/2)4/3 = 5,512,500 \text{ Hz},$$

or approximately 5.5 MHz. However, since scan lines are not actually immediately adjacent, the resolution is reduced slightly, so that the modulation frequency is slightly lower. But an audio signal must accompany the video, which brings the frequency requirement back to approximately 5.5 MHz. Also, the carriers available to television broadcasting, since radio was already firmly established by the late 1940's, were in the 50 MHz range. A 50 MHz carrier modulated at 5.5 MHz carries appreciable sidebands from 45 to 55 MHz. This further increases required bandwidth to 10 MHz.

The 60 Hz field frequency, the 30 Hz picture frequency, the 525 line, and other specifications resulted from the fact that only 6 MHz bandwidth could possibly be allocated to color television transmission. The NTSC developed ingenious methods by which to reduce a 10 MHz to a 6 MHz bandwidth. The methods fall into two main categories: those which take advantage of the character of visual perception, and those which directly reduce transmission bandwidth. The conservation methods of the former category are: interlaced scanning, in which a 2:1 field-to-picture ratio permits an imperceptable flicker frequency without requiring more pictures per second which would increase required bandwidth; band-saving, in which those colors, blue, and to a lesser extent, red, with which the eye perceives substantially less detail need not be transmitted with bandwidths as large as green and achormatic colors; frequency interlace, which, viewed in terms of frequency analysis, permits the harmonic components of a luminance signal to be interwoven with the harmonic components of a chrominance signal (these signals have yet to be defined).

Those methods directly conserving bandwidth are: single-sideband transmission, in which the lower sideband of harmonics of a modulated carrier are eliminated, since identical information is carried in the upper sideband; and phase modulation, by which the two components of the chrominance signal are transmitted on the same carrier but a quarter cycle out of phase with one antoher. These methods are explained in detail by most texts on color television, or in Reference (37), (40), or (45). Two of these methods are further described here so that the signal equations used in the image processor design may be derived.

The band-saving method requires that chromatic and achromatic information be differentiated. First, an "achromatic" luminance signal is derived. It was shown in the previous section that luminance of a color $\bar{S}$ can be written:

$$L_S = L_R R + L_G G + L_B B$$

Just as the tristimulus values R, G, and B were normalized to r, g, and b, the luminance factors may be normalized by:

$$L_r = \frac{L_R}{L_R + L_G + L_B}, \quad L_g = \frac{L_G}{L_R + L_G + L_B}, \quad L_b = \frac{L_B}{L_R + L_G + L_B}$$

The equation for luminance can then be rewritten:

$$Y_s = L_r R + L_g G + L_b B, \qquad 3.2.1.$$

where the normalized Y_s has replaced L_S, such that

$$L_S = (L_R + L_G + L_B) Y_s$$

The values of L_r, L_g, and L_b with respect to Standard Illuminant C may be determined. This can be done simply from the knowledge of the

chromaticities of the NTSC primaries and Illuminant C, and the fact that for Illuminant C, tristimulus values R, G, and B are equal. Equivalences are set up between the chromaticity points for the NTSC primaries and their luminances, both specified in the CIE XYZ System:

$$0.67L_R\bar{X} + 0.33L_R\bar{Y} + 0.00L_R\bar{Z} \equiv 0.67\bar{X} = 0.33\bar{Y} + 0.00\bar{Z}$$

$$0.21L_G\bar{X} + 0.71L_G\bar{Y} + 0.08L_G\bar{Z} \equiv 0.21\bar{X} + 0.71\bar{Y} + 0.08\bar{Z}$$

$$0.14L_B\bar{X} + 0.08L_B\bar{Y} + 0.78L_B\bar{Z} \equiv 0.14\bar{Z} + 0.08\bar{Y} + 0.78\bar{Z}$$

But, as explained in the previous section, the luminances of the X and Z tristimulus values are zero. Therefore:

$$0.33L_R\bar{Y} \equiv 0.67\bar{X} + 0.33\bar{Y} + 0.00\bar{Z}$$

$$0.71L_G\bar{Y} \equiv 0.21\bar{X} + 0.71\bar{Y} + 0.08\bar{Z}$$

$$0.08L_B\bar{Y} \equiv 0.14\bar{X} + 0.08\bar{Y} + 0.78\bar{Z}$$

Solving for L_R, L_G, and L_B:

$$L_R \equiv \frac{0.67}{0.33}\bar{X} + \bar{Y}$$

$$L_G \equiv \frac{0.21}{0.71}\bar{X} + \bar{Y} + \frac{0.08}{0.71}\bar{Z}$$

$$L_B \equiv \frac{0.14}{0.08}\bar{X} + \bar{Y} + \frac{0.78}{0.08}\bar{Z}$$

Now, Illuminant C may be specified by:

$$\bar{S}_C = R\bar{R} + G\bar{G} + B\bar{B}$$

But, for Illuminant C, R = G = B, so that:

$$\bar{S}_C \propto \bar{R} + \bar{G} + \bar{B}$$

In luminance terms:

$$(L_r + L_g + L_b)L_C \equiv L_rL_R + L_gL_G + L_bL_B,$$

since L_r, L_g, and L_b are proportional to L_R, L_G, and L_B. Also,

$L_r + L_g + L_b = 1$, so that:

$$L_C \equiv L_r L_R + L_g L_G + L_b L_B$$

Substituting the equivalences for L_R, L_G, and L_B into L_C, above:

$$L_C \equiv \frac{0.67}{0.33} L_r \bar{X} + L_g \bar{Y}$$
$$+ \frac{0.21}{0.71} L_g \bar{X} + L_g \bar{Y} + \frac{0.08}{0.71} L_g \bar{Z}$$
$$+ \frac{0.14}{0.08} L_b \bar{X} + L_b \bar{Y} + \frac{0.78}{0.08} L_b \bar{Z}$$

Just as the equivalences were set up for the NTSC primaries, an equivalence may be set up between the chromaticity point and the luminance of Illuminant C, whose chromaticity is x = 0.3101, y = 0.3163, and z = 0.3736:

$$0.3101 L_C \bar{X} + 0.3163 L_C \bar{Y} + 0.3736 L_C \bar{Z} \equiv 0.3101 \bar{X} + 0.3163 \bar{Y} + 0.3736 \bar{Z}$$

Again, L_x and L_z are zero; therefore, solving for L_C:

$$L_C \equiv \frac{0.3101}{0.3136} \bar{X} + \bar{Y} + \frac{0.3736}{0.3163} \bar{Z}$$

Now, equating the corresponding terms of the two equivalences for L_C:

$$\frac{0.67}{0.33} L_r + \frac{0.21}{0.71} L_g + \frac{0.14}{0.08} L_b = \frac{0.3101}{0.3163}$$

$$L_r + L_g + L_b = 1$$

$$\frac{0.08}{0.71} L_g + \frac{0.78}{0.08} L_b = \frac{0.3736}{0.3163}$$

Solving simultaneously:

$$L_r = 0.2988, \; L_g = 0.5868, \; L_b = 0.1144$$

Even though the phosphors then available, and several improvements since the time of the NTSC recommendations, do not match the chromaticities of the NTSC primaries, these values of L_r, L_g, and L_b are universally used.

The equation specifying the luminance at any point $\bar{S}$ in a scene, Equation 3.2.1., is then:

$$Y_S = 0.2988R + 0.5868G + 0.1144B \qquad 3.2.2.$$

The second scheme used to help differentiate chromatic and achromatic information in the band-saving method of bandwidth conservation is the derivation of chromaticity-difference, or chrominance, signals. Luminance information, in terms of the Y equation, could be transmitted along with any two color signals, from which the third color signal is recovered. However, it is advantageous to transmit chrominance signals in the form of R - Y and B - Y information. First, R - Y and B - Y can be transmitted at low definitions, or in small bandwidth, since the eye perceives little detail in R and less in B colors. The Y signal is then added to R - Y and B - Y to recover R and B by simple, economical, low frequency circuits at the receiver. The G signal is recovered from the Y signal, $Y = 0.2988R + 0.5868G + 0.1144B$, where R and B have been determined. Second, since for achromatic colors (white, greys, and black), $R = G = B$, and for $Y = L_rR + L_gG + L_bB$, $L_r + L_g + L_b = 1$, it follows that $Y = R = G = B$. Thus, for white, greys, and black, the chrominances, R - Y, and B - Y, are automatically zero. The actual voltages produced for Y, R - Y and B - Y may be written E_Y, $E_R - E_Y$, and $E_B - E_Y$, which are directly proportional to the colorimetric quantities, respectively.

The remaining method described here, phase modulation, directly conserves transmission bandwidth, by transmitting the two chrominance signals, $E_R - E_Y$ and $E_B - E_Y$, on the same carrier, but 45° out of phase with one another. Figure 3.2.1. is helpful in illustrating this method.

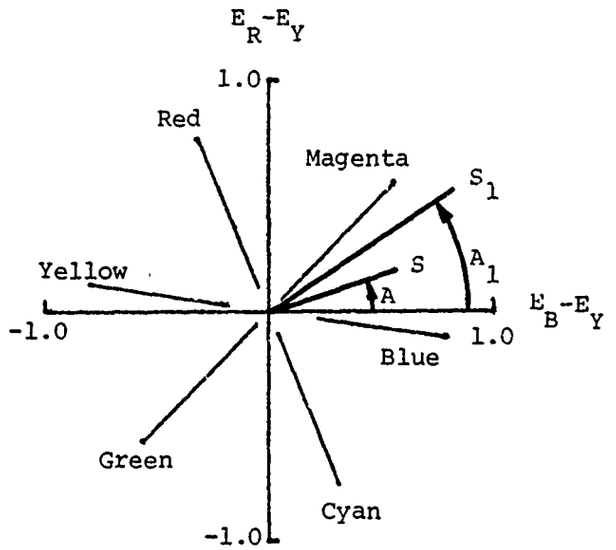

Figure 3.2.1. An amplitude-phase representation of the chromaticity difference signals showing specific hue regions and two color points S and S_1.

The hue and saturation components of chrominance are depicted in the figure by two of their quantitative descriptors, dominant wavelength and purity, which require definition. The dominant wavelength of a given color is specified on the Chromaticity Diagram by the intersection with the spectrum locus of a line formed by the chromaticity point of that color and the chromaticity point of a given neutral standard. The purity of a given color is the ratio of two lengths on the Chromaticity Diagram, the first being the distance between the chromaticity point of that color and the chromaticity point of a given neutral standard, and the second being the distance from the neutral standard point, straight through the color point, to the intersection point with the spectrum locus or purple line. Now, for a given color, the two out-of-phase modulations of a single carrier result in a single amplitude modulation at a particular phase. This amplitude is proportional to the product of luminance and purity.

The phase is proportional to dominant wavelength. In terms of Figure 3.2.1. the length OS indicates amplitude and the phase angle, A, dominant wavelength. The origin represents the chromaticity of Standard Illuminant C, regardless of luminance. Thus, with little error, point S_1 may be considered of different hue and higher saturation than point S.

The proportionality factor between phase and dominant wavelength alters the aboslute positions of the chrominance axes. Before introducing this alteration, however, a practical constraint in the standard maximum amplitude of the chrominance signals requires that they be reduced prior to transmission, to avoid overloading the transmitter. The reduction factors are 0.877 for the $E_R - E_Y$ signal and 0.493 for $E_B - E_Y$. These signal axes are plotted in Figure 3.2.1. To continue, the charominance signals are shifted off the 0.877 ($E_R - E_Y$) and 0.493 ($E_B - E_Y$) axes by 33°. The choice of 33° is interesting. It was the desire of the NTSC that when image detail reached such fineness that the $E_B - E_Y$ signal was no longer significant, the color range remaining be parallel to the orange to blue-green direction. Practical tests confirmed that these particular color contrast permitted maximum resolution to be visually perceived. These shifted axes in Figure 3.2.2. were called the E_I signal, or In Phase component of the carrier, and the E_Q signal, or the Quadrature component of the carrier. By the usual rotaion of axes transformation, the two sets of axes are related as follows:

$$E_I = 0.877(E_R - E_Y)\cos 33^\circ - 0.493(E_B - E_Y)\sin 33^\circ$$

$$E_Q = 0.877(E_R - E_Y)\sin 33^\circ - 0.493(E_B - E_Y)\cos 33^\circ,$$

or

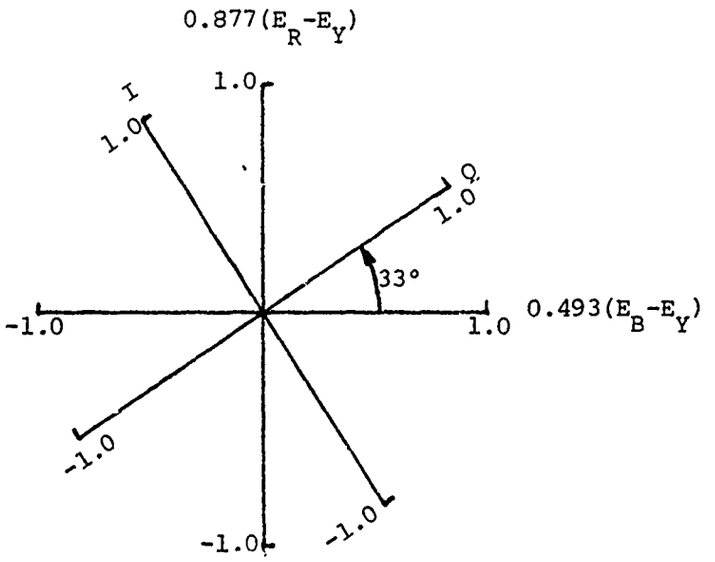

Figure 3.2.2. An amplitude-phase representation of the chromaticity difference signals where the axes have been rescaled to account for the practical transmission constraints. Also shown are the chrominance axes which are shifted by 33° to account for the proportionality factor between the phase and dominant wavelength.

$$E_I = 0.736(E_R - E_Y) - 0.268(E_B - E_Y)$$
$$E_Q = 0.478(E_R - E_Y) - 0.413(E_B - E_Y) \qquad 3.2.3.$$

The total NTSC signal transmitted, E_M, then, combines the luminance and chrominance signals, which are frequency interlaced, and the components of the chrominance signals, which are phase modulated, as follows:

$$E_M = E_Y + E_Q \sin(wt + 33^\circ) + E_I \cos(wt + 33^\circ), \qquad 3.2.4.$$

where

$$E_Y = 0.2988E_R + 0.5868E_G + 0.1144E_B$$
$$E_Q = 0.478(E_R - E_Y) - 0.413(E_B - E_Y)$$
$$E_I = 0.736(E_R - E_Y) - 0.268(E_B - E_Y)$$

These equations are used in the design of the image processors, described in the next sections.

In summary, Section 3.1. and 3.2. have described tristimulus color-matching theory and the means by which it was transformed into the internationally accpeted CIE Standards of Colorimetry. The CIE Standard was described in such detail that the signal equations of color television theory could be conveniently derived, and the limitations of color television reproduction understood. Finally, the restrictions of color television transmission were explained, since the signals representing straightforward colorimetric quantities of a scene are transformed into obscured "transmission primaries" with which the image processor must deal.

3.2.2. Luminance Processor Design Model

This section describes briefly how colorimetric theory is applied in the luminance processor. Detailed hardware design is presented in Chapter IV of Reference (29).

It has been shown that luminance is a linear combination of tristimulus values, Equation 3.2.1.:

$$Y = L_r R + L_g G + L_b B$$

where L_r, L_g, $L_b > 0$. Now a binary function, L(x,y), is defined for any x and y such that:

$$L = 1 \quad \text{iff } Y > Y_{thr}$$

$$= 0 \quad \text{otherwise,}$$

where Y_{thr} is the preset luminance threshold. Y is proportional to the signal E_y, so that:

$$L = 1 \quad \text{iff } E_Y > E_{Y_{thr}}$$

$$= 0 \quad \text{otherwise.}$$

$E_{Y_{thr}}$ may be set under computer control, see Chapter IV of Reference (29). This function, L(x,y), is generated by the luminance processor and stored in computer memory for manipulation or printout.

The absolute luminance of a scene presented to the camera may produce a voltage below the minimum preset under computer program control. The computer algorithm, see Chapter V of Reference (29), initializes at zero the voltage produced by the luminance circuit. When the scene produces a voltage below this level, negative values for luminance cannot be handled by the program algorithm. But the circuit voltage may be set to a lower minimum by adjustment of the 5K ohm variable resistor of the luminance circuit. This adjustment will enable the program luminance scale, from 0 to 255, to be matched to the actual scene and camera signals.

3.2.3. Hue Processor Design Model

In Section 3.1.2., approximately constant hue planes in the RGB space were introduced. The equations of these planes may be written as follows:

$$h_r R + h_g G + h_b B = 0 \qquad 3.2.5.$$

where h_r, h_g, and h_b may be positive or negative tristimulus specifications. Now, from the scene image, a binary hue function, h(x,y), may be defined as follows:

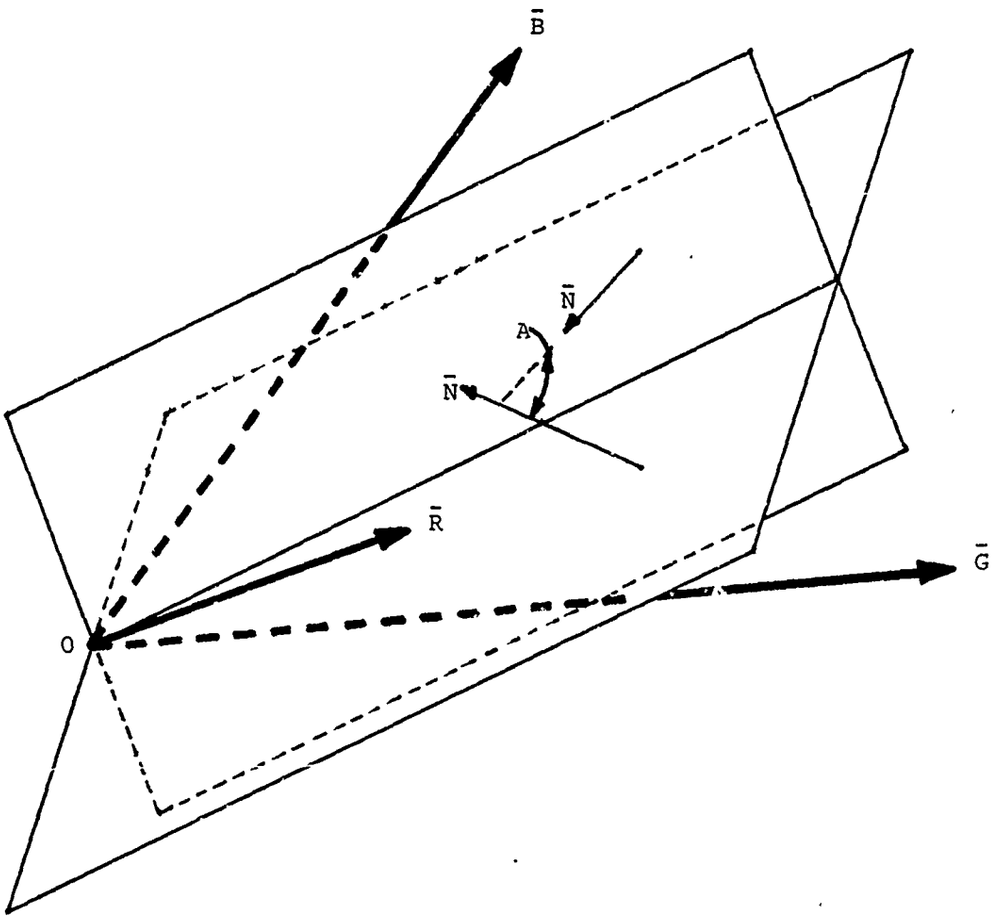

Figure 3.2.3. Two isohue planes in RGB space showing the angle A between the normal vectors of the planes.

$$h = 1 \quad \text{iff } h_{1r}R + h_{1g}G + h_{1b}B < 0 \text{ and}$$
$$h_{2r}R + h_{2g}G + h_{2b}B > 0 \qquad 3.2.6.$$
$$= 0 \quad \text{otherwise.}$$

These conditions actually define a binary hue range, the bounding planes of which are shown in Figure 3.2.3. The angle between the normals of the two isohue planes is given by:

$$\cos A = \frac{h_{1r}h_{2r} + h_{1g}h_{2g} + h_{1b}h_{2b}}{[(h_{1r}^2 + h_{1g}^2 + h_{1b}^2)(h_{2r}^2 + h_{2g}^2 + h_{2b}^2)]^{1/2}} \qquad 3.2.7.$$

Now, referring back to the television camera signals, and substituting Equations 3.2.3. into Equation 3.2.4., where the bandwidth of E_I is limited to 500 kHz:

$$E_M = E_Y + 0.493(E_B - E_Y)\sin wt + 0.877(E_R - E_Y)\cos wt \qquad 3.2.8.$$

Now consider the relation

$$\frac{0.877(E_R - E_Y)}{0.493(E_B - E_Y)} = \tan A \qquad 3.2.9.$$

Substituting for E_Y, from the signal equivalent of Equation 3.2.2., into Equation 3.2.9.:

$$h_R E_R + h_G E_G + h_B E_B = 0 \qquad 3.2.10.$$

where

$$\begin{aligned} h_R &= (\ 1.247 + 0.299\tan A) \\ h_G &= (-1.066 + 0.599\tan A) \qquad 3.2.11. \\ h_B &= (-0.203 - 0.866\tan A) \end{aligned}$$

Assuming the constants of proportionality between E_R, E_G, and E_B and R, G, and B are identical, Equation 3.2.10. is also an equation of iso-hue planes.

Equation 3.2.9., then, may be represented by the plot of Figure 2.2.2. This plot is repeated in Figure 3.2.4. showing a point S_R representing a saturated red color with $E_R = 1$, and $E_B = E_G = 0$. The coordir tes of this point are

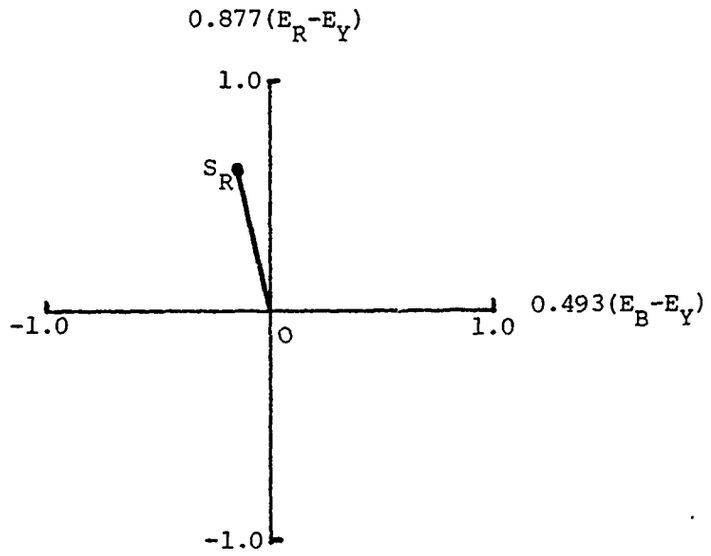

Figure 3.2.4. The point S_R depicting a "red" color on the amplitude-phase chrominance diagram.

$$0.493(E_B - E_Y) = -0.147$$

$$\text{and } 0.877(E_R - E_Y) = 0.615$$

where $E_Y = 0.2988(1.0) + 0.5868(0.0) + 0.1144(0.0) = 0.2988$. Thus for any $E_R = c_1 + c_2$ and $E_B = E_G = c_2$, where

$$0 \leq c_1 + c_2 \leq 1$$

$$0 \leq c_1 \leq 1$$

$$0 \leq c_2 \leq 1$$

it follows that,

$$\frac{0.877(E_R - E_Y)}{0.493(E_B - E_Y)} = \frac{0.877(\ 0.7012c_1)}{0.493(-0.2988c_1)} = -4.175$$

This represents the loci of all points on line OS_R. Thus, all colors of this particular red fall on line OS_R. Similar lines may be constructed in Figure 3.2.4. for all colors.

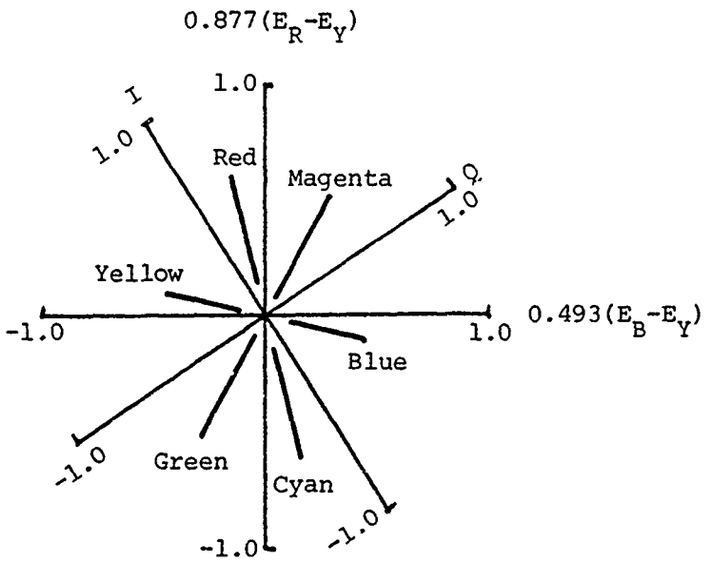

Figure 3.2.5. The complete amplitude-phase chrominance diagram showing the chrominance axes' shift and scaling and the shifted primary color lines with points of full saturation (purity) indicated.

Consider the chrominance portion of the complete NTSC transmitted signal, Equation 3.2.4.:

$$E_{M_C} = 0.493(E_B - E_Y)\sin wt + 0.877(E_R - E_Y)\cos wt \qquad 3.1.12.$$
$$= \{[0.493(E_B - E_Y)]^2 + [0.877(E_R - E_Y)]\}^{1/2} \sin(wt + \emptyset)$$

where

$$\tan \emptyset = \frac{0.877(E_R - E_Y)}{0.493(E_B - E_Y)} \qquad 3.1.13.$$

Equations 3.2.13. and 3.2.9. are equivalent, indicating that the chrominance signals' phase difference represents hue to a first approximation. Figure 3.2.5. shows the chrominance signal and shifted I, Q axes, with the primary and complementary color lines and full saturation points indicated. The definition of the binary hue function, Equation 3.2.4.,

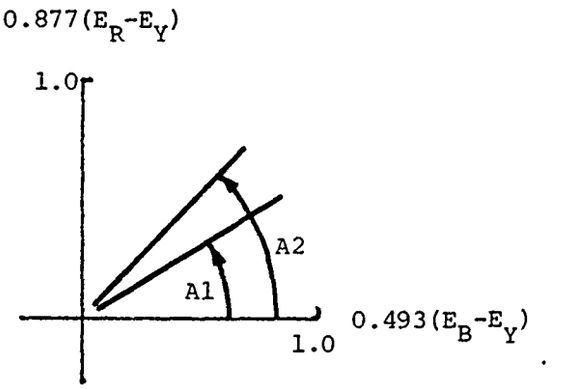

Figure 3.2.6. Chrominance diagram representation of the angles of two isohue planes.

can be rewritten in terms of color television camera signals as follows:

$$h = 1 \quad \text{iff} \quad \tan A1 < \frac{0.877(E_R - E_Y)}{0.493(E_B - E_Y)} < \tan A2 \qquad 3.2.14.$$

$$= 0 \quad \text{otherwise}$$

To obtain the angle between two isohue planes in terms of A1 and A2, substitute Equations 3.2.11. into Equation 3.2.7.:

$$\cos A = \qquad 3.2.15.$$

$$\frac{1 - 0.0231(\tan A1 + \tan A2) + 0.4177(\tan A1)(\tan A2)}{[(1 - 0.0462\tan A1 + 0.4177\tan^2 A1)]^{1/2}[(1 - 0.0462\tan A2 + 0.4177\tan^2 A2)]^{1/2}}$$

Note that Equation 3.2.14. cannot represent all colors of Equation 3.2.6. But Equation 3.2.14. can operate on all colors possibly reproduced by the television camera. The camera is, of course, limited in the luminance range it can reproduce. Equation 3.2.14. can be represented graphically by Figure 3.2.6. The angles A1 and A2 are the parameters which specify the initial and final values of a chosen color range, and are used directly by the algorithm in the Jagadeesh System.

CHAPTER IV

4.0 Introduction: Specimen and Photographic Considerations

The first of the two sections which follow describes the procedure developed for fixation and staining of the biological specimen used to exemplify the quantification methods developed in this thesis. For convenience, the animal chosen was the rabbit and the specimen was the thoracic aorta including the eight intercostal ostia. A step-by-step protocol for the procedure appears as Appendix E. The purpose of this section is to describe and justify this procedure. It should be understood that each species and each anatomical location may require the optimization of general fixing and staining procedures. The primary requisite is that working procedures be standardized.

The second section of this chapter describes the procedure developed to record the specimen image photographically so that it may be interfaced with computing and image processing facilities. Much of the justification for this procedure is found in Section 1.1. of this thesis Again, a step-by-step protocol is presented as Appendix F.

4.1. Specimen Preparation and Staining Methods

The procedure that follows was developed by an associate of the author, Dr. Murina Levesque, at The Ohio State University (46). The method applies only to the rabbit aorta. Advantages of the method are speed, simplicity, and repeatability. Since the thrust of this investigation is development of the technique of colorimetric topography, the epidemiologic factors of the animals' backgrounds are not important here.

In future application of this technique; however, it is the correlation between these factors and the results of colorimetric topography that will be sought.

Prior to sacrifice with pentobarbitol sodium, the rabbit is heparinized to prevent subsequent coagulation of the blood, and thereby, facilitating easier cleaning of the excised specimen. Immediately after sacrifice the heart is exposed to allow cannulation of the left ventricle as an input port for clearing and fixing fluids. The right iliac artery is then exposed and cannulated as the output port. This allows the entire aortic path to be cleared and fixed in situ at physiological pressure. Fixation at physiological pressure is necessary to reduce dimensional distortion of the specimen as it is opened along the ventral aspect and flattened for photography. The fixative is a 4% solution of formaldehyde which is volume perfused through the aortic pathway. After excision, opening, and cleaning of the fixed specimen it is rinsed in 70% ethanol and stained in Sudan IV. After another ethanol rinse, the specimen is stored in 4% formaldehyde until photographed. See Appendix E for exact preparation and staining procedures. The method of stain differentiation was developed experimentally to produce well-defined, healthy background tissue (2).

4.1.1. Non-Stained Specimens and Other Stains

An imaging system is capable of preprocessing on hues other than the characteristic red of Sudan IV stained lipids. The yellow cast always associated with lipid deposits and the uptake of Evans Blue with permeable proteins, which has been shown to follow endothelial damage

and precede lesion development (47), suggest two additional colors on which to preprocess. It was shown in Chapter III that the NTSC signal, employed in the Jagadeesh System, allots severely restricted bandwidth to blue so that the signal-to-noise ratio in the hue processor for blue hues is poor and very precise preprocessing on blue would be impossible. As will be discussed in Chapter VI, however, the NTSC signal is bypassed in other television image hardware designs so that the original RGB signals are used by the luminance and hue processors. This arrangement eliminates the NTSC conversion and associated electronics, and thereby produces signal-to-noise ratios equivalent for all preprocessed hues.

4.2. Specimen Photography

The staining procedure just described is restricted to the rabbit aorta. The photographic procedure, on the other hand, is quite general, and, except for the actual subject matter photographed, applies equally well to all species and anatomical locations. The general protocol, with reference to the rabbit descending thoracic aorta as subject matter, is presented in Appendix F. This procedure has been optimized to interface with television image processing systems. This section then explains the choices made for the lighting and film, calibration references, and the principles of partitioning and landmark selection.

4.2.1. Lighting and Film

The specimen must be photographed under repeatable conditions. These conditions must therefore be controlled. The most easily controlled conditions occur under artificial lighting with a color-matched film.

Tungsten photoflood lighting has become a standard for "still-life" photography, and lamps and film are readily available. Though a photoflood lamp releasing energy correlated to a Plankian radiator at 3400°K is standard, a "daylight" or "blue" photoflood, correlated to 5500°K, is suitable if the film's spectral sensitivity character matches the spectral emission distribution of that lamp. This is the case with the daylight photoflood and daylight balanced film. The only criteria, then, is that illumination on the subject be precise and controllable and match the spectral sensitivity of the film. Once this requirement is satisfied, availability, processing ease, and simplicity of use may be considered.

These latter considerations suggest that the 35 mm format be used since this format is by far the most widely used by serious amateur and professional photographers. Film, cameras, and accessories are standardized and readily available. This format also interfaces well with image processing systems.

4.2.2. Calibration References

This is a most important concept in colorimetric topography. For data, in terms of specimen photographs, to be analyzed at a central computing facility, it must take on some standard form or be convertible to a standard form. The protocols for specimen preparation and staining, and photography, Appendixes E and F, lead the way in producing standardized data which incorporates all required information. But several variables involved in producing this data cannot be standardized, or can be only with much effort and expense. Therefore, the calibration

procedures, explained next, were developed to minimize uncontrollable variation and convert existing conditions to standardized conditions at minimum expense.

The calibration procedure assures proper exposure of the chosen film by the scene of the specimen. To understand this procedure, one must appreciate the design model which relates a meter's response to scene illumination to the film's response to that scene. The vast majority of photographic meters integrate the illumination they sense over the surface area they include in that measurement. In this way, they present one number, indicative of the entire scene, on which to base exposure of the film. The assumption made in meter design is that the scene consists of equal areas of light and dark objects, or bright and dim light sources; that is, the scene contains all grey values equally stepped from white to black. This "grey scale" always reflects 18% of the incident illumination. Thus, a meter, measuring illumination reflected from the scene, assumes that a completely white scene reflects 18% of the incident illumination and that a completely black scene reflects 18% of the incident illumination. Both conclusions are, of course, incorrect. Furthermore, a meter, measuring illumination incident upon a scene, assumes that the scene, whether it be completely white, black, or whatever, reflects 18% of the illumination incident on the meter's sensor. As a result, two photographs, both exposed as indicated by metering, one of a completely white and the other of a completely black surface, appear identical, that is both are an 18% reflectance grey. Obviously, both photographs are improperly exposed. Absolutely proper exposure is indicated by a meter when the scene is an equally stepped,

black to white, grey scale. Thus, the calibration procedure developed in this thesis requires exposure of a grey scale. These exposures are bracketed to ± 3 f-stops centered at the meter-indicated exposure. The processed photographs are then judged to determine that one which is "properly" exposed. The properly exposed photograph is the meter-indicated exposure only if the meter accurately integrates to the 18% reflectance standard. Otherwise, a different photograph is judged to be properly exposed and the meter-indicated exposure must receive a correction factor in all subsequent exposure readings. The protocol for this procedure constitutes Appendix F.

The explanation of a "properly" exposed grey scale is in order. When an equally stepped, black to white, grey scale is properly exposed, the photograph of all grey level values integrates to the 18% reflectance standard, and the central grey level step in the scale actually reflects (or transmits, in the case of a transparency) 18% of the incident illumination. A densitometer is used to verify this fact. The densitometric reading, furthermore, can be used to indicate the exposure correction required for an improperly exposed photograph. However, the densitometer is an expensive tool, rarely found in a biomedical research laboratory. The grey scale is, itself, a photometric tool, but quite inexpensive and readily available. In combination with a camera and exposure meter, the grey scale is a powerful tool. To interpret the wealth of information it carries, one must not only appreciate the design of the meter but also the response of the film.

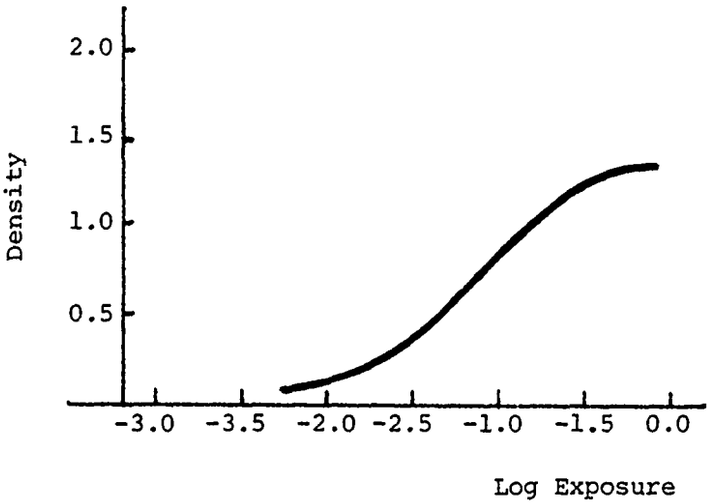

Figure 4.2.1. Characteristic curve for typical negative black and white film.

Generally, the response of a negative film to various illumination levels is linear only for moderate values. At the extreme illumination levels in a given range the film response is nonlinear, as shown in Figure 4.2.1. This figure shows the "characteristic curve" of a typical negative film, indicating the linear and nonlinear relationships between the film optical density and the log exposure producing that density. It is obvious that densities on the linear portion of the curve maintain the relative brightness relationship in the scene. The linear portion of the curve, therefore, faithfully reproduces the actual scene, except for contrast indicated by the linear slope. This is further discussed later. The relative brightness relationship is not maintained by the lower nonlinear portion, or toe, and the upper nonlinear portion, or shoulder, of the curve, corresponding to low and high levels of illumination, respectively. The decreasing slopes of these regions cause low illumination levels to merge into a single, low density and high levels

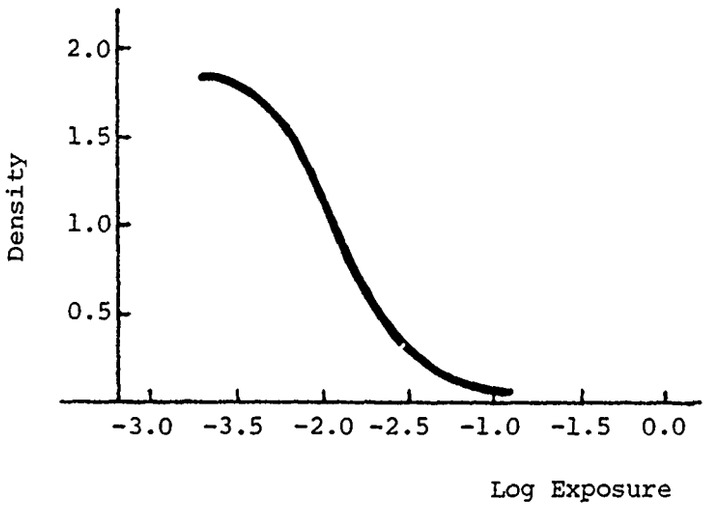

Figure 4.2.2. Characteristic curve for typical reversal, or positive, color film.

into a single, high density. Information is thereby lost. For faithful reproduction, then, the entire brightness range in the scene must fall on the linear portion of the film's characteristic curve. With this background, the protocol's grey scale calibration procedure is easily understood. The meter must be calibrated so as to indicate the exposure that places the central portion of the grey scale at the center of the linear portion of the characteristic curve. If the film's character has a much narrower log exposure range beneath the linear portion of the curve, the whitest portions and blackest portions of the grey scale may merge, but this will only simplify the choice of the photograph that places the central grey scale region at the center of the linear portion of the curve. If several photographs of the bracketed sequence reproduce the entire grey scale faithfully, the middle photograph is "properly" exposed. However, this slight difficulty should not arise in practice since the linear portion of the curve is much narrower in color reversal

film than in negative film. This is shown in Figure 4.2.2.

The matter of contrast warrants discussion. The greater the slope of the linear portion of the curve the greater is the film's contrast character. Accurate reproduction occurs at a contrast indicated by a density/log exposure slope of 1.00. The contrast of the transparency analyzed by the image processor can be increased or decreased electronically by decreasing or increasing the scale of the range of luminance thresholds preset for processing (see Sections 2.2.2. and 3.2.). To do this, the actual contrast of the transparency must be known or be capable of determination. This is the purpose of the first calibration photograph required by the protocol. This and the remaining two calibration photographs are now discussed.

The first calibration photograph of the standard grey scale is analyzed to determine the darkest and lightest greys linearly reproduced for the given film and emulsion number. These two grey levels, regardless of the range they define, are assigned the minimum (zero) and maximum preset luminance thresholds, respectively. The number of thresholds from zero to maximum is constant. The only assumption made is that the relative optical density ranges of all films processed are very similar. This is indeed the case for all but those special purpose films which use the protocol prohibits. For example, the characteristic curves of films A and B of Figure 4.2.3. differ in contrast, but are similar in relative optical density range. This first calibration photograph, then, is used to eliminate contrast variation in the various films processed. Note that contrast may differ among films from different manufacturers and among films of different emulsion number from the same manufacturer.

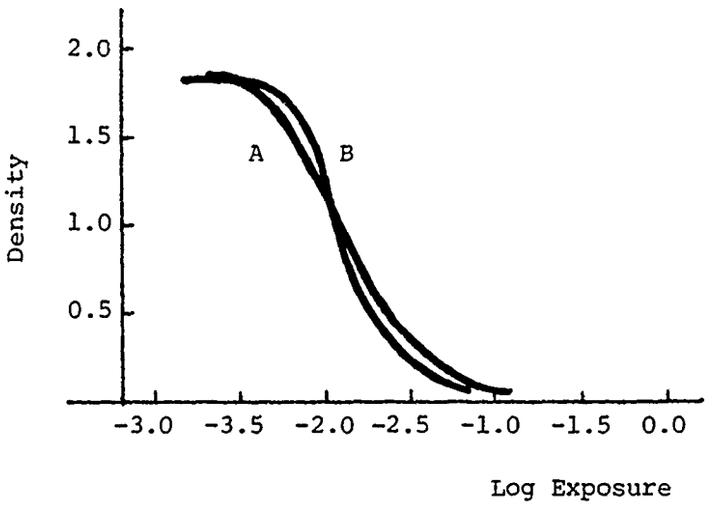

Figure 4.2.3. Characteristic curves for two films of differing contrast characters.

The second calibration photograph is of the 18% reflectance neutral grey test card. The purpose of photographing this plain, uniform field is for a convenient future application of colorimetric topography. Any spatial variation in the incident illumination for specimen photography, due to poor quality, or perhaps dented, reflectors for the photofloods, or improper lamp positioning, will be apparant on an otherwise uniform field. The slide of this field is used to perform a grey level correction for non-uniform illumination at the subject plane. Each point (x,y) of f(x,y) (see Section 2.2.) may exhibit a luminance differing from adjacent points. When the photograph is of a uniform field, this variation is, of course, undesirable. Therefore, all pixels may be corrected by respective factors to bring all pixels to the same luminance. The factor for each pixel is stored in computer memory and then applied to all specimen scenes which were photographed using the identical non-uniform illuminating field. In this way, the individual investigator who performs

the specimen photography need not be overly concerned with making the field uniform. Gross shadows or hot spots must, of course, be eliminated at the time of photographing. In this way, a specific region of the specimen analyzed by colorimetric topography will not be falsely interpreted as above (or below) a specific luminance threshold, due to a hot spot (or shadow) in the incident illumination.

The final calibration photograph, like the second, need be taken only when the photographic setup is altered (see Appendix F). This photograph is of a 1 cm by 1 cm white patch with the 18% reflectance surface as background. As this slide is analyzed at O.S.U., a luminance threshold will be chosen for which only this patch is above threshold, that is, only those pixels of f(x,y) which define the white patch assume the binary value of 1. All other pixels in the scene are 0. The ratio, then, of 1.00 cm^2 to the number of pixels above threshold gives the area occupied per pixel. This scale factor permits highly accurate specimen areas to be determined. Also, since the pixel aspect ratio is known, highly accurate specimen dimensions may be determined.

4.2.3. Partitioning and Landmark Selction

A photograph of the entire specimen under study could be analyzed. The prepared aorta, for example, whose aspect ratio might range from 1:30 to 1:10, would yield a photograph which must be analyzed on the standard vidicon with an aspect ratio of 3:4. Even "fitting" the aortic image into the vidicon field diagonally, only about 7 to 21% of the available pixels comprise the aortic image. The smaller the area-to-pixel ratio discussed in the previous section, the greater is the resolution

at which the analysis can be made. Therefore, a smaller, frame-filling region of the aorta, called a partition, is photographed. Of course, several partitions need be taken in order that the entire specimen be analyzed. The specific region of the specimen enclosed in one partition is standardized; the partitioning of the rabbit descending thoracic aorta is detailed in Appendix F. In general, partition selection depends upon the species and anatomical location.

As the partition is analyzed by computer image processing, the pixels comprising the partition are stored as an array. In the final graphical representation of the specimen, these partitions must be reunited. Adjacent partitions are united by bringing certain points, which lie on the adjacent edges of those partitions, and are common to both partitions, into coincidence. When these common points are registered, the common boundary between the two partitions disappears. This process is repeated until the entire specimen is restored. These common points, which are simply elements of a continuous array forming the entire specimen, are not arbitrarily chosen, but are the coordinates of "landmarks" which appear both on the specimen itself and its binary mapping. Typically, a landmark is a specified ostium on the image of the prepared specimen. As outlined in Appendix F, the third, fifth, and seventh pairs of intercostal ostia define the common landmarks in the rabbit descending thoracic aorta. The first intercostal ostial pair and the eighth ostial pair define terminal landmarks, since only the descending thoracic aorta is investigated here, and these ostia terminate this region of the aorta. In general, landmarks are selected so that the partition they enclose assumes a 3:4 aspect ratio. Partitioning and the use of landmarks as registration

indices are further discussed in Chapter V.

CHAPTER V

5.0 Introduction: Software Development

As mentioned in previous chapters, the output of the Jagadeesh and other television image processing systems is a digitized planar map of the original scene. The map is stored in computer memory as a two dimensional array. In colorimetric topography, the value of an array element, is attributed to the luminance of the corresponding pixel in the image. To economize memory requirements, the range of luminance values in a single map is not continuous: indeed, a dichotomy is established by encoding each array element as above or below a given luminance, called a threshold. The resulting dichotomous array is referred to as a binary map. Of course, to completely specify an image whose pixels may assume any of numerous (approx. fifty) digitized luminance values, several binary maps, each dichotomous about a different luminance threshold, must be produced by the processor. As these binary maps are overlaid in proper registration, a three dimensional representation of the image is built; the dimensions in the horizontal plane being the length and width of the image, and the vertical dimension representing luminance.

An image processing system can not only digitize an image by thresholding on luminance, but can also initially preprocess the image on hue so that only a specific color of interest is thresholded. As explained in Chapters II and III, uninteresting colors remain at zero luminance throughout the subsequent thresholding process.

In this case, the vertical dimension, of a three dimensional representation of the image, represents the saturation of the interesting color, since luminance of a monochromatic image is synonomous with saturation, though they are inversely proportional.

Therefore, the "topography" of the image is not spatial, but "colorimetric" in the vertical dimension. For the image of an arterial specimen prepared to exhibit sudanophilia, colorimetric topography produces a topographical map which depicts saturation of Sudan IV for any given point along the length and width of the specimen. In this way, diseased tissue is differentiated from healthy tissue by degree of staining, with accurate location information retained.

The purpose of this chapter is to explain the methods by which preliminary but fundamental binary maps are processed to produce the final colorimetrically topographical map to be used for pathological interpretation. To generalize the binary map produced by the television image processor, simulated maps were generated manually from known specimen images of rabbit descending thoracic aortae, prepared according to Protocol, Appendix E. Sudanophilia were defined at increasing luminance thresholds as rectangular areas on the specimen; this permitted the effects of subsequent transformation to be easily grasped visually, and also proved convenient in construction of the simulated data files. Three luminance thresholds were simulated to correspond to zero, forty, and eighty percent levels of maximum luminance. The aortae were partitioned as required by the Protocol,

Appendix F. Presented, then, for computer processing were five complete images, each of a different aortic specimen, each divided into four partitions, and each mapped at the zero, forty, and eighty percent luminance levels.

This chapter explains in detail the sequence of major processing steps applied to the digitized specimen image. First, the zero luminance binary maps of the four partitions of a given specimen are printed. After preparation, these four binary maps are concatenated to restore the complete image at, of course, only the zero luminance level. This procedure is described in Section 5.1. Second, this concatenated binary map is transformed geometrically into the "standard specimen", the procedure for which is described in Section 5.2. Third, this binary standard specimen is overlaid by a grid which is required by the computer algorithm to produce a contour map. Fourth, steps one, two, and three are repeated for the 40% and 80% luminance level binary maps. Fifth, the three contour maps are overlaid in proper registration to build the graphics of colorimetric topography. These graphics take the forms of a multi-level contour map and a three dimensional plot. Steps three, four, and five are described in Section 5.3. Sixth, steps one through five are repeated for the four remaining specimens. Lastly, the ten resulting graphs, five graphs for each of 2 graphic forms, are manipulated to produce statistically meaningful information. The sixth and last steps are described in Section 5.4.

5.1 Restoration of Specimen Image

The photographic protocol requires that the complete specimen be photographed by overlapping partitions. The purpose of this procedure is to optimize the number of artery pixels in a vidicon field with an aspect ratio of 3:4 (see Section 4.2.3.). Since each partition has an aspect ratio of about 3:5, much more efficient use is made of the vidicon field. Partitioned image processing, thus greatly increases resolution, or number of pixels per unit area. However, since a single partition is not of interest here, these four overlapping partitions must be reunited with overlap eliminated. Furthermore, since the partitions are photographed by the investigator with a manual copy stand arrangement, some misalignment of the specimen image with respect to the photographic boundaries of each partition will occur. This misalignment must be corrected. The restoration schemes described in this section solve these problems.

Throughout Sections 5.1., 5.2., and 5.3.1., the discussion centers on the processing of a single luminance level, or one complete binary map. This is due to the fact that once one partition, in terms of a photographic transparency, is projected onto the camera vidicon, all pixels maintain the same array locations in computer memory; that is, there is no relative movement between the transparency and the vidicon. (This is insured in work with the Jagadeesh and other systems by securely mounting the transparency projector and the television camera on a rigid optical bench.) Since thresholding is performed electronically, exact physical alignment is maintained throughout this process. As the second

transparency (partition) replaces the first in the projector, a new set of conditions exists, but, again, are maintained for the second partition throughout the thresholding process. In this way, any given ostium on the specimen partition forms a landmark, whose array location has the same coordinates in all thresholded binary maps for that partition. These landmarks are used to exactly and precisely register the thresholded binary maps and their standard transformation to produce the final graphs. In addition, the ostial landmarks have three further important functions: to permit truncation of partition overlap regions, to permit concatenation of partitions, and to form transformation vertices. These functions are covered in Section 5.2. and 5.3.; the next section discusses the procedure for landmark specification.

5.1.1. Landmark Specification

The number of pixels per unit area generally depends upon the lines per field and horizontal sampling frequency of the camera vidicon. Consider a 500 X 500 vidicon pixel array, somewhat larger than most consumer oriented televisions. Assuming that a partition consisting of a region containing three ostial pairs nearly fills the vidicon area, an ostium of 1-2 mm diameter would be comprised of from 400 to 1600 pixels. Human interaction with the computer is required at this point to reduce 1000 pixel ostia to a single pixel landmark. The pixel chosen is the visual center of the small ostial field. The landmark is defined by the coordinates of that pixel. If interactive processing is not possible the partition could be printed in the form of

its binary map at a luminance threshold where the ostia (and black background of the artery photograph) are below threshold and encoded as a field of zeros. Scales on the printed graph are then used to determine the coordinates of the chosen landmark pixel.

The resolution of the simulated binary maps presented in this thesis results in a ostial field of three to eight pixels for simplicity of data file construction. The pixels chosen as landmarks in this case were consistently either the central or the right lateral and distal pixel of the ostial field. As the number of pixels per ostial field increases the error in determination of the landmark becomes insignificant. The accuracy of the presentation here is sufficient to confirm the applicability of colorimetric topography. The partitions used here have array dimensions of 80 X 120 pixels which conforms to the aspect ratio of the 35 mm transparency, that is, 24 X 36 mm. Figure 5.1.1. shows a typical binary map of a partition used here at a luminance threshold of 0% of maximum. (See Section 3.2.2.) All pixels above that threshold are encoded as ones and below as zeros. Note that the ostial fields of zeros have been chosen interactively and encoded as 2's for clarity.

5.1.2. Truncation at Terminal and Concatenate Ostial Landmarks

The region under study here is the rabbit descending thoracic aorta, from the first to the eighth intercostal ostia. Figure 5.1.2. shows the photographic partitioning of this region. As mentioned

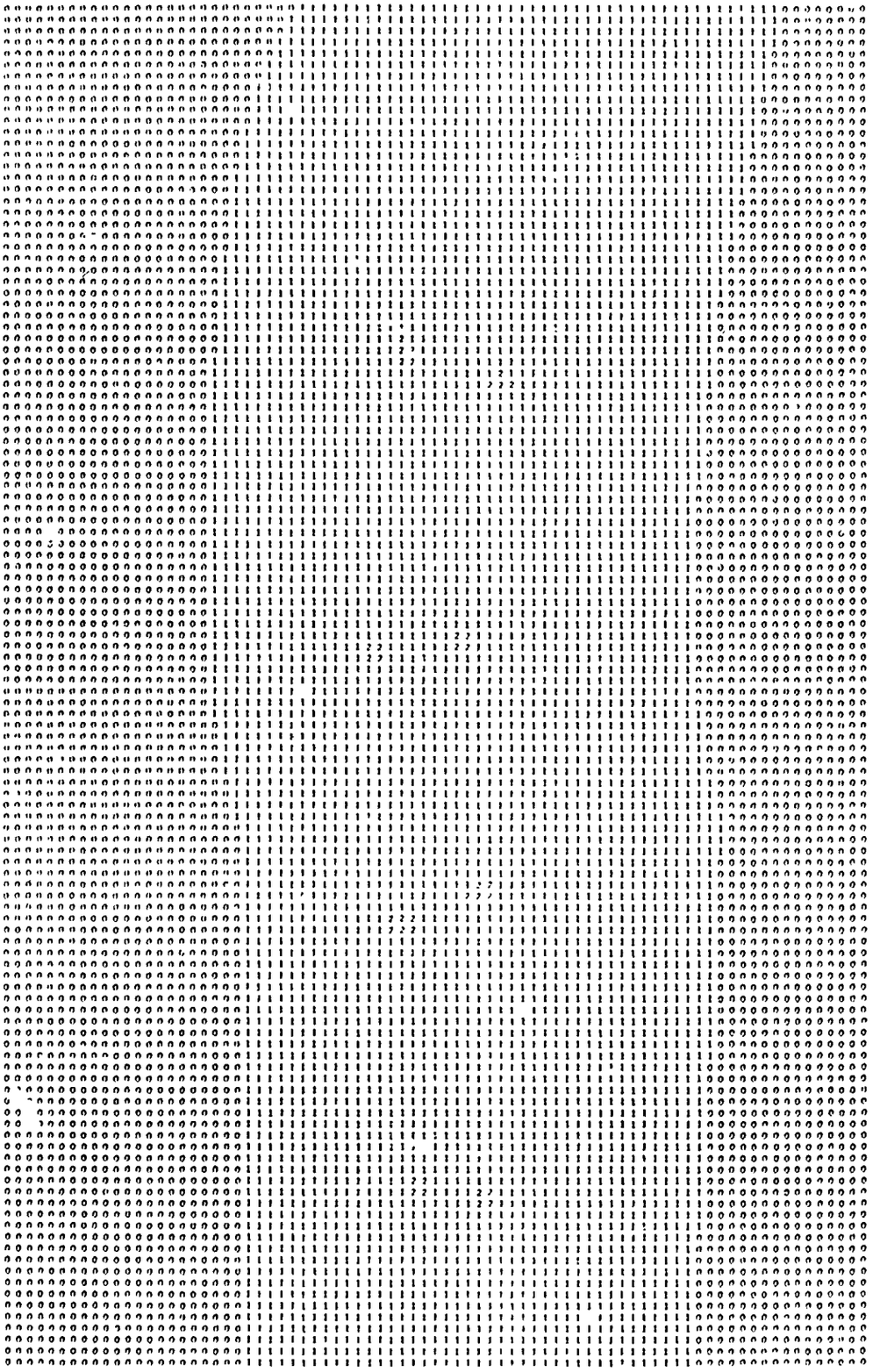

Figure 5.1.1. Typical binary map at minimum luminance threshold.

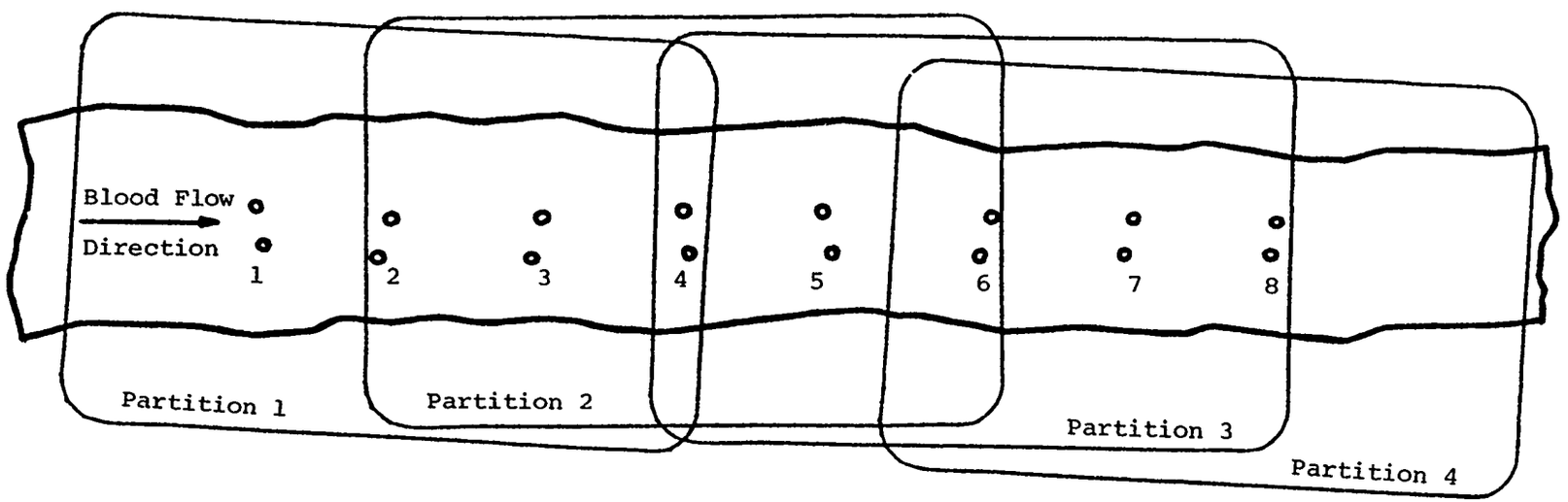

Figure 5.1.2. Photographic partitioning of the rabbit descending thoracic aorta. Numbered are the intercostal ostia pairs 1 through 8.

earlier, the overlapping and/or terminal regions of these partitions must be eliminated to permit concatenation of the partitions. To show how this is performed, the truncation procedure is applied to Partition 1 of Figure 5.1.2. Note that ostial pairs one and eight are terminal ostia since concatenation is not required at these junctions. Partition 1 is represented by its 0% luminance binary map in Figure 5.1.3. Since Partition 1 is defined by ostial pairs 1 and 3, truncation must be applied at these pairs. First, specify the landmarks for ostia pair 1. These landmarks, or more correctly, their coordinates determine a line, which is represented by the upper solid line in the Figure. All pixels above this line are nullified (assigned a value of zero). Similarly, specify the landmarks for ostial pair 2, and nullify all pixels below the line so determined. The computer algorithm for this procedure nullifies a given pixel when, for a specified x value, the y value of the given pixel is less than the y value which lies on the upper truncation line, and similarly, when the y value of the given pixel is greater than the y value which lies on the lower truncation line. Note the origin and direction of the x-y coordinate axes in the upper left of the Figure. As a result of this procedure, those pixels on and between the upper and lower truncation lines remain unchanged. The computer program which produces and stores this new data file is listed in Appendix A . The process is repeated on the first luminance level binary map of the remaining three partitions of specimen image A, then applied to remaining binary maps of the partitions of specimen image A, and finally applied similarly to specimen images B, C, D, and E.

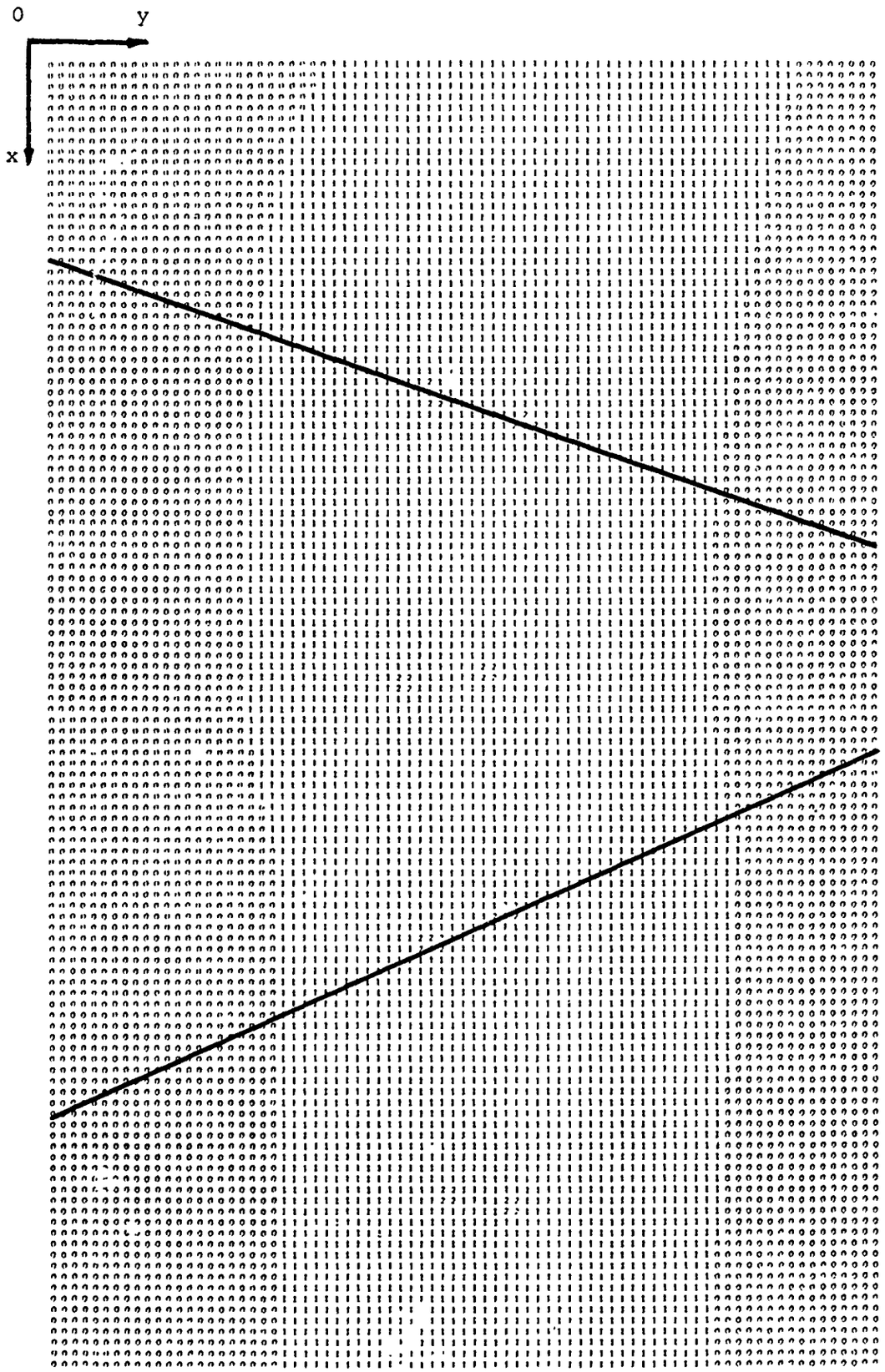

Figure 5.1.3. Typical binary map showing truncation at landmarks.

5.1.3. Translation and Rotation of Partitions

To correct any translational and rotational misalignment of partitions, resulting unavoidably from the specimen photography, two algorithms are required. These algorithms make use of ostial pairs 3, 5, and 7 to concatenate the partitions at truncation lines. Refer to Figures 5.1.4. In Figure 5.1.4.a, Partitions 1 and 2 are shown in the form immediately after truncation. Note the separate sets of coordinate axes with origins at different x values. In Figure 5.1.4.b, ostium 3R of ostial pair 3 on Partition 2 (P2) has been made to coincide with ostium 3R of Partition 1 (P1). The algorithm has translated P2 by adding the required Δx and Δy values to all pixel coordinates of P2, so that the landmark coordinates of ostium 3R in P1 and P2 are identical. Note the translated coordinate system $x_2' - y_2'$. In Figure 5.1.4.c, the entire coordinate system $x_2' - y_2'$ of P2 has been rotated so that the landmark coordinates of 3L in P1 and P2 are also identical. The algorithm computes the angle A from landmarks 3L in P1, 3R, and 3L in P2, and applies this rotation to system $x_2' - y_2'$ about landmark 3R. Again, this process is repeated at concatenate ostial pairs 5, and 7, applied to remaining luminance levels, and applied similarly to the remaining specimen images. Note that each time the process is applied only the subsequent partition is translated and rotated. In this way, P1 is never translated or rotated, and P4 receives the effects of translations and rotations of P2, P3, and P4. The program is listed in Appendix A.

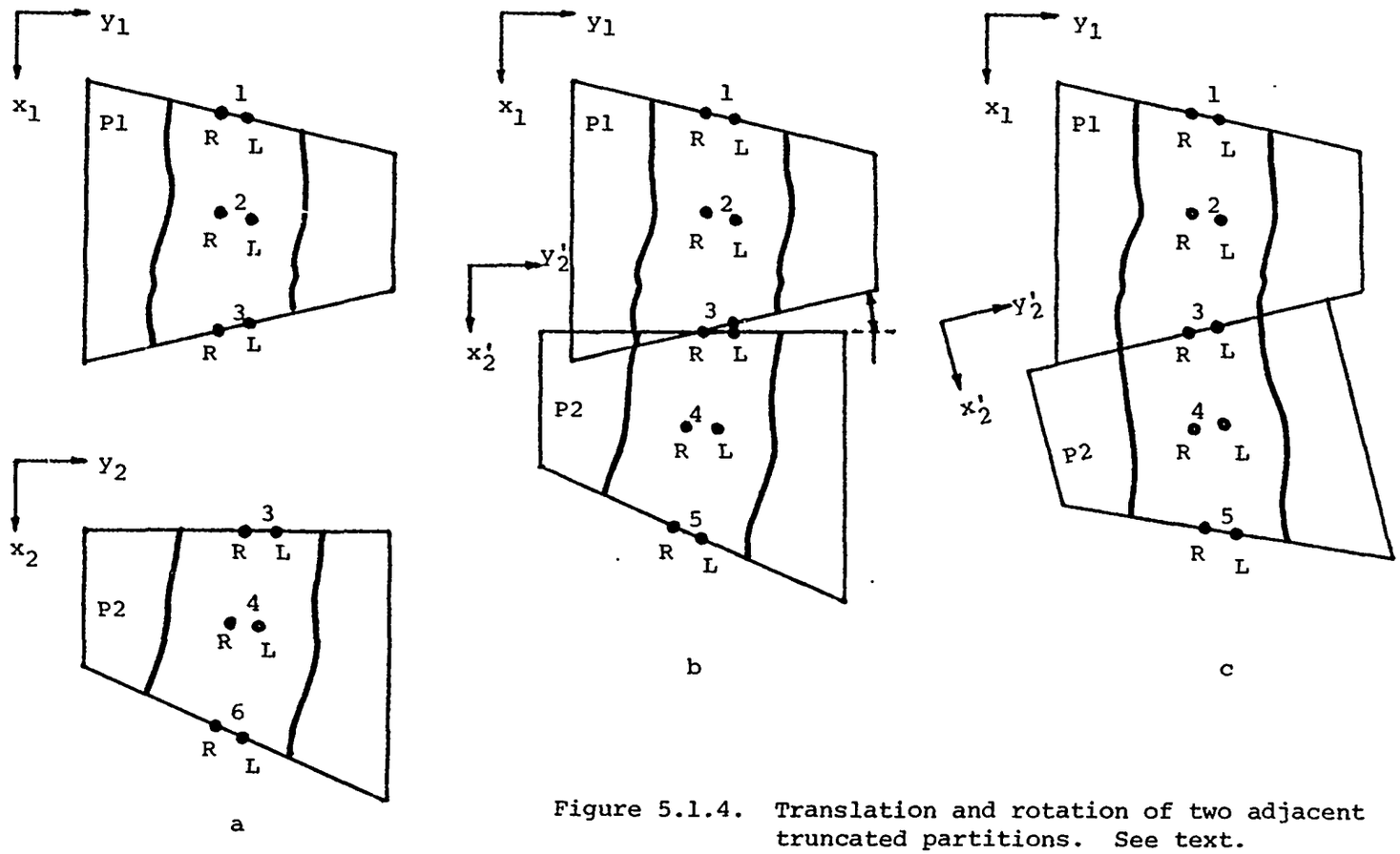

Figure 5.1.4. Translation and rotation of two adjacent truncated partitions. See text.

5.1.4 Concatenation of Partitions

Concatenation has, in effect, been produced by the operations described above. All that remains is to eliminate the redundant specification of the $x_2' - y_2'$ coordinate system. Since it is coincidental with the $x_1 - y_1$ system, $x_2' - y_2'$ specification is erased from computer memory. The origin of the x_1-y_1 system is taken at the 1R landmark in P1. Note that the ability to interactively choose identical landmark pixels for 3R & 3L of P1 and 3R & 3L of P2, affects the accuracy of concatenation; at high resolution, however, the error is quite insignificant. Accuracy-affecting interaction may be eliminated; see Chapter VI.

5.2. Transformation to Reference Standard

The general concept of the transformation employed here is the unpublished work of Donald Fry, at the National Institutes of Health, Bethesda, Maryland*. In essence, the concept is as follows: given the coordinates of the three vertices of a triangle, all points on and within that triangle may be linearly transformed into another triangle of different size and shape. The transformation functions are discussed in detail in Section 5.2.3.

Why is this transformation necessary? It is not required if only one specimen image is to be studied. However, as pointed out in Chapters I and II, the biological variation, especially in physical dimensions, is great, even within common age, sex, specie and epidemiological

* No further documentation available.

classes. Therefore, to effectively judge atherosclerotic lesions for general or specific trends, a statistical number of specimens is required. This transformation permits numerous specimens of common class to be studied without uncontrollable biological variation by transforming each slightly varied specimen into standard physical dimensions of choice. Section 5.2.2 describes one such "standard specimen". In Section 5.2.1. the specification of vertices is described.

5.2.1. Specification of Transformation Vertices

The triangles used in Fry's transformation are clearly limited in biological application by the availability of reference vertices, which can be commonly specified for all arterial specimens. In the midthoracic aorta, the ostial landmarks have proven to be convenient choices. Figure 5.2.1. shows how triangles were formed for the transformation used in this thesis. Obviously, other arrangements could be formed, but the one employed here, using six triangles between each ostial pair, has proven to be efficient in computer time and memory requirements, without sacrificing accuracy. Note in the Figure that the intersections of the lines determined by paired landmarks and the severed edges of the specimen also form vertices. Note also that the triangles are confined to the region of the artery and do not enclose areas which were "background" in the original photographs. (There is one exception to this, however. See Section 5.2.3.) The vertices and triangles are numbered for reference as shown in Figure 5.2.2. Vertex landmarks must be specified interactively on all five simulated specimen images. This can be done by reading the coordi-

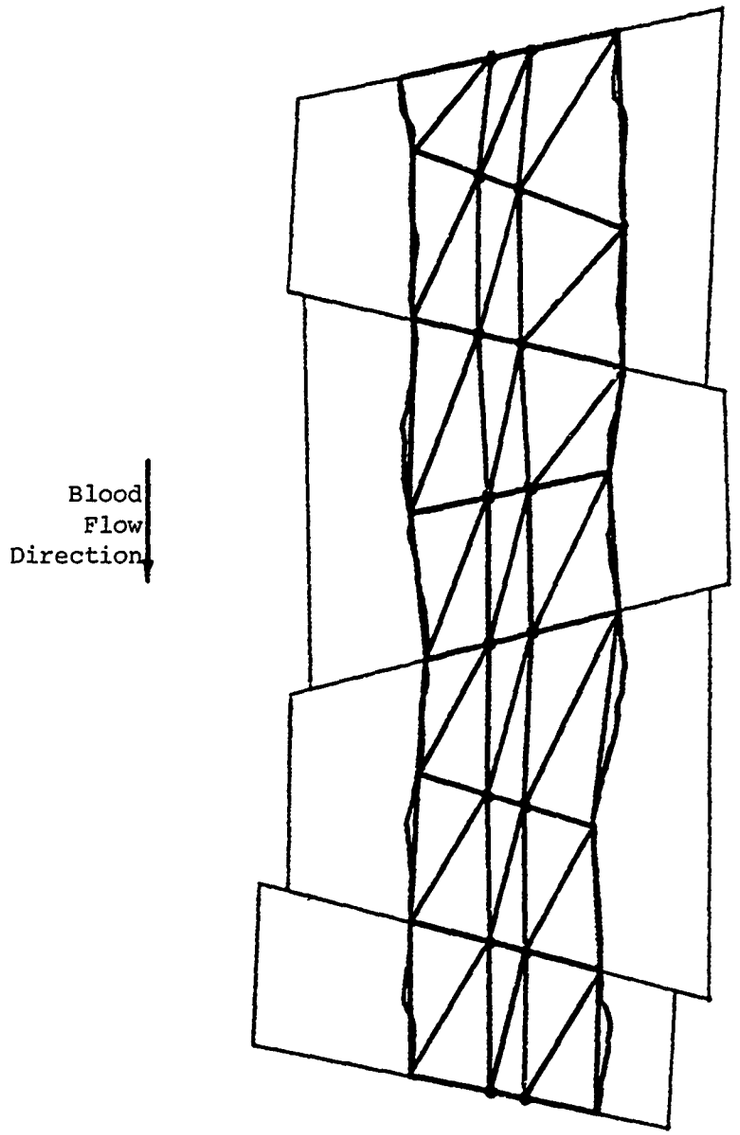

Figure 5.2.1. Arrangement of triangles using intercostal ostia and specimen borders as vertices. See text.

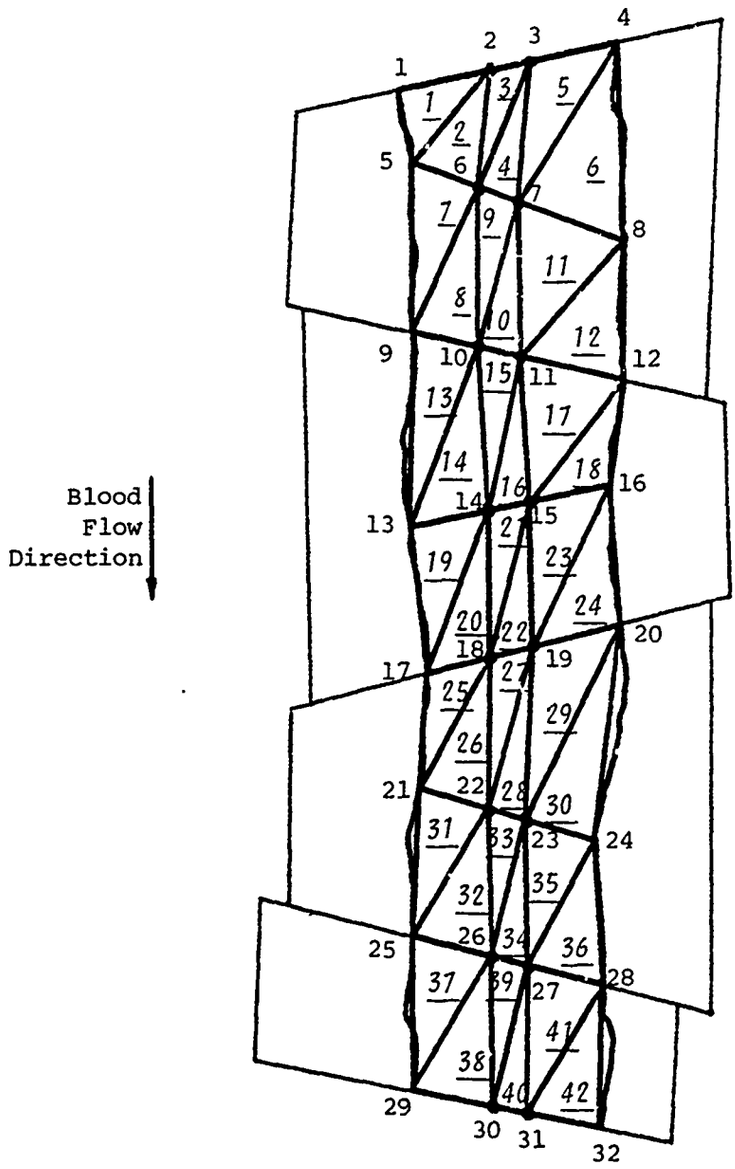

Figure 5.2.2. Reference numbering of triangles and vertices. See text.

nate scales on the printout of the entire data set at each landmark location, or by direct interaction at a CRT display. See Chapter VI.

5.2.2. The Standard Specimen

Since the taper of the descending thoracic aorta in the adult rabbit is slight, and the slope of the line passing through one ostial pair is randomly distributed about zero, a rectangular standard specimen of the typical aspect ratio. 2:7, and with side-by-side evenly spaced ostial arrangement was constructed. This appears in Figure 5.2.3. with transformation triangles included. Note that vertex and triangle numbering must be consistent with the reference. The vertex coordinates, which are also standardized for this standard specimen, are listed in Table 5.2.1. All five simulated specimens are mapped into this standard specimen, since they represent specimens of common age, sex, specie and epidemiology. Of course, a standard specimen should be quite similar in gross respects to all specimens that are mapped into it. The purpose of the standard is to overcome biological variability, not variability in age, sex, and so on; a new standard must be constructed for each different grouping. This grouping is the essence of most pathological research.

5.2.3 Transformation Functions

This section describes the transformation in detail and the algorithm to implement it on computer. The program listing is Appendix B.

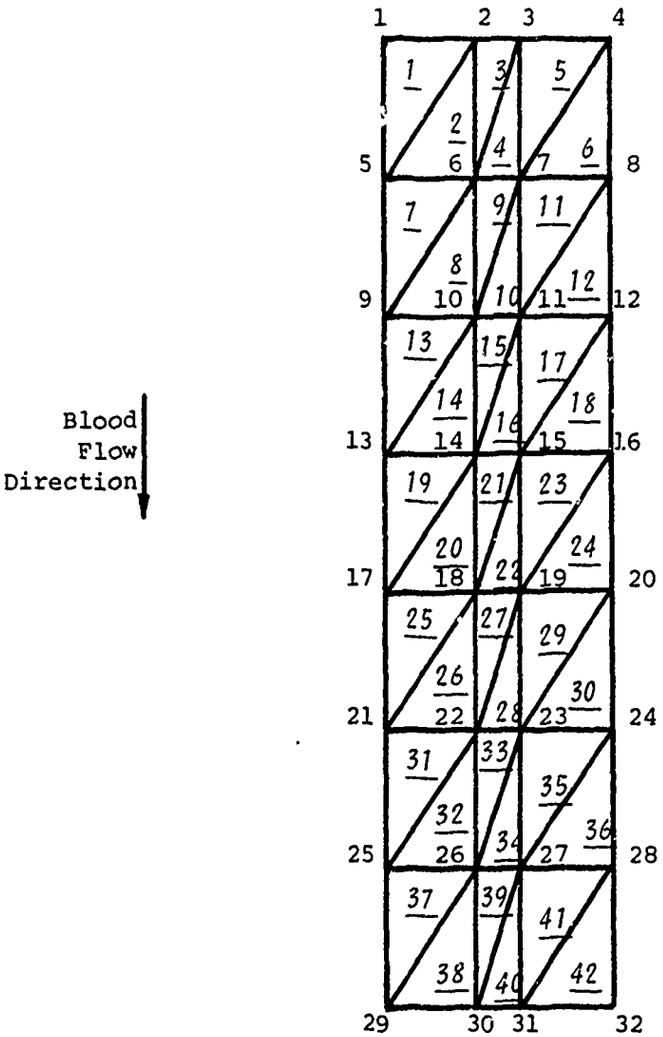

Figure 5.2.3. Triangle and vertex specification of the Standard Specimen.

Vertex Number	Coordinates (x,y)
1	(0,0)
2	(0,20)
3	(0,30)
4	(0,50)
5	(30,0)
6	(30,20)
7	(30,30)
8	(30,50)
9	(60,0)
10	(60,20)
11	(60,30)
12	(60,50)
13	(90,0)
14	(90,20)
15	(90,30)
16	(90,50)
17	(120,0)
18	(120,20)
19	(120,30)
20	(120,50)
21	(150,0)
22	(150,20)
23	(150,30)
24	(150,50)
25	(180,0)
26	(180,20)
27	(180,30)
28	(180,50)
29	(210,0)
30	(210,20)
31	(210,30)
32	(210,50)

Table 5.2.1. Coordinates of the vertices for the Standard Specimen.

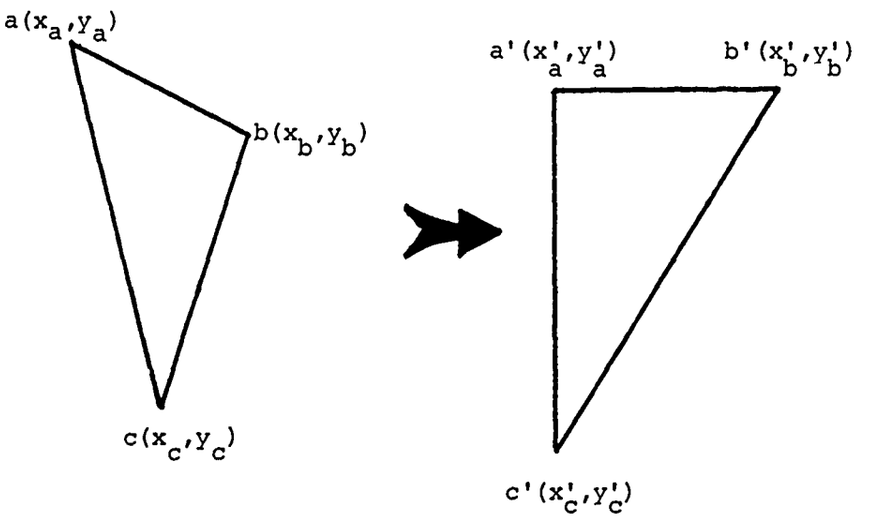

Figure 5.2.4. Triangle a'b'c' into which abc is mapped by the Fry transformation.

Refer to Figure 5.2.4. Given a, b, c, a , b , and c , solve for the transformation coefficients, A, B, C, D, E, and F as follows:

$$A = y'_a - Bx_a - Cy_a$$

$$B = \frac{y'_c - y'_a - C(y_c - y_a)}{x_c - x_a}$$

$$C = \frac{(y'_b - y'_a)(x_c - x_a) + (y'_c - y'_a)(x_a - x_b)}{(y_b - y_a)(x_c - x_a) + (y_c - y_a)(x_a - x_b)}$$

$$D = x'_a - Ex_a - Fy_a$$

$$E = \frac{x'_c - x'_a - F(y_c - y_a)}{x_c - x_a}$$

$$F = \frac{(x'_b - x'_a)(x_c - x_a) + (x'_c - x'_a)(x_a - x_b)}{(y_b - y_a)(x_c - x_a) + (y_c - y_a)(x_a - x_b)}$$

Now, compute

$$f(y) = C_1 + M_1 x, \quad \text{where } M_1 = \frac{y_b - y_a}{x_b - x_a}, \quad C_1 = y_a - M_1 x$$

$$g(y) = C_2 + M_2 x, \quad \text{where } M_2 = \frac{y_b - y_c}{x_b - x_c}, \quad C_2 = y_c - M_2 x_c$$

$$h(y) = C_3 + M_3 x, \quad \text{where } M_3 = \frac{y_c - y_a}{x_c - x_a}, \quad C_3 = y_a - M_3 x_a$$

These are the equations of the lines which form sides ab, bc, and ca, respectively. The algorithms to implement these equations are straightforward.

With these equations, the coordinates of those pixels within the triangle abc must be determined. This is due to the fact that only the pixels within a given triangle can be correctly transformed using the coefficients determined by the vertices of that triangle. Obviously, pixels outside that triangle can be correctly transformed only by the equations developed from the adjacent triangle within which those pixels lie. The algorithm which searches the data set to determine pixel inclusion in a triangle was developed by Edward Herderick at The Ohio State University. The algorithm, employing polar coordinates, first specifies an angle formed by any two legs of the triangle. One side of that angle is referenced to zero degrees, so that the other side lies at the computed angle. For example, in angle bca of Figure 5.2.5., side bc lies on the zero degree reference, and side ca lies at the computed 30°angle. Next the algorithm specifies an angle formed by a different set of legs of the same triangle, say,

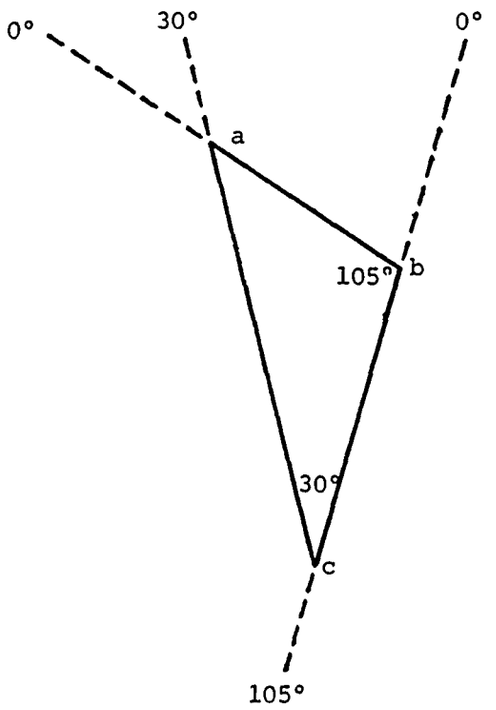

Figure 5.2.5. Reference angles specified by the algorithm on a typical triangle abc.

angle abc of Figure 5.2.5. Similarly, a 0° reference and 105° angle are specified. Then, the algorithm causes the data set to be searched and tests each pixel (pixel coordinates) to determine if its angular position, calculated first with respect to bc, is between 0° and 30°, and calculated second with respect to ab, is between 0° and 105°. If both tests are positive, the pixel is judged to be within the triangle.

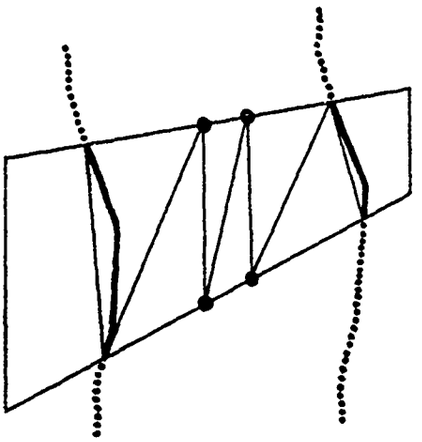

Figure 5.2.6. Specimen region between two ostial pairs showing transformation triangles. See text.

The coordinates of each pixel so judged are then transformed by the following equations:

$$y' = A + Bx + Cy$$

$$x' = D + Ex + Fy$$

where x and y are the coordinates of the pixel judged to be within the original triangle, and x' and y' are the coordinates of the corresponding pixel within the transformed triangle. This procedure is then repeated for the standard number of triangles, in this case, forty-two.

Note in Figure 5.2.6. a typical specimen region between two ostial pairs prior to transformation. Due to careless incision in opening the excised artery along the ventral aspect, very rough

edges are apparent. This fact permits the leftmost triangle in the figure to enclose several pixels of background, and the rightmost triangle to omit several specimen pixels. Though this problem was not alleviated in this preliminary study, the procedure for doing so is straightforward and discussed in Chapter VI. This problem is apparent in the figures of Section 5.3. and 5.4. where "background" pixels included in transformation triangles were interpreted by the algorithm to be below threshold lesion areas. Otherwise, small irregularities in the ventral incision are insignificant since the resulting edges are transformed into straight lines in the standard specimen.

5.3. Graphical Representation of Standard Specimen

As mentioned in the introduction, the graphics of colorimetric topography take two forms: a contour, or "topographical", map and a three dimensional plot. Though both forms are highly quantitative, the contour map permits convenient visual examination and extraction of quantified data. However, since the 3-D plot displays quantified data in a much more striking visual manner, it is included for comparison and to allow the non-mathematical investigator to gain a better "feel" for the data.

The next section describes how these graphics are generated and the following section is a brief discussion as to how the graphs should be interpreted.

5.3.1. Registration of Overlaid Binary Maps

To generate the final graphics for one complete specimen image, the three concatenated and transformed binary maps, each at a different luminance threshold, must be over laid. Since the coordinates of the corresponding array elements are identical (received identical translation, rotation, and transformation) and have the same origin, it is a simple matter to register the maps exactly. As the "packaged" contour and 3-D plot routines are called, the same coordinate is drawn from each and every binary map and used to build a vertical dimension upon the same coordinate pair in the horizontal plane. The spacing of the points in the vertical dimension is arbitrary, though chosen for easy readability. Of course, on the contour plot a closed contour representing the plane at a specified vertical dimension is drawn on the horizontal plane. Examples of contour and 3-D plots are shown in the figures of Section 5.4.

The order in which the luminance level binary maps are overlaid and the interpretation of the graphics follows.

5.3.2. Interpretation of Colorimetric Topography

As the luminance threshold is raised in the image processor to produce binary maps, the "darker" areas fall below threshold first, followed by "moderate" areas and finally by "lighter" areas. Thus, black pixels are the first to change from a value of 1 (above threshold) to 0 (below threshold), if, in fact, those pixels ever registered above threshold. (In any case, minimum luminance threshold is an

electronically controllable parameter; see Section 3.2.2.) Highly saturated red lines, or "deep reds" (assuming preprocessing on red), next change from 1 to 0 as the luminance increases from minimum. Then moderately saturated red pixels, and next, slightly saturated red, or "pale pink", pixels change from values of 1 to 0 as their luminance values are passed by the increasing luminance threshold. Finally only white, or healthy specimen areas, remain encoded by 1's. On a 3-D plot, difficult to show on paper, one would see an "inverted mountain" built of 1's, floating in a sea of 0's. Obviously, it is the inversion of this plot that would be meaningful. In Figure 5.4.1.e. this "mountain" of 1's is righted and the 0's are eliminated for clarity so that the surface denotes the three dimensional boundary between the 1's and 0's which were distributed in 3-space. The height of the surface, then, indicates increasing saturation, or "deepness", of red hue. This, in turn, is indicative of the concentration of Sudan IV staining.

Thus, the pale-to-deep red sudanophilia, with which the pathologist and investigator are quite familiar, are represented by a highly quantitative, colorimetrically topographical map of that arterial surface.

5.4. Statistical Synthesis of Standard Specimens

The usefulness of colorimetric topography lies in the statistical nature by which numerous arterial specimens may be grouped and compared according to the investigator's needs to quantify regressive or progressive trends in atherogenesis. For this thesis, five specimens of

similar age, sex, and epidemiology were simulated and processed by the algorithms already discussed. The first two sections that follow describe the procedures to produce the statistical graphics. The final section outlines the use of these graphics.

5.4.1. Grid Overlay and Interpolation

The pixel arrangement and orientation is quite precise and regular in the preliminary binary map. Not only the map, but also the stored array positions are located by whole number coordinates. For the low resolution specimen images processed here, those coordinates, for one partition, are x = 1, 2, 3, ..., 120; and y = 1, 2, 3, ..., 80. However these numbers are stored as real numbers; they must be operated upon by continuous functions. The results of the translation, rotation, and transformation operations are rational and irrational numbers for pixel coordinates. The pixel, itself, represents a minute, rectangular area in the image, and its value, an average over that area, is stored at a given set of x-y coordinates. These coordinates may receive translation and rotation in Partitions 2, 3, and 4, a process that destroys the regular pattern of pixel arrangement, and thus the regularity of coordinate increments. Furthermore, the Fry transformation produces, by design, a linear distortion of successive coordinate positions. Now, the transformation functions are different for each specimen image, as they are for each triangle. This is obviously due to the fact that the actual coordinates of the standard vertex choices will, in general, be different in different specimens. (This, of course, is not true in the standard specimen, where not only the vertex choices but also their

corresponding coordinates are standardized as listed in Table 5.2.1.) Therefore, the linear distortion will be different for each specimen.

Several standard specimens, from different specimen images, must be overlaid to permit statistical graphics. When these overlays are registered at any common landmark, all other landmarks will be in exact registration, since the corresponding landmarks (and vertices) of all standard specimens are coincidental, with identical coordinates. However, due to dissimilar linear distortions in successive standard specimens, the coordinates of a non-vertex pixel in one standard specimen *will not* be coincidental with the coordinates of a pixel in an adjacent standard specimen. Indeed, non-vertex pixels, themselves, *will not*, in general, correspond.

This lack of correspondence of pixel locations in the vertical dimension of overlaid standard specimens, causes a problem in combining these maps for statistical graphics. Therefore, a convenient "packaged" computer program overlays a grid onto each standard specimen, applies an interpolation scheme to the standard specimen's coordinates about given, standard, and regular positions on the grid. For each luminance level binary map of the standard specimen, a weighting factor of $1/d^2$ is applied to pixels neighboring a specific grid position, where d is the distance from a pixel location to that grid position location. This weighted interpolation, then, assigns a given, standard, and regular set of positions for pixel location on the standard specimen and also assigns a value of 0 or 1, depending upon the neighborhood, to each pixel so located. These computer programs form Appendix C.

5.4.2. Probabilistic Graphics for Standard Specimens

Now that the standard specimens, or corresponding luminance levels, can be overlaid with all corresponding pixels in registration, a useful design for the vertical dimension can be determined. Two components of information are available in the vertical dimension of several overlaid standard specimens. The first is saturation level, as discussed in Section 5.3.2. Second is the number of pixels at a given saturation level encoded as 1's, that is, above that "saturation threshold". The actual number will depend upon the particular specimen examined. It is more useful, therefore, to determine the number of pixels, at a given saturation level, which are encoded as 1's for 100% of the standard specimens. This "number of pixels" present in 100% of the standard specimens is then determined at all saturation levels. Remember that not only the number of pixels but also the location of each pixel is explicitly known.

This design can be best displayed in contour and 3-D plots as discussed in Section 5.3.1. In this case, however, separate plots are made for each probability chosen. (For brevity, "the number of pixels encoded as 1's for a given saturation level" will henceforth be called "lesion area".) Note that lesion areas which exist for less than 100% of the standard specimens, are actually specified in terms of percentiles; that is, a lesion area that occurs for 80% of the standard specimens will be larger than, and therefore enclose, those lesion areas which occur for more than 80% of the standard specimens. The probability percentiles chosen for output in this

thesis are the 100th, 80th, 60th, 40th, and 20th. Figures 5.4.1. show the contour plots of these respective probability percentiles. To exemplify the 3-D plot, Figure 5.4.1.d. is repeated in 3-D as Figure 5.4.1.e. The packaged programs to produce these plots form Appendix D.

5.4.3. Comparison of Colorimetric Topographies

The 100th probability percentile is perhaps the most important display of sudanophilia. The areas and location of those areas would indicate that, for the specimens analyzed, sudanophilia of the given saturation always occur at those arterial locations. By comparing one statistical standard specimen with another, built of specimens of different age, sex, or treatment, and so on, progression, regression, and static behavior would be clearly evident; and changes would be very accurately quantified, in terms of location and severity, if progression or regression had occurred. Furthermore, the importance of a single statistical sample in one statistical standard specimen should not be ignored.

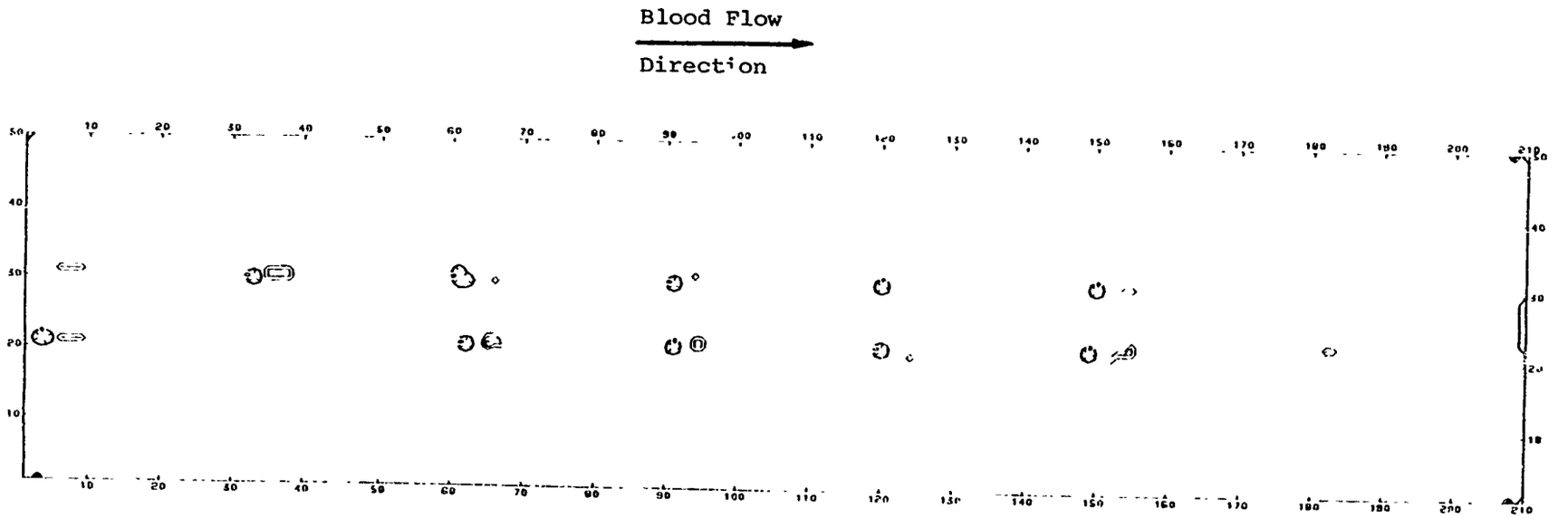

Figure 5.4.1.a. 100th probability percentile.

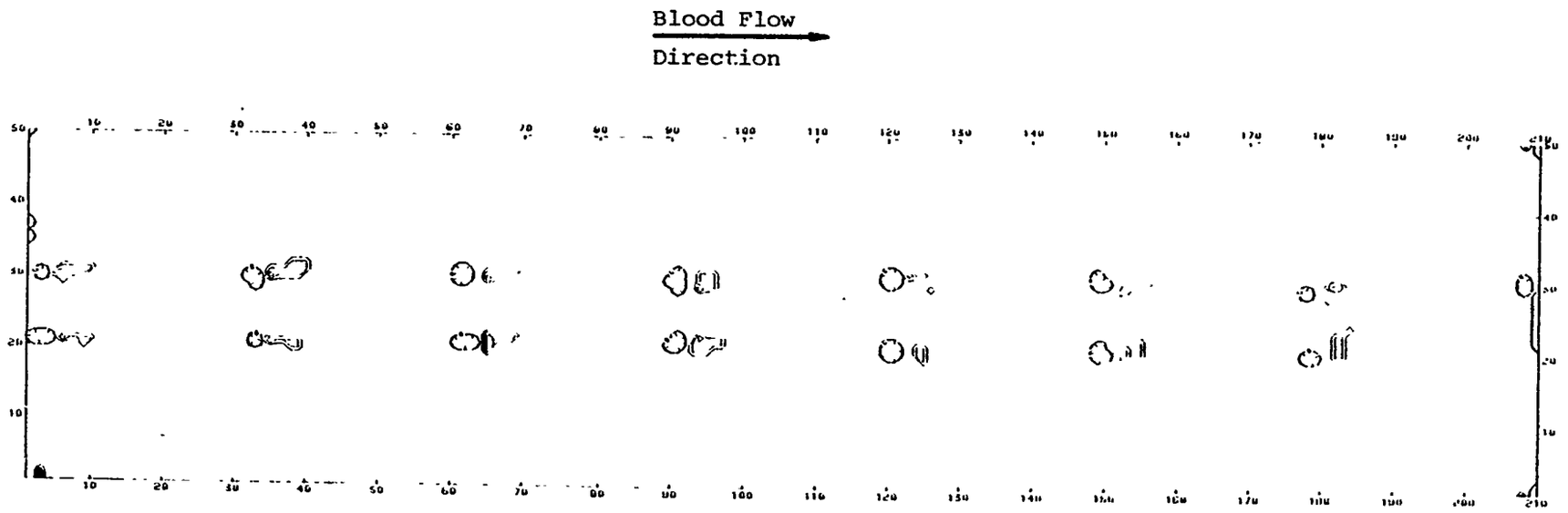

Figure 5.4.1.b. 80th probability percentile.

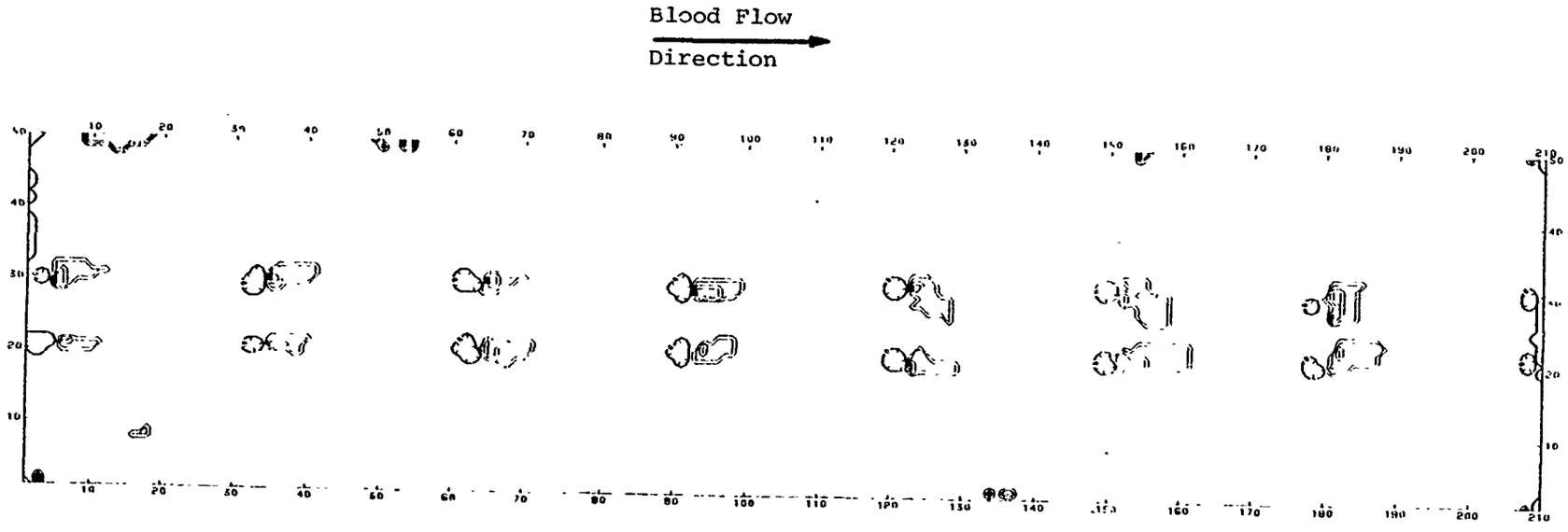

Figure 5.4.1.c. 60th probability percentile.

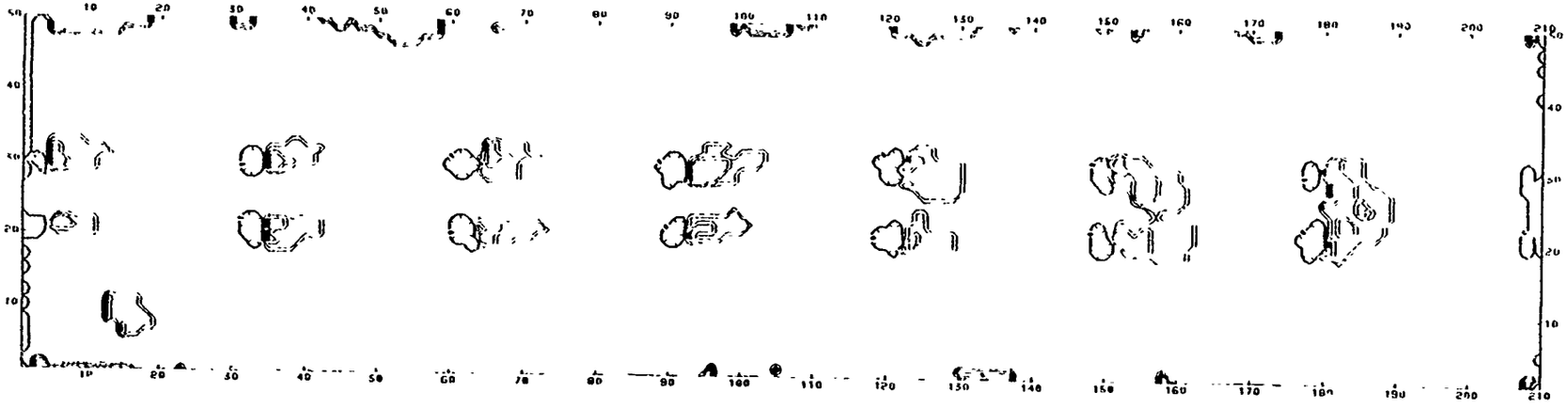

Blood Flow
Direction

Figure 5.4.1.d. 40th probability percentile.

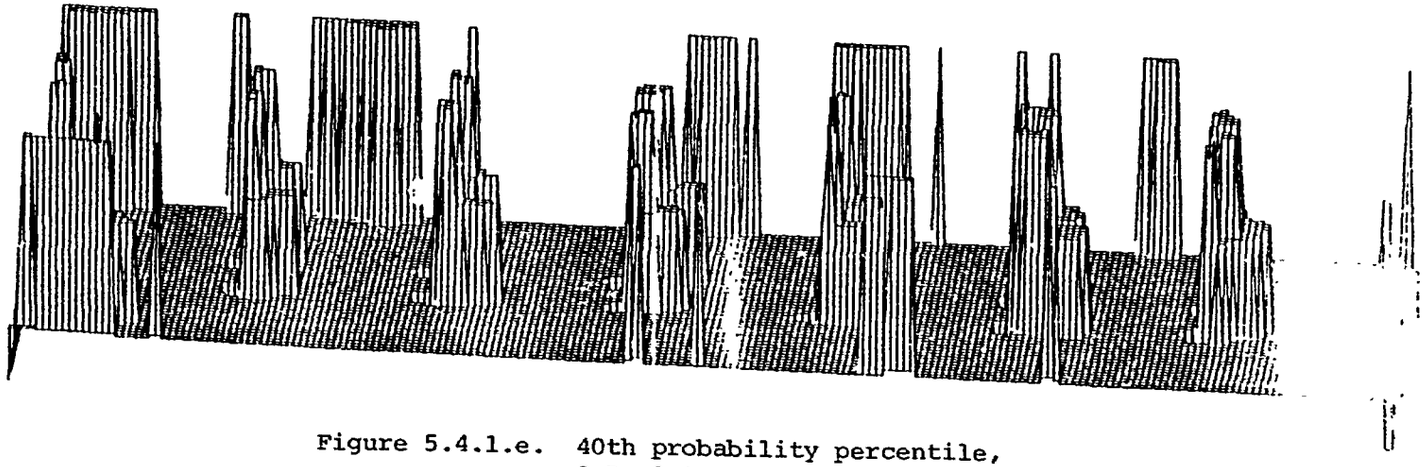

Figure 5.4.1.e. 40th probability percentile,
3-D plot.

Blood Flow

Direction

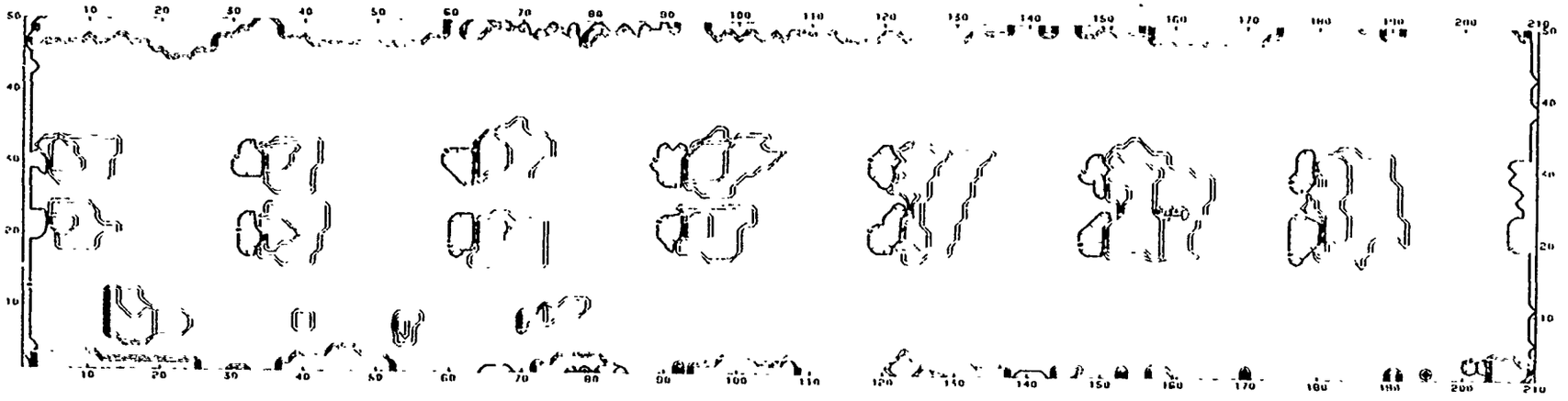

Figure 5.4.1.f. 20th probability percentile.

CHAPTER VI

6.0 Introduction: Conclusion and Recommendations for Future Work

Any field of research employing advanced electronic hardware is subject to constant change and improvement. Image processing technology, though well developed, is only now coming into widespread use: this is due primarily to substantial cost reductions in electronic hardware. Along with this use will come industrial incentive for further development and increased versatility of packaged processing systems.

With packaged systems will come dedication of equipment to the image processing requirement. The tools will then be easy to assemble and operate. System design emphasis will be on increased accuracy and precision. All these factors will benefit the image processing user and bring this labor-saving technique into common usage and acceptance.

The next section summarizes and concludes the presentation of the work of this thesis. The section that follows briefly outlines specific recommendations for further development of colorimetric topography, which should result in increased accuracy, precision and convenience of use.

6.1. Conclusion

Employing the standard digitized image derived from the existing theory of image processing, this thesis documents the development of a standard photographic protocol, a high resolution processing scheme, and the graphical representation and analysis for the quantification

of atherosclerosis as manifest by sudanophilia. The problem statement is analyzed and the need for "another" solution justified by brief critiques of the results of existing methods. The limitations of the proposed technique are presented by developing television image processing theory from fundamentals. After developing a convenient, standard protocol for the photography and presentation of the necropsy specimen image to the television camera, a computer processing scheme is developed to reduce the overwhelming data complex to a tractable form for presentation to the research scientist.

Colorimetric topography has been shown to produce highly quantitative graphical representations of the specimen image. The accuracy is limited only by the resolution of the television image, which is, at this juncture, due to photographic partitioning, far beyond measurement requirements. The precision of the system is limited only by the human interaction presently required for the specification of landmarks and transformation vertices. The Fry transformation, by design, introduces no error into the accuracy of measurement, but transforms, by controlled, reversible, linear conversion, one planar map into another. Proper operation of the computer algorithms is exemplified by analysis of simulated specimens. Finally, the precision of this preliminary system can be increased by the interactive techniques presented next.

6.2. Future Work

Recommendations for further refinement of hardware design and computer processing are presented next.

6.2.1. "Real Time" Image Processing

Binary maps are produced by the thresholding process to reduce memory requirements. In the Jagadeesh System, thresholding also avoids the necessity to digitize the television field by sampling at a frequency sufficient to complete the entire field in 1/60 second. (The Jagadeesh System samples at 180/scan line for only one of two fields.) A digitizer capable of sampling at 180/scan line in 1/60 second was prohibitively expensive at the time that this system was designed.

However, systems available today can economically sample at even higher resolution and for both fields within 1/30 second without difficulty. These systems are commonly used for television animation. Since only one television image is produced in 1/30 second, digitization can easily keep pace with the field frequency. Also, since memory is less expensive today, the entire image digitization process can occur in "real time" with respect to the television image. No longer need a map be dichotomous about a given threshold; one map could easily carry the 50 discrete luminance values of the example cited in Chapter II.

In this case, it would not be required to specify landmarks for the overlay of separate luminance levels. However, landmarks are still required for overlay of several standard specimens.

6.2.2. RGB vs NTSC

The Jagadeesh System derived a color specification (the angle A, see Section 3.2.2.) from a scheme using the NTSC transmission primaries,

I, Q, and Y, as input. In effect, the NTSC primaries were converted back to the RGB primaries, which were initially available, though with difficulty, at the camera. High quality cameras today have conveniently available RGB signals. Thus the NTSC conversion, with its inherent broadcast limitations (see Section 3.2.1.), can be completely bypassed. A linear combination of high quality RGB signals, then, specifies the color on which preprocessing can operate.

6.2.3. Computer Specification of Landmarks

As mentioned in Sections 5.1.1. and 5.1.4., the landmarks within an ostial field of 0's can be specified by computer, eliminating precision limiting interaction. Interaction is required only to isolate the ostial field so that a simple algorithm can numerically integrate to determine the geographic center of the field. This process would be quite precise. The isolation could be performed at an interactive CRT as could vertex specification, described next.

6.2.4. CRT Interaction for Vertex Specification

The specification of transformation vertices on the concatenated specimen array was performed manually in this thesis by reading the scales on a computer printout. Much more accurate and precise results could be attained by specifying the vertices with a sensor-pen at an interactive CRT terminal. This equipment was not available at the time of this work, however.

6.2.5. Artifacts of Transformation and Plotting Routines

In the specimens simulated for this study, lesion areas were placed in typical pathological locations. Thus, the lesions occupied areas downstream of ostia. Some lesions were placed elsewhere to typify non-ostial lesions, but no lesions were simulated at the artery borders. Note, however, that the graphics show lesions in this area. This is due to the inclusion of "background" zeros in the border triangles and subsequent processing of these zeros as lesion area, since lesions are also encoded as zeros. Refer to Figure 5.2.6.

This problem is not difficult to overcome. Two possible corrections involve the encoding by the image processor and the manner by which the specimen array is entered into computer memory. In the first corrective measure, the "background" of the specimen image is encoded with a character other than zero or one. This is possible, since at the minimum luminance threshold only those pixels representing "background" are below threshold; all the specimen surface is above threshold. At this threshold only, then, below threshold is encoded with 3's and above with 1's. In subsequent thresholds the 0, 1 arrangement is applied. Thus all background information can be separated from lesion area and the former pixels excluded from the transformation.

The second corrective measure is perhaps simpler to implement. The data array from the specimen image is input to computer by reading across columns of the data file (specimen image) from each side toward the center. The file is begun only upon encountering a 1, that is,

specimen area. Thus background pixels are not included in the data set and the transformation not applied to them. Note that since 0's may occur at specimen borders due to existing border lesions, but will, incorrectly, be deleted from the data set, this procedure is again restricted to a luminance threshold map where background information is encoded with a unique character.

Due to the poor resolution of the simulated specimens, especially ostial fields restricted to approximately 0.5% of the 400-1600 pixels/field produced by television image digitization, the grid overlay interpolation procedure obscures the ostia pixels in the 100th probability percentile contour map. In the processing of an image digitized by television, however, this artifact does not exist.

REFERENCES

1. McGill, H.C. 1977. Atherosclerosis: Problems in Pathogenesis. Atheroscl R 2:27-65.

2. Holman, R.L.; McGill, H.C.; Strong, J.P.; Geer, J.C. 1958. The Natural History of Atheroselerosis. Am J Path 34(2):209-235.

3. Klotz, O.; Manning, M.F. 1911. Fatty Streaks in the Intima of Arteries. J Pathology 16:211-220.

4. WHO 1958. Classification of Atherosclerotic Lesions. Technical Report Series # 143.

5. Roberts, J.C.; Moses, C.; Wilkins, R.H. 1959. Autopsy Studies In Atherosclerosis. Circulation 20:511-526.

6. Louisiana State Univ., Sch. of Medicine, Dept. of Pathology, New Orleans; and Instituto de Nutricion de Centro America y Panama, Guatemala. 1962. Standard Operating Protocol. International Atherosclerosis Project.

7. Insull, W. 1967. Stain for Differentiation and Quantification of Gross Lesions of Atherosclerosis. Arch Path 83:474-478.

8. Smith, E.B.; Smith, R.H. 1976. Early Changes in Aortic Intima. Atheroscler R 1:119-136.

9. Wilens, S.L. 1937. The Post Mortem Elasticity of the Adult Aorta. Am J Path 13:811-819.

10. Gore, I.; Tejada, C. 1957. The Quantitative Appraisal of Atherosclerosis. Atheroscler 33(5):875-885.

11. Holman, R.L.; et al 1960. An Index for the Evaluation of Atheroselerotic Lesions in the Abdominal Aorta. Circulation 22:1137-43.

12. Daoud, A.S.; Goodale, F.; Floretin, R.; Beadenkopf, W.G. 1962. Chemicoanatomic Studies in Geographic Pathology. Arch Path 73:74-93.

13. Kagan, A.; Uemura, K. 1962. Grading Atherosclerosis in Aorta and Coronary Arteries Obtained at Autopsy. B WHO 27:667-679.

14. Cranston, W.I.; Mitchell, J.R.A.; Russell, R.W.R.; Schwartz, C.J. 1964. Assessment of Aortic Disease. J Atheroscl 4:29-39.

15. Mitchell, J.R.A.; Schwartz, C.J. 1965. Arterial Disease. Oxford, England: Blackwell Scientific Publishing, Ltd.

16. Kuthan, F. 1968. The Quantitation of Aortic and Coronary Atherosclerotic Lesions. J Atheroscl 8:981-982.

17. Al-Hashimi, A.S.; Williams, G. 1971. A Morphometric Method for Assessment of Atheroselerotic Lesions. Atheroscler 14:401-409.

18. Solberg, L.A.; et al 1972. Evaluation of Atherosclerotic Lesions in Cerebral Arteries by Unaided Visual Estimation. Atheroscler 16:155-167.

19. Cornhill, J.F.; Roach, M.R. 1974. Quantitative Method for the Evaluation of Atherosclerotic Lesions. Atheroscler 20:131-136.

20. Eggen, D.A.; Strong, J.P.; McGill, H.C. 1962. An Objective Method for Grading Atherosclerotic Lesions. Lab Inv 11(9): 732-742.

21. Robbins, S.L.; Fish, S.J. 1964. A New Angiographic Technic Providing a Simultaneous Permanent Cast of the Coronary Arterial Lumen. Am J Clin P 42(2):156-163.

22. Crawford, D.W.; et al 1974. Grading of Coronary Atherosclerosis. Atheroscler 19:231-241.

23. Aldridge, H.E. 1977. Better Visualization of the Asymmetric Lesion in Coronary Arteriography Utilizing Cranial and Caudal Angulated Projections. Chest 71(4):502-507.

24. Barndt, R.; Crawford, D.W. 1977. A New Three-Dimensional Postmortem Method to Study the Topography of Atherosclerosis Using Profilametry. Atheroscler 27:121-128.

25. Crawford, D.W.; et al 1977. Computer Densitometry for Angiographic Assessment of Arterial Cholesterol Content and Gross Pathology in Human Atherosclerosis. J L Cl Med 89(2):378-392.

26. Hata, Y.; et al 1978. A Xerographic Method for the Quantitative Assessment of Atherosclerotic Lesions. Atheroscler 29:251-258.

27. Loewenson, R.B.; Bearman, J.E.; Resch, J.A. 1972. Reliability of Measurements for Studies of Cerebrovascular Atherosclerosis. Biometrics 28:557-569.

28. Chernukh, A.M.; Gorizontova, M.P.; Shinkarenko, V.S. 1977. Quantitative Evaluation of Disturbances of Vascular Permeability by Means of a Television Analyzing System. B Ex B Med 84(10):507-509.

29. Jagadeesh, J.M. 1974. Real Time Image Processing System Using a Color Television Camera. PhD Dissertation, The Ohio State Univ., Columbus.

30. Antti Manuikko 1978. Personal Communication. Dept. of Forensic Medicine, Univ. of Helsinki, Finland.

31. McGill, H.C.; et al 1968. General Findings of the International Atherosclerosis Project. Lab Inv 18(5): 498-502.

32. Rosenfeld, A.; Kak, A.C. 1976. Digital Picture Processing. New York: Academic Press.

33. Bishop, P.O. 1968. The Visual System: the neural basis of visual perception. P Int Union Physl 6:262-278

34. MacNichol, E.F., Jr. 1964. Three-pigment Color Vision. Sci Am 211(6):48.

35. Neisser, U. 1968. The Processes of Vision. Sci Am 219(3):204.

36. Guyton, A.C. 1971. Textbook of Medical Physiology. Philadelphia: W.B. Saunders Co.

37. Judd, D.B.; Wyszecki, G. 1975. Color in Business, Science, and Industry, 3rd Ed. New York: Wiley-Interscience.

38. Billmeyer, F.W., Jr.; Saltzman, M. 1966. Principles of Color Technology. New York: Wiley-Interscience.

39. Bureau Central de la Commission International de l'Eclairage 1971. Colorimetry, Official Recommendations of the International Commission on Illumination. Publication CIE No. 15 (E-1.3.1).

40. Wentworth, J.W. 1955. Color Television Engineering. New York: McGraw-Hill, Inc.

41. Wyszecki, G.; Stiles, W.S. 1967. Color Science. New York: Wiley & Sons, Inc.

42. Cornsweet, T.N.; Pinsker, H.M. 1965. Luminance Discrimination of Brief Flashes under Various Conditions of Adaptation. J Physiol 176:294-308.

43. Guild, J. 1931. The Colorimetric Properties of the Spectrum. Phi T Roy B A230:149-157.

44. Wright, W.D. 1928-9. A Re-determination of the Trichromatic Coefficients of the Spectral Colors. T Op Soc Lon 30:141-156.

45. Hunt, R.W.G. 1975. The Reproduction of Color. London: Fountain Press.

46. Levesgue, M. 1979. Personal Communication

47. Somer, J.B.; Evans, G.; Schwartz, C.J. 1972. Influence of Experimental Aortic Coarctation on the Pattern of Aortic Evans Blue Uptake *in vivo*. Atherscler 16:127-138.

APPENDIX A

Program "CUTTST" for truncation, translation, and rotation of partitions.

```
      DIMENSION TNP(80),ICHRS(3),VALS(3),TITL(6),INUMS(9)
      DIMENSION OABV(2,2),OBLW(2,2),NABV(2,2),NBLW(2,2)
      DIMENSION PTS(10000,3)
      INTEGER TITL
      REAL NABV,NBLW
      DATA TITL/'    ','    ','PICT','    ','    ','    '/
      DATA VALS/0.,1.,2./
      DATA ICHRS/':::::','....','****'/
      DATA INUMS/'   1','   2','   3','   4','   5','   6','   7',
     X     '   8','   9'/
      DATA IRW/'RAW '/,ITN/'TRAN'/
      NVAL=3
      NTL=6
      NPGX=3
      NPGY=1
      NPIC = 0
      READ(8,3)TITL(1)
    3 FORMAT(A4)
    1 READ(8,5,END=900)NABV(1,1),NABV(1,2),NABV(2,1),NABV(2,2)
    5 FORMAT(4F10.2)
      READ(8,5)NBLW(1,1),NBLW(1,2),NBLW(2,1),NBLW(2,2)
      NPIC=NPIC+1
      WRITE(6,700)NPIC
  700 FORMAT('1',T40,'PICTURE ',I3)
      WRITE(6,702)
  702 FORMAT('0',T10,'BEFORE CUT')
      WRITE(6,705)NABV(1,1),NABV(1,2),NABV(2,1),NABV(2,2),
     X            NBLW(1,1),NBLW(1,2),NBLW(2,1),NBLW(2,2)
  705 FORMAT(T30,'NEW ABOVE : ',4F10.2,/,T30,'NEW BELOW ',4F10.2)
      CALL CUTIT(NABV,NBLW)
      WRITE(6,707)
  707 FORMAT('0 AFTER CUT')
      WRITE(6,705)NABV(1,1),NABV(1,2),NABV(2,1),NABV(2,2),
     X            NBLW(1,1),NBLW(1,2),NBLW(2,1),NBLW(2,2)
      IF(NPIC .NE. 1)GO TO 10
              OBLW(1,1)=NABV(1,1)
              OBLW(1,2)=NABV(1,2)
              OBLW(2,1)=NABV(2,1)
              OBLW(2,2)=NABV(2,2)
              OABV(1,1)=0.0
              OABV(1,2)=0.0
              OABV(2,1)=0.0
              OABV(2,2)=0.0
   10 CONTINUE
      IIN=10
      IOUT=17
      TITL(4)=INUMS(NPIC)
```

```
      TITL(6)=IRW
      IXSP=0
      IYSP=0
      OSTVAL=2.0
      CALL PLOTIT(PTS,NPTS,ICHRS,VALS,NVAL,XMIN,XMAX,YMIN,YMAX,NPGX,
     X        NPGY,TITL,NTL,IXSP,IYSP,OSTVAL,IOUT,IIN)
      CALL ROTAT(OBLW,OABV,NBLW,NABV)
      OBLW(1,1)=NBLW(1,1)
      OBLW(1,2)=NBLW(1,2)
      OBLW(2,1)=NBLW(2,1)
      OBLW(2,2)=NBLW(2,2)
      IIN=21
      IOUT=18
      TITL(6)=ITN
      IYSP=1
      YMIN=-50.0
      YMAX=50.0
      OSTVAL=999
      CALL PLOTIT(PTS,NPTS,ICHRS,VALS,NVAL,XMIN,XMAX,YMIN,YMAX,NPGX,
     X        NPGY,TITL,NTL,IXSP,IYSP,OSTVAL,IOUT,IIN)
      GO TO 1
  900 CONTINUE
      STOP
      END
```

```
      SUBROUTINE CUTITIN(NABV,NBLW)
      DIMENSION NABV(2,2),NBLW(2,2),TINP(80)
      REAL NABV,NBLW
      REWIND 10
C SLOPE & INTERCEPT
      SLOPE1=(NABV(1,1)-NABV(2,1)) / (NABV(1,2)-NABV(2,2))
      TINT1 = NABV(1,1)-(SLOPE1*NABV(1,2))
      SLOPE2=(NBLW(1,1)-NBLW(2,1)) / (NBLW(1,2)-NBLW(2,2))
      TINT2=NBLW(1,1)-(SLOPE2*NBLW(1,2))
      WRITE(6,77)SLOPE1,TINT1,SLOPE2,TINT2
   77 FORMAT('0SLPS',4F10.2)
C CHECK POINTS
      X=0.
    1 READ(5,5)IST,TINP
    5 FORMAT(I3,T1,80F1.0)
      IF(IST.EQ.999)GO TO 900
      X=X+1.
      DO 10 I=1,80
            Y=FLOAT(I)
CC
CC GUT OF BOUNDS?
CC
            TST1=(SLOPE1*Y)+TINT1
            TST2=(SLOPE2*Y)+TINT2
            IF(X.LT.TST1 .OR. X.GT.TST2)GO TO 10
C POINT OK TRANSLATE & OUTPUT
            XT=X-NABV(1,1)
            Y=Y-NABV(1,2)
C NOTE IN THIS ROUTINE WHEN I SAY TRANSLATE IT IS WITH RESPECT TO
CC    THE UPPER LEFT HAND OSTIA POINT .  FINAL ROTATION AND TRANSLATION
CC    WILL TAKE PLACE LATER.
C
            WRITE(10)XT,Y,TINP(I)
   30 FORMAT(3F10.2)
   10 CONTINUE
      GO TO 1
  900 CONTINUE
C ADJUST ABOVE & BELOW OSTIA POINTS TO REFLECT TRANSLATION
C
      NABV(2,1)=NABV(2,1)-NABV(1,1)
      NABV(2,2)=NABV(2,2)-NABV(1,2)
      NBLW(1,1)=NBLW(1,1)-NABV(1,1)
      NBLW(1,2)=NBLW(1,2)-NABV(1,2)
      NBLW(2,1)=NBLW(2,1)-NABV(1,1)
      NBLW(2,2)=NBLW(2,2)-NABV(1,2)
      NABV(1,1)=0
      NABV(1,2)=0
      ENDFILE 10
```

```
      REWIND 10
      RETURN
      END
```

```
      SUBROUTINE PLOTIT(PTS,NPTS,ICHRS,VALS,NVAL,XMIN,XMAX,YMIN,YMAX,
     X          NPGX,NPGY,TITL,NTL,IXSP,IYSP,OSTVAL,IOUT,IIN)
      DIMENSION PTS(10000,3),ICHRS(NVAL),VALS(NVAL),TITL(NTL),
     X          IOUPT(38,111)
      INTEGER TITL
      IPG=0
      NXLNES=38
      NYLNES=111
      IF(IYSP .EQ. 0)YMIN=99999
      IF(IYSP .EQ. 0)YMAX=-99999
      IF(IXSP .EQ. 0)XMIN=99999
      IF(IXSP .EQ. 0)XMAX=-99999
      NPTS=0
   60 READ(IIN,END=70)X,Y,VAL
   50 FORMAT(3F10.2)
      IF(VAL .EQ. 0)GO TO 60
      NPTS=NPTS+1
      PTS(NPTS,1)=X
      PTS(NPTS,2)=Y
      PTS(NPTS,3)=VAL
      IF(IXSP .EQ. 1)GO TO 52
      IF(X.LT. XMIN)XMIN=X
      IF(X.GT.XMAX)XMAX=X
   52 CONTINUE
      IF(IYSP .EQ. 1)GO TO 53
      IF(Y.LT.YMIN)YMIN=Y
      IF(Y.GT.YMAX)YMAX=Y
   53 CONTINUE
      GO TO 60
   70 CONTINUE
      YINC=(YMAX-YMIN)/FLOAT(NPGY)
      XINC=(XMAX-XMIN)/FLOAT(NPGX)
      DO 5 I=1,NPGX
            DO 7 J=1,NPGY
                  PXMX = (FLOAT(I)*XINC) + XMIN
                  PXMN=(FLOAT(I-1)*XINC)+XMIN
                  PYMX=(FLOAT(J)*YINC)+YMIN
                  PYMN=(FLOAT(J-1)*YINC)+YMIN
                  IF(OSTVAL .EQ. 999)GO TO 23
                  IPG=IPG+1
                  WRITE(IOUT,20)OSTVAL,IPG
   20 FORMAT('1',T45,'LOCATION OF OSTIA POINTS, VALUE = ',F8.2,
     X      T120,'PAGE ',I3)
                  WRITE(IOUT,21)
   21 FORMAT(///,' ',T21,'X VALUE',T31,'Y VALUE',T41,'Z VALUE')
   23             CONTINUE
                  CALL FILL(PTS,NPTS,IOUPT,PXMX,PXMN,PYMX,PYMN,ICHRS,
     X                              VALS,NVAL,NXLNES,NYLNES,OSTVAL,IOUT)
```

```
                    IPG = IPG + 1
                    CALL PRNT(IOUPT,PXMX,PXMN,PYMX,PYMN,TITL,NTL,
     X             NXLNES,NYLNES,IPG,IOUT,OSTVAL)
 7          CONTINUE
 5  CONTINUE
    REWIND IIN
    RETURN
    DEBUG SUBCHK
    END
```

```
      SUBROUTINE PRNT(IOUPT,PXMX,PXMN,PYMX,PYMN,TITL,NTL,NXLNES,NYLNES,
     X      IPG,IOUT,OSTVAL)
      DIMENSION IOUPT(NXLNES,NYLNES),TITL(NTL),TY(23),TX(60)
      INTEGER TITL
C     PRINT TITLE
      IF(OSTVAL .EQ. 999 .AND. IPG .NE. 1)GO TO 90
      WRITE(IOUT,3)IPG
    3 FORMAT('1',T120,'PAGE ',I3)
      WRITE(IOUT,10)(TITL(J),J=1,NTL)
   10 FORMAT('0',T50,20A4)
C     WRITE FIRST Y LABEL
      ECHY=(PYMX-PYMN)/FLOAT(22)
      DO 20 I=1,23
            TY(I) = ((I-1)*ECHY) + PYMN
   20 CONTINUE
      WRITE(IOUT,30)(TY(J),J=2,23,2)
   30 FORMAT('0',T10,12(3X,F7.2))
      WRITE(IOUT,40)(TY(J),J=1,23,2)
   40 FORMAT(' ',T7 ,12(1X,F7.2,1X,'|'))
      WRITE(IOUT,50)
   50 FORMAT(' ',T11,'|',T12,11('     |     |'))
   90 CONTINUE
      WRITE(IOUT,12)
   12 FORMAT(T11,111('-'))
      NSTOP=NXLNES-1
      ECHX=(PXMX-PXMN)/FLOAT(NSTOP)
      DO 60 I=1,NXLNES
            TX(I)=((I-1)*ECHX)+PXMN
   60 CONTINUE
      DO 70 I=1,NXLNES
            ILF=MOD(I,2)
            IF(ILF .EQ. 0)GO TO 75
            WRITE(IOUT,80)(IOUPT(I,J),J=1,111)
   80 FORMAT(' ',T10,'I',T11,111A1,'I')
            GO TO 70
   75       WRITE(IOUT,85)TX(I),(IOUPT(I,J),J=1,111),TX(I)
   85 FORMAT(' ',F7.2,T9,'-I',T11,111A1,'I-',F9.2)
   70 CONTINUE
      WRITE(IOUT,17)
   17 FORMAT(' ',T11,111('-'))
      IF(OSTVAL .EQ. 999)GO TO 92
      WRITE(IOUT,50)
      WRITE(IOUT,40)(TY(J),J=1,23,2)
      WRITE(IOUT,30)(TY(J),J=2,23,2)
   92 CONTINUE
      RETURN
      DEBUG SUBCHK
      END
```

```
      SUBROUTINE FILL(PTS,NPTS,IOUPT,PXMX,PXMN,PYMX,PYMN,ICHRS,VALS,
     X          NVAL,NXLNES,NYLNES,OSTVAL,IOUT)
      DIMENSION PTS(10000,3),ICHRS(NVAL),VALS(NVAL),IOUPT(NXLNES,NYLNES)
      DATA IBLNK/' '/
C
      ECHX=(PXMX-PXMN)/FLOAT(NXLNES)
      ECHY=(PYMX-PYMN)/FLOAT(NYLNES)
C     BLANK OUT OUTPUT ARRAY
      DO 5 I=1,NXLNES
      DO 5 J=1,NYLNES
            IOUPT(I,J)=IBLNK
    5 CONTINUE
C   FILL ARRAY
      DO 10 I=1,NPTS
            X=PTS(I,1)
            Y=PTS(I,2)
C DETERMINE X & Y SUBSCRIPT VALUES
            TX=(X - PXMN)/ECHX
            IX = TX
            IF(TX .NE. IX)IX = IX + 1
            TY = (Y - PYMN)/ ECHY
            IY=TY
            IF(TY .NE. IY)IY = IY +1
C CHECK BOUNDS
            IF(IX .LE. 0 .OR. IX .GT. NXLNES)GO TO 10
            IF(IY .LE. 0 .OR. IY .GT. NYLNES)GO TO 10
C POINT OK, DETERMINE PLOTTING CHARACTER
            IF(PTS(I,3) .NE. OSTVAL)GO TO 18
            WRITE(IOUT,15)X,Y,PTS(I,3)
   15 FORMAT(T21,F8.2,T31,F8.2,T41,F8.2)
   18 CONTINUE
            IPT=0
            DO 20 J=1,NVAL
                  IF(VALS(J) .EQ. PTS(I,3))IPT=J
   20       CONTINUE
            ICH=ICHRS(IPT)
            IOUPT(IX,IY)=ICH
   10 CONTINUE
      RETURN
      DEBUG SUBCHK
      END
```

```
      SUBROUTINE ROTAT(OBLW,OABV,NBLW,NABV)
      DIMENSION OBLW(2,2),OABV(2,2),NBLW(2,2),NABV(2,2)
      REAL NBLW,NABV
      REWIND 10
      REWIND 21
      X1=OBLW(1,1)
      X2=OBLW(2,1)
      Y1=OBLW(1,2)
      Y2=OBLW(2,2)
      X3=NABV(1,1)
      X4=NABV(2,1)
      Y3=NABV(1,2)
      Y4=NABV(2,2)
      WRITE(6,79)
   79 FORMAT('0 AT ENTRY ROTATE :')
      WRITE(6,80)OABV(1,1),OABV(1,2),OABV(2,1),OABV(2,2),
     X      OBLW(1,1),OBLW(1,2),OBLW(2,1),OBLW(2,2),
     X      NABV(1,1),NABV(1,2),NABV(2,1),NABV(2,2),
     X      NBLW(1,1),NBLW(1,2),NBLW(2,1),NBLW(2,2)
   80 FORMAT('0',T30,'OABOVE : ',4F10.2,/,
     X           T30,'OBELOW : ',4F10.2,/,
     X           T30,'NABOVE : ',4F10.2,/,
     X           T30,'NBELOW : ',4F10.2)
C
CC ADJUST NEW ABOVE LINE TO OLD BELOW LINE
C
      DIFX=X1-X3
      DIFY=Y1-Y3
C
      X3=X3+DIFX
      X4=X4+DIFX
      Y3=Y3+DIFY
      Y4=Y4+DIFY
      CALL ANGL(X1,Y1,X2,Y2,ANG1)
      CALL ANGL(X3,Y3,X4,Y4,ANG2)
C
CC CALCULATE ANGLE NEW MUST BE ROTATED BY TO ALIGN WITH OLD
C
      TANG=ANG1-ANG2
      WRITE(6,82)ANG1,ANG2,TANG,DIFX,DIFY
   82 FORMAT('0  TRANSFORM : ANGLE1 = ',F10.4,5X,'ANGLE2 = ',F10.4,
     X      5X,'DIFFERENCE = ',F10.4,5X,'MOVEX = ',F10.2,5X,'MOVEY = ',
     X      F10.2)
      NPTS=0
C
C TRANSFORM THE POINTS
C
    1 READ(10,END=30)XRAW,YRAW,TLUM
```

```
   20 FORMAT(3F10.2)
C
CC ROTATE AROUND ABOVE(1,1)
C
      XROT=(XRAW*COS(TANG))-(YRAW*SIN(TANG))
      YROT=(YRAW*COS(TANG))+(XRAW*SIN(TANG))
C
CC TRANSLATE
C
      XTRNS=XROT+DIFX
      YTRNS=YROT+DIFY
C
CC WRITE OUT
C
      WRITE(11)XTRNS,YTRNS,TLUM
      WRITE(21)XTRNS,YTRNS,TLUM
      GO TO 1
   30 CONTINUE
C
      ENDFILE 21
      REWIND 21
      REWIND 10
C
CCC RECOMPUTE NEW ABOVE & BELOW TO REFLECT ROTATION
C
      DO 40 I=1,2
            XROT=(NABV(I,1)*COS(TANG))-(NABV(I,2)*SIN(TANG))
            YROT=(NABV(I,2)*COS(TANG))+(NABV(I,1)*SIN(TANG))
            XTRN=XROT+DIFX
            YTRN=YROT+DIFY
            NABV(I,1)=XTRN
            NABV(I,2)=YTRN
            XROT=(NBLW(I,1)*COS(TANG))-(NBLW(I,2)*SIN(TANG))
            YROT=(NBLW(I,2)*COS(TANG))+(NBLW(I,1)*SIN(TANG))
            XTRN=XROT+DIFX
            YTRN=YROT+DIFY
            NBLW(I,1)=XTRN
            NBLW(I,2)=YTRN
   40 CONTINUE
      WRITE(6,87)
   87 FORMAT('0 AT RETURN ROTATE : ')
      WRITE(6,80)OABV(1,1),OABV(1,2),OABV(2,1),OABV(2,2),
     X      OBLW(1,1),OBLW(1,2),OBLW(2,1),OBLW(2,2),
     X      NABV(1,1),NABV(1,2),NABV(2,1),NABV(2,2),
     X      NBLW(1,1),NBLW(1,2),NBLW(2,1),NBLW(2,2)
      RETURN
      END
```

```
      SUBROUTINE ANGL(X1,Y1,X2,Y2,ANGLE)
      RISE=Y2-Y1
      RUN=X2-X1
      VAL=RISE/RUN
      VALPOS=ABS(VAL)
      ANGLE=ATAN(VALPOS)
      WRITE(6,40)X1,Y1,X2,Y2,ANGLE
   40 FORMAT('0IN ANGLE : ',5F10.4)
      IF(RUN .LT. 0)ANGLE=3.141592654-ANGLE
      IF(RISE .GT. 0)GO TO 10
            WRITE(6,30)X1,Y1,X2,Y2,RISE,RUN
   30       FORMAT('0 YOU BLEW IT  IN ANGLE ROUTINE "RISE" IS LT 0 : ',
     X             6F10.2)
   20 ANGLE=ANGLE*(-1.0)
   10 CONTINUE
      RETURN
      END
```

APPENDIX B

Program "SUPERB" for concatenation of partitions and transformation.

```
      DIMENSION TRIANG(100,3,2),STAND(100,3,2),XBND(100,2),YBND(100,2),
     X          COEF(100,6),LST(100)
      NTRG=0
      READ(3,210)ITIT
  210 FORMAT(A4)
      WRITE(6,200)ITIT
  200 FORMAT('1',58X,A4,'STANDARD MAP',/,
     X       ' ',36X,'RAW COORDINATES',T70,'STANDARD COORDINATES')
    1 CONTINUE
      NTRG = NTRG + 1
      READ(8,5,END=20)TRIANG(NTRG,1,1),TRIANG(NTRG,1,2),
     X          TRIANG(NTRG,2,1),TRIANG(NTRG,2,2),
     X          TRIANG(NTRG,3,1),TRIANG(NTRG,3,2)
      READ(9,5,END=20)
     X          STAND(NTRG,1,1),STAND(NTRG,1,2),
     X          STAND(NTRG,2,1),STAND(NTRG,2,2),
     X          STAND(NTRG,3,1),STAND(NTRG,3,2)
    5 FORMAT(4X,6(1X,F6.1))
      WRITE(6,205)NTRG,((TRIANG(NTRG,I,J),J=1,3),I=1,3),
     X       ((STAND(NTRG,I,J),J=1,3),I=1,3)
  205 FORMAT(T5,I5,T14,9(F5.1,1X),10X,9(F5.1,1X))
      CALL MXMN(TRIANG,NTRG,XBND,YBND)
      CALL COEF(TRIANG,STAND,COEF,NTRG)
      GO TO 1
C
CC PROCESS POINTS
C
   20 NRD=0
      NTRG = NTRG - 1
      NOUT=0
   50 READ(1,END=100)X,Y,Z
      NRD=NRD+1
C
CC BUILD LIST OF POSSIBILITIES
C
      NPSB=0
      DO 60 I=1,NTRG
            IF(X .LT. XBND(I,1) .OR. X .GT. XBND(I,2))GO TO 60
            IF(Y .LT. YBND(I,1) .OR. Y .GT. YBND(I,2))GO TO 60
C
CC THIS TRIANGLE IS A POSSIBILITY
C
            NPSB=NPSB+1
            LST(NPSB)=I
   60 CONTINUE
C
CC IF NO POSSIBILITIES THEN EXCLUDE POINT
C
```

```
      IF(NPSB .EQ. 0)GO TO 50
C
CC  FIND WHICH ONE
C
      DO 70 I=1,NPSB
            CALL ISIT(X,Y,TRIANG,LST(I),IANS)
            IF(IANS .EQ. 0)GO TO 70
C
CCC YES ITS IN TRIANGLE LST(I)
C
            CALL OUTP(X,Y,Z,COEF,LST(I),NOUT)
   70 CONTINUE
C
CCC EVEN THOUGH THE POINT WAS THOUGHT TO BE IN A TRIANGLE , IT WASN'T
C
      GO TO 50
  100 CONTINUE
      X=0
      Y=0
      Z=0
      WRITE(12)X,Y,X,Y,Z
      Y=50
      WRITE(12)X,Y,X,Y,Z
      X=210
      Y=0
      WRITE(12)X,Y,X,Y,Z
      Y=50
      WRITE(12)X,Y,X,Y,Z
      NOUT=NOUT+4
      WRITE(6,105)NPD,NOUT
  105 FORMAT('0NORMAL END OF PROCESSING ',I5,' POINTS READ, ',
     X       I5,' POINTS OUTPUT')
      STOP
      END
```

```
      SUBROUTINE COEF(TRIANG,STAND,COEF,NTRG)
      DIMENSION TRIANG(100,3,2),STAND(100,3,2),COEF(100,6),ICOF(6)
      DATA ICOF/'AAAA','BBBB','CCCC','DDDD','EEEE','FFFF'/
      AX=TRIANG(NTRG,1,1)
      AY=TRIANG(NTRG,1,2)
      BX= TRIANG(NTRG,2,1)
      BY=TRIANG(NTRG,2,2)
      CX=TRIANG(NTRG,3,1)
      CY=TRIANG(NTRG,3,2)
      AXP=STAND(NTRG,1,1)
      AYP= STAND(NTRG,1,2)
      BXP=STAND(NTRG,2,1)
      BYP=STAND(NTRG,2,2)
      CXP=STAND(NTRG,3,1)
      CYP=STAND(NTRG,3,2)
C
C  SOLVE COEF F
C
      TNUM=((BXP-AXP)*(CX-AX)) + ((CXP-AXP)*(AX-BX))
      TDEN=((BY-AY)*(CX-AX)) + ((CY-AY)*(AX-BX))
      IF(TDEN .NE. 0)GO TO 10
      WRITE(6,50)ICOF(6),TNUM,TDEN,AX,AY,BX,BY,CX,CY,AXP,AYP,BXP,BYP,
     X          CXP,CYP
   50 FORMAT('0***ERROR WHILE ATTEMPTING TO COMPUTE COEFFICIENT',A4,
     X       'DENOMINATOR = 0 ',2F10.2,/,' ',12F10.2)
      F=0.0
      GO TO 15
   10 CONTINUE
      F=TNUM / TDEN
C
C  COMPUTE COEFF E
C
   15 CONTINUE
      TNUM= CXP - AXP - (F*(CY-AY))
      TDEN = CX - AX
      IF(TDEN .NE. 0)GO TO 20
      WRITE(6,50)ICOF(5),TNUM,TDEN,AX,AY,BX,BY,CX,CY,AXP,AYP,BXP,BYP,
     X          CXP,CYP
      F=0.0
      GO TO 25
   20 CONTINUE
      E=TNUM / TDEN
C
C  COMPUTE COEFF D
C
   25 CONTINUE
      D = AXP - (F*AX) - (E*AY)
C
```

```
C  COMPUTE COEFF C
C
      TNUM = ((BYP-AYP)*(CX-AX)) + ((CYP-AYP)*(AX-BX))
      TDEN= ((BY-AY)*(CX-AX)) + ((CY-AY)*(AX-BX))
      IF(TDEN .NE. 0)GO TO 30
      WRITE(6,50)ICOEF(3),TNUM,TDEN,AX,AY,BX,BY,CX,CY,AXP,AYP,BXP,BYP,
     X          CXP,CYP
      C=0.0
      GO TO 35
   30 CONTINUE
      C = TNUM / TDEN
C
C  COMPUTE COEFF B
C
   35 CONTINUE
      TNUM = CYP - AYP - (C*(CY-AY))
      TDEN = CX-AX
      IF(TDEN .NE. 0)GO TO 40
      WRITE(6,50)ICOEF(2),TNUM,TDEN,AX,AY,BX,BY,CX,CY,AXP,AYP,BXP,BYP,
     X          CXP,CYP
      B=0.0
      GO TO 45
   40 CONTINUE
      B=TNUM / TDEN
C
C  COMPUTE COEFF A
C
   45 CONTINUE
      A=AYP - (B*AX) - (C*AY)
C
C  PUT INTO ARRAY
C
      COEF(NTRG,1)=A
      COEF(NTRG,2)=B
      COEF(NTRG,3)=C
      COEF(NTRG,4)=D
      COEF(NTRG,5)=E
      COEF(NTRG,6)=F
      RETURN
      END
```

```
      SUBROUTINE MXMN(TRIANG,NTRG,XBND,YBND)
      DIMENSION TRIANG(100,3,2),XBND(100,2),YBND(100,2)
      YMX=-99999
      YMN=99999
      XMX=-99999
      XMN=99999
      DO 5 I=1,3
            IF(TRIANG(NTRG,I,1) .LT. XMN)XMN=TRIANG(NTRG,I,1)
            IF(TRIANG(NTRG,I,1) .GT. XMX)XMX=TRIANG(NTRG,I,1)
            IF(TRIANG(NTRG,I,2) .LT. YMN)YMN=TRIANG(NTRG,I,2)
            IF(TRIANG(NTRG,I,2) .GT. YMX)YMX=TRIANG(NTRG,I,2)
    5 CONTINUE
      XBND(NTRG,1)=XMN
      XBND(NTRG,2)=XMX
      YBND(NTRG,1)=YMN
      YBND(NTRG,2)=YMX
      RETURN
      END
```



```
      SUBROUTINE OUTP(X,Y,Z,COEF,IWCH,NOUT)
      DIMENSION COEF(100,6)
      NOUT = NOUT + 1
C
C  TRANSFORM
C
      A=COEF(IWCH,1)
      B=COEF(IWCH,2)
      C=COEF(IWCH,3)
      D=COEF(IWCH,4)
      E=COEF(IWCH,5)
      F=COEF(IWCH,6)
      XP=D + (E*X) + (F*Y)
      YP=A + (B*X) + (C*Y)
      WRITE(12)X,Y,XP,YP,Z
      RETURN
      END
```

```
      SUBROUTINE ISIT(X,Y,TRIANG,IWCH,IANS)
      DIMENSION TRIANG(100,3,2),XT(3),YT(3)
      XT(1)=TRIANG(IWCH,1,1)
      YT(1)=TRIANG(IWCH,1,2)
      XT(2)=TRIANG(IWCH,2,1)
      YT(2)=TRIANG(IWCH,2,2)
      XT(3)=TRIANG(IWCH,3,1)
      YT(3)=TRIANG(IWCH,3,2)
      IANS=0
      CALL BET(X,Y,XT(1),YT(1),XT(2),YT(2),XT(3),YT(3),IBANS)
         IF(IBANS .EQ. 0)RETURN
      CALL BET(X,Y,XT(2),YT(2),XT(1),YT(1),XT(3),YT(3),IBANS)
         IF(IBANS .EQ. 0)RETURN
      IANS=1
      RETURN
      END



      SUBROUTINE BET(X,Y,X1,Y1,X2,Y2,X3,Y3,IBANS)
      IBANS=0
      AX=X2-X1
      AY=Y2 - Y1
      BX=X3 - X1
      BY = Y3 - Y1
      CX= X - X1
      CY=Y - Y1
      CALL ANGL(AX,AY,ANGLE1)
      CALL ANGL(BX,BY,ANGLE2)
      ANGMIN=ANGLE1
      IF(ANGLE2 .LT. ANGLE1)ANGMIN=ANGLE2
      ANGMAX=ANGLE1
      IF(ANGLE2 .GT. ANGLE1)ANGMAX=ANGLE2
      ANGDIF=ANGMAX-ANGMIN
      CALL ANGL(CX,CY,ANGLE3)
      IF(ANGLE3 .LT. 999)GO TO 10
         IBANS=1
         RETURN
   10 CONTINUE
      ANGTST=ANGLE3-ANGMIN
      IF(ANGTST .LT. 0)ANGTST=ANGTST + 360.0
      IF(ANGTST .GT. ANGDIF .AND. ANGDIF .LT. 180.0)IBANS=1
      IF(ANGTST .LT. ANGDIF .AND. ANGDIF .LT. 180.0)IBANS=1
      IF(ANGTST .EQ. ANGDIF)IBANS=1
      RETURN
      END
```

```
      SUBROUTINE ANGL(X,Y,ANGLE)
      HYP=SQRT((X*X)+(Y*Y))
      RISE=ABS(Y)
      IF(HYP .GT. 0)GO TO 10
         ANGLE=999.
         RETURN
   10 CONTINUE
      SIN1=RISE/HYP
      ANGLE=ARSIN(SIN1)
      ANGLE=(ANGLE/(2.0*3.141592654))*360.0
      IF(X .LT. 0.0 .AND. Y .GT.  0.0)ANGLE=180.0-ANGLE
      IF(X .LT. 0.0 .AND. Y .LT. 0.0)ANGLE=180.0+ANGLE
      IF(X .GT. 0.0 .AND. Y .LT. 0.0)ANGLE=360.0 - ANGLE
      IF(X .EQ. 0.0 .AND. Y .LT. 0.0)ANGLE=180.0 + ANGLE
      IF(X .LT. 0.0 .AND. Y .EQ. 0.0)ANGLE=180.0 - ANGLE
      RETURN
      END

      DIMENSION PTS(10000,3),ICHRS(3),VALS(3),TITL(5),TITL2(5)
      INTEGER TITL,TITL2
      DATA TITL/'RAW ','TRIA','NGLE','    ','    '/
      DATA TITL2/'TRAN','SFOR','MED ','    ','    '/
      DATA ICHRS/'$$$$','....','****'/
      DATA VALS/0.,1.,2./
      NVAL=3
      NTL=5
      NPGX=3
      NPGY=1
      IIN=10
      IOUT=17
      IXSP=0
      IYSP=1
        YMIN=-50.0
      YMAX=50.0
      OSTVAL=999.0
      READ(5,5)ILM
    5 FORMAT(A4)
      TITL(5)=ILM
      TITL2(5)=ILM
      CALL PLOTIT(PTS,NPTS,ICHRS,VALS,NVAL,XMIN,XMAX,YMIN,YMAX,NPGX,
     X        NPGY,TITL,NTL,IXSP,IYSP,OSTVAL,IOUT,IIN)
      IIN=20
      YMAX=60.0
      CALL PLOTIT(PTS,NPTS,ICHRS,VALS,NVAL,XMIN,XMAX,YMIN,YMAX,NPGY,
     Y        NPGY,TITL2,NTL,IXSP,IYSP,OSTVAL,IOUT,IIN)
      STOP
      END
```

```
      SUBROUTINE PLOTIT(PTS,NPTS,ICHRS,VALS,NVAL,XMIN,XMAX,YMIN,YMAX,
     X          NPGX,NPGY,TITL,NTL,IXSP,IYSP,DSIVAL,IOUT,IIN)
      DIMENSION PTS(10000,3),ICHRS(NVAL),VALS(NVAL),TITL(NTL),
     X          IOUPT(38,111)
      INTEGER TITL
      IPG=0
      NXLNES=38
      NYLNES=111
      IF(IYSP .EQ. 0)YMIN=99999
      IF(IYSP .EQ. 0)YMAX=-99999
      IF(IXSP .EQ. 0)XMIN=99999
      IF(IXSP .EQ. 0)XMAX=-99999
      IFLG=0
      IF(IIN .EQ. 10)GO TO 72
      IIN=10
      IFLG=1
   72 CONTINUE
      NPTS=0
   60 READ(IIN,END=70)X,Y,XP,YP,VAL
   50 FORMAT(3F10.2)
      IF(IFLG .NE. 1)GO TO 100
         XV=XP
         YV=YP
      GO TO 105
  100 XV=X
      YV=Y
  105 CONTINUE
      NPTS=NPTS + 1
      PTS(NPTS,1)=XV
      PTS(NPTS,2)=YV
      PTS(NPTS,3)=VAL
      IF(IXSP .EQ. 1)GO TO 52
         IF(XV .LT. XMIN)XMIN=XV
         IF(XV .GT. XMAX)XMAX=XV
   52 CONTINUE
      IF(IYSP .EQ. 1)GO TO 53
         IF(Y .LT. YMIN)YMIN=YV
         IF(Y .GT. YMAX)YMAX=YV
   53 CONTINUE
      GO TO 60
   70 CONTINUE
      YINC=(YMAX-YMIN)/FLOAT(NPGY)
      XINC=(XMAX-XMIN)/FLOAT(NPGX)
      DO 5 I=1,NPGX
            DO 7 J=1,NPGY
                  PXMX = (FLOAT(I)*XINC) + XMIN
                  PXMN=(FLOAT(I-1)*XINC)+XMIN
                  PYMX=(FLOAT(J)*YINC)+YMIN
```

```
                PYMN=(FLOAT(J-1)*YINC)+YMIN
                IF(OSTVAL .EQ. 999)GO TO 23
                IPG=IPG+1
                WRITE(IOUT,20)OSTVAL,IPG
20 FORMAT('1',T45,'LOCATION OF OSTIA POINTS, VALUE = ',F8.2,
   X      T120,'PAGE ',I3)
                WRITE(IOUT,21)
21 FORMAT(///,' ',T21,'X VALUE',T31,'Y VALUE',T41,'Z VALUE')
23              CONTINUE
                CALL FILL(PTS,NPTS,IOUPT,PXMX,PXMN,PYMX,PYMN,ICHRS,
   X                      VALS,NVAL,NXLNES,NYLNES,OSTVAL,ITIT)
                IPG = IPG + 1
                CALL PRNT(IOUPT,PXMX,PXMN,PYMX,PYMN,TITL,ATI,
   X              NXLNES,NYLNES,IPG,IOUT,OSTVAL)
 7          CONTINUE
 6  CONTINUE
    REWIND IIN
    RETURN
    DEBUG SUBCHK
    END
```

```
      SUBROUTINE PRNT(IOUPT,PXMX,PXMN,PYMX,PYMN,TITL,NTL,NXLNES,NYLNES,
     X     IPG,IOUT,OSTVAL)
      DIMENSION IOUPT(NXLNES,NYLNES),TITL(NTL),TY(23),TX(60)
      INTEGER TITL
C     PRINT TITLE
      IF(OSTVAL .EQ. 999 .AND. IPG .NE. 1)GO TO 90
      WRITE(IOUT,3)IPG
    3 FORMAT('1',T120,'PAGE ',I3)
      WRITE(IOUT,10)(TITL(J),J=1,NTL)
   10 FORMAT('0',T50,20A4)
C     WRITE FIRST Y LABEL
      ECHY=(PYMX-PYMN)/FLOAT(22)
      DO 20 I=1,23
         TY(I) = ((I-1)*ECHY) + PYMN
   20 CONTINUE
      WRITE(IOUT,30)(TY(J),J=2,23,2)
   30 FORMAT('0',T10,12(3X,F7.2))
      WRITE(IOUT,40)(TY(J),J=1,23,2)
   40 FORMAT(' ',T7 ,12(1X,F7.2,1X,'|'))
      WRITE(IOUT,50)
   50 FORMAT(' ',T11,'|',T12,11('     |     |'))
   90 CONTINUE
      WRITE(IOUT,12)
   12 FORMAT(T11,111('-'))
      NSTOP=NXLNES-1
      ECHX=(PXMX-PXMN)/FLOAT(NSTOP)
      DO 60 I=1,NXLNES
         TX(I)=((I-1)*ECHX)+PXMN
   60 CONTINUE
      DO 70 I=1,NXLNES
         ILF=MOD(I,2)
         IF(ILF .EQ. 0)GO TO 75
         WRITE(IOUT,80)(IOUPT(I,J),J=1,111)
   80 FORMAT(' ',T10,'I',T11,111A1,'I')
         GO TO 70
   75    WRITE(IOUT,85)TX(I),(IOUPT(I,J),J=1,111),TX(I)
   85 FORMAT(' ',F7.2,T9,'-I',T11,111A1,'I-',F9.2)
   70 CONTINUE
      WRITE(IOUT,17)
   17 FORMAT(' ',T11,111('-'))
      IF(OSTVAL .EQ. 999)GO TO 92
      WRITE(IOUT,50)
      WRITE(IOUT,40)(TY(J),J=1,23,2)
      WRITE(IOUT,30)(TY(J),J=2,23,2)
   92 CONTINUE
      RETURN
      DEBUG SUBCHK
      END
```

```
      SUBROUTINE FILL(PTS,NPTS,IOUPT,PXMX,PXMN,PYMX,PYMN,ICHRS,VALS,
     X           NVAL,NXLNES,NYLNES,OSTVAL,IOUT)
      DIMENSION PTS(10000,3),ICHRS(NVAL),VALS(NVAL),IOUPT(NXLNES,NYLNES)
      DATA IBLNK/' '/
C
      ECHX=(PXMX-PXMN)/FLOAT(NXLNES)
      ECHY=(PYMX-PYMN)/FLOAT(NYLNES)
C     BLANK OUT OUTPUT ARRAY
      DO 5 I=1,NXLNES
      DO 5 J=1,NYLNES
            IOUPT(I,J)=IBLNK
    5 CONTINUE
C   FILL ARRAY
      DO 10 I=1,NPTS
            X=PTS(I,1)
            Y=PTS(I,2)
C DETERMINE X & Y SUBSCRIPT VALUES
            TX=(X - PXMN)/ECHX
            IX = TX
            IF(TX .NE. IX)IX = IX + 1
            TY = (Y - PYMN)/ ECHY
            IY=TY
            IF(TY .NE. IY)IY = IY +1
C CHECK BOUNDS
            IF(IX .LE. 0 .OR. IX .GT. NXLNES)GO TO 10
            IF(IY .LE. 0 .OR. IY .GT. NYLNES)GO TO 10
C POINT OK, DETERMINE PLOTTING CHARACTER
            IF(PTS(I,3) .NE. OSTVAL)GO TO 18
            WRITE(IOUT,15)X,Y,PTS(I,3)
   15 FORMAT(T21,F8.2,T31,F8.2,T41,F8.2)
   18 CONTINUE
            IPT=0
            DO 20 J=1,NVAL
                  IF(VALS(J) .EQ. PTS(I,3))IPT=J
   20       CONTINUE
            ICH=ICHRS(IPT)
            IOUPT(IX,IY)=ICH
   10 CONTINUE
      RETURN
      DEBUG SUBCHK
      END
```

APPENDIX C

Program "GRID" for generation of grid overlay and Program "PRNTGRID" for overlay on standard specimen.

```
      NPTS=0
    1 READ(11,END=10)X,Y,XP,YP,VAL
      NPTS=NPTS+1
      IF(VAL .EQ. 0)TVAL=10.0
      IF(VAL .EQ. 1)TVAL=0.
      IF(VAL .EQ. 2)TVAL=-10.0
      WRITE(14,5)XP,YP,TVAL
    5 FORMAT(3F5.1)
      GO TO 1
   10 WRITE(6,20)NPTS
   20 FORMAT('0','POINTS = ',I5)
      STOP
      END
```

```
      DIMENSION PTS(210,50),IOUT(50),TJUNK(20),ICHRS(3)
      DIMENSION IP(3)
      DATA IP/0,1,2/
      DATA ICHRS/' ','.','*'/
      READ(9)ICOLX,IRWY,IJ
      READ(9)TJUNK
      DO 5 I=1,IRWY
         READ(9)(PTS(J,I),J=1,210)
         DO 10 J=1,210
            VAL=PTS(J,I)
            IF(VAL .LT. -5.0)PTS(J,I)=2
            IF(VAL .GE. -5.0 .AND. VAL .LE. 5.0)PTS(J,I)=1
            IF(VAL .GT. 5.0)PTS(J,I)=0
   10    CONTINUE
    5 CONTINUE
      DO 20 I=1,210
         DO 30 J=1,50
            DO 3 K=1,3
               IF (PTS(I,J) .EQ. IP(K))IOUT(J)=ICHRS(K)
    3       CONTINUE
   30    CONTINUE
         WRITE(6,40)I,IOUT
   40    FORMAT(' ',5X,I3,10X,50A1)
      WRITE(10,45)(PTS(I,J),J=1,50)
   45 FORMAT(50F2.0)
   20 CONTINUE
      STOP
      END
```

APPENDIX D

Program "Surface II" for contour and 3-D graphics.

```
      DIMENSION IV(210,50)
      DO 1 I=1,210
      READ(5,10)I2
      READ(5,11)(IV(I,J),J=1,50)
    1 CONTINUE
      DO 20 I=1,210
      READ(5,10)(IV(I,J),J=1,50)
      CONTINUE
      DO 40 J=1,50
      WRITE(6,70)(IV(I,J),I=1,210)
   70 FORMAT(210I2)
      CONTINUE
      STOP
      END
```

APPENDIX E

Procedure for Staining of Rabbit Aorta

Preparation of Animal

Prior to a lethal injection of phenobarbitol, the animal is heparinized (1000 units/animal). Immediately following sacrifice, the chest is opened to expose the heart, which is cannulated through the wall of the left ventricle. The right iliac artery is exposed and cannulated for drainage. This flow path is perfused with 5% glucose, by weight, in 0.9% saline until drainage is clear of blood. The path is then volume perfused with 4% aqueous formaldehyde (formalin 1:10 with distilled water) at physiological pressure by elevation of a 1 liter reservoir with drip-drainage at the iliac (about one hour).

Excision of Specimen

Excise the entire aorta from fibrous ring including the aortic valve leaflets to beyond the iliac bifurcation. Care must be taken to retain coronary anastomoses and maximal lengths of aortic branches.

Preparation of Specimen

Clean the specimen with extreme care with forceps and scissors, severing the aortic branches without mechanical distortion at the aortic wall, after careful dissection of fibrous and fatty tissue from the aortic wall. Open the aortic tube by making a very regular and smooth incision longitudinally along the ventral aspect of the aorta, being careful to maintain the ventral position of the cut.

Staining of Specimen

Rinse the specimen in 70% ethanol until all loose matter is removed. Submerge in stock Sudan IV (5 grains crystalline Sudan IV dissolved in 500 ml of 80% ethanol and 500 ml acetone) for 15 minutes, agitating the solution on the minute. Repeat ethanol rinse. Submerge in 80% ethanol for 20 minutes. Adherence to the 20 minute time is critical. Now, soak the specimen in distilled water until the ethanol is displaced and the specimen sinks. Store in 4% formaldehyde.

APPENDIX F

Procedure for Specimen Photography

Camera

The 35 mm camera format is used, with the standard full frame size, 24 x 36 mm. Any camera which can produce 35 mm film transparencies is suitable. The focal length of the camera lens is unimportant as long as it does not produce intentional image distortion, such as produced by the "fisheye" short focal length lens, of about 40 mm or less, nor large brightness intensity fall off near the edges of the film frame.

Lighting

The light source required is the photographic photoflood. (Fluorescents must not be used.) The lamp wattage is unimportant as long as it provides convenient and adequate exposure to the film. One hundred fifty watt lamps are recommended. The color temperature of the lamp must match the color balance characteristic of the film used. This will be discussed in the section on Film and Processing. The lamps should be used only for their useful life, typically three hours and then replaced. The lighting should be as uniform across the subject matter as possible. This usually requires the use of two to four lamps.

Set-Up

A copy stand should be used. Both the camera and lamps should be secured to the stand so that both may be adjusted. The lamps' positions can be adjusted to vary the radiant intensity at the subject plane. The

camera position is adjusted to produce appropriate image composition and magnification. Composition and magnification are discussed in detail in the section on Photographic Partitioning. Lamp position must be adjusted to totally prevent specular reflections, or glare, from the subject matter. The board on which the subject specimen is laid may be incl.ned up to 5° from the horizontal to reduce glare, if necessa.y. A piece of rigid, transparent material, such as glass or plexiglass, should be laid over that portion of the specimen to be photographed to maintain flatness. The dimensions of t.. s retainer must be just larger than the field of view at the photographic magnification used; the edges of the retainer, indeed, that a retainer is being used, must not be visible in the final photcgraph. Furthermore, if the retainer is too large, the following procedure will be difficult to perform correctly. Water should be injected as an interface between the specimen surface and the retainer to fill the gaps where intimate contact cannot be made; note that excessive pressure should not be applied to the retainer to insure uniform contact as this dimensionally distorts the specimen. The background for the specimen must be flat black. A black velvet surface is recommended for sufficient softness to allow slight pressure on the retainer and maintain the water interface by surface tension. In some setups it may be necessary to submerge the entire specimen in water to reduce glare. This also prevents the specimen from drying out from the heat of the lamps, though the lamps should only be on while the actual exposure is being made. The procedure is inconvenient, however, and should be avoided. The primary method of glare prevention should be adjustment of lamp position and introduction of a film of water between

the specimen surface and the transparent retainer. The camera's film plane must be horizontal, that is parallel, to the subject plane (except for the allowable 5° subject plane inclination). Of course, sharp focus must be maintained.

Film and Processing

Conventional color transparency film is required. Avoid high contrast, orthochromatic, and other special purpose films. Film sensitivities from ASA 25 to 200 (DIN 15 to 24) are recommended. The film color balance character should be matched to the photoflood; no colored filters should be introduced between the film and subject except for this purpose. For example, a daylight balanced film must be exposed by a daylight balanced (often called blue) photoflood, and a 3400K (tungsten) balanced film must be exposed by a 3400K photoflood (the most commonly used photoflood lamp). Color balancing (color shifting) filters may be used to match a film with an otherwise unmatched photoflood. Other color temperature ratings are not commonly encountered. Film storage prior to exposure and the immediate laboratory processing thereafter, must be according to manufacturer's recommendations. If the film is user processed, do so immediately after exposure and under strictly controlled processing conditions to maintain manufacturer's recommended tolerances. The processed and mounted slides must be carefully packaged for shipment to the image processing facility.

Calibration Exposure

Proper exposure must be assured by the use of a precise exposure meter. The exposure calibration procedure, which must be performed for any meter used, depends somewhat on the meter type. The two types, reflected light meters and incident light meters, and their calibration procedures are described next. Note that proper calibration must not be assumed; the following tests must be performed.

The reflected light meter is commonly used in 35 mm single lens reflex (SLR) cameras, which usually meter the light actually passing through the camera lens. The procedure to be described also applies to separate, hand held reflected light meters. The scene to be photographed is a stepped grey scale the background for which is an 18% reflectance neutral grey test card (both scale and card are furnished by O.S.U.). Exposures of this scene are bracketed by 3 f-stops in 1/2 f-stop increments centered about the meter-indicated exposure setting. If a hand-held reflected light exposure meter is used, insure that only the area comprised by the grey scale and test card background are being metered. The meter should be adjusted as the manufacturer recommends to the film sensitivity number (AS or DIN). For example, suppose the meter is set for ASA 200 (DIN 24) and indicates for the given lighting condition an exposure of 1/60 second at f8.0. Thirteen exposures should be made of the calibration scene at the following shutter speed and aperture combinations, or their equivalents:

1/30 at f4; 3 f-stops overexposed
1/30 at f4-f5.6; 2½ f-stops overexposed
1/60 at f4; 2 f-stops overexpsed
1/60 at f4-f5.6; 1½ f-stops overexposed
1/60 at f5.6; 1 f-stop overexposed
1/60 at f5.6-f8; ½ f-stop overexposed
1/60 at f8; meter indicated exposure
1/60 at f8-f11; ½ f-stop underexposed
1/60 at f11; 1 f-stop underexposed
1/60 at f11-f16; 1½ f-stops underexposed
1/60 at f16; 2 f-stops underexposed
1/125 at f11-f16; 2½ f-stops underexposed
1/125 at f16; 3 f-stops underexposed

where f4-f5.6 indicates the half-stop between f4 and f5.6, for example. Maintain a record of the exposure settings. This film should be promptly processed in exactly the same way as the specimen films will be processed. Upon return and examination of these slides, you must choose that exposure which best depicts the central portion of the grey scale. The choice is made by the following criteria. If the film used has a narrow exposure latitude, none of the 13 slides will have differentiated all the steps of the grey scale; some adjacent steps will have merged into a common black or a common white. In this case, the properly exposed slide is one which depicts well-differentiated grey steps in the central portion of the scale, that is, the slide which depicts a number of merged, undifferentiated, black steps equal to the number of merged, undifferentiated, white steps. In the more usual case however, all steps of the grey scale will appear differentiated on one or more slides. Here the properly exposed slide is that one, single slide or the "middle" one if a series of slides differentiates all the steps. Returning to the example, suppose this properly exposed slide received an exposure of 1/60 at f5.6-f8. According to the meter-indicated exposure, this slide is 1/2 f-stop overexposed. However, for purposes here, this slide is to

be considered properly exposed, so that the meter indicates a consistent 1/2 f-stop overexposure. For all specimen slides taken for the O.S.U. analysis then, your meter-indicated exposure must be corrected to conform with the result of this calibration procedure. For the example cited, the exposure setting on the camera must be 1/2 f-stop LESS than the meter-indicated exposure, or 1/60 second at f8-f16. Rather than remembering to "underexpose" all your slides by 1/2 f-stop, a convenient method of correction is to change the film sensitivity setting on the meter from ASA 200 (DIN 24) to ASA 283 (DIN 25) (or as close to ASA 283 as possible). To obtain a film ASA, number corrected for a given number of f-stop(s), modify the uncorrected ASA number as follows:

To "underexpose" by:	½	Multiply uncorrected ASA number by:	1.4
	1		2
	1½		2.8
	2		4
	2½		5.6
	3		8

To "overexpose" by:	½	Divide uncorrected ASA number by:	1.4
	1		2
	1½		2.8
	2		4
	2½		5.6
	3		8

To obtain a corrected DIN number, modify the uncorrected DIN number as follows:

To "underexpose" by:	½	Add 1.5 to uncorrected DIN number
	1	3
	1½	4.5
	2	6
	2½	7.5
	3	9

To "overexpose" by:	½	Subtract 1.5 from uncorrected DIN number
	1	3
	1½	4.5
	2	6
	2½	7.5
	3	9

Your reflected light meter is now calibrated and may be used to determine proper exposure by the method described in the section entitled Photographic Protocol.

Though the underlying reasons for calibration of incident light meters differ from those for reflected light meters, the practical calibration procedure is similar. The meter-indicated exposure reading must be made at the subject position with the incident light meter facing the camera, not the light source. This is standard procedure for most incident light meters. The photographed scene must include the grey scale, but in this case, need not include the 18% reflectance neutral grey test card as background. From this point on, the procedures for film exposure, processing, and analysis, and correction of film sensitivity number are identical to the reflected light meter procedures discussed above.

Calibration Standards

The image analysis by computer requires that calibration and normalization standards be included in the actual film strip on which the necropsy specimens are photographed. The standards need not, and in most cases, can not, be included in each slide. The standards must be photographed each time there is a change in the photographic set-up. These include: changes in magnification, whether produced by lens focal length change, or change in camera-to-subject distance; changes in lamp or lamp position; changes in ambient lighting (ambient fluorescent lighting must be switched off); changes in film emulsion number; and each time a photographic session is begun. Each time one of these changes is made, two or three calibration photographs must be taken preceding the sequence

of specimen photographs which may have required that change.

The first calibration photograph need be taken only at the beginning of each photographic session and when a new emulsion number is loaded in the camera. This photograph is of the 20 step grey scale with the 18% reflectance neutral grey test card as background. Area outside the perimeter of the 18% reflectance card must not appear in the photograph. The grey scale should be centered in a the viewfinder.

The second calibration photograph, to be taken each time there is ANY change in the photographic set-up, is of the 18% reflectance card surface, only, which must be positioned at the subject plane and at the same inclindation from the horizontal as the actual specimen board is to be inclined (up to 5%). The camera's viewfinder must be completely filled by this surface; area outside the perimeter of the card surface must not appear in the photograph.

The third calibration photograph, again to be taken each time there is ANY change in the photographic set-up, is of the white reference patch on the 18% reflectance background. Again, area outside the perimeter of the 18% reflectance card must not appear in the photograph. The 1 cm by 1 cm patch is sufficiently small so that the patch, surrounding margins of 18% reflectance surface, and the "1 cm^2" label, are all visible in the viewfinder at the magnification you employ.

All calibration standards are supplied. They should be cared for meticulously, kept clean, and stored in complete darkness.

Photographic Partitioning

To increase the accuracy of the computer analysis, not only is the entire specimen included in one photograph, but also several overlapping regions of the specimen are photographed individually. Each photographed region is called a partition. That region of the specimen included in one partition will in general vary with the species of the animal and that specimen's anatomical location. The four photographic partitions of the descending thoracic aorta of the rabbit, prepared according to standard protocol, are shown in Figure F1. The scene in the camera viewfinder for each partition must be as shown. The edges of the transparent retainer, described earlier, must be outside the camera viewfinder and not visible in the photograph; all that should be apparent in the photograph is the arterial region and black background above and below. All photographs, including calibration photographs, must be ordered and numbered for submission.

Photographic Protocol

Rabbit Descending Thoracic Aorta

Set up for Exposure #4. Photograph, order, and number the slides as follows:

Exposure #	Description
1.	18% reflectance neutral grey test card
2.	Grey Scale on 18% reflectance neutral grey background
3.	White reference patch on 18% reflectance neutral grey background
4.	Intimal surface of entire gross specimen

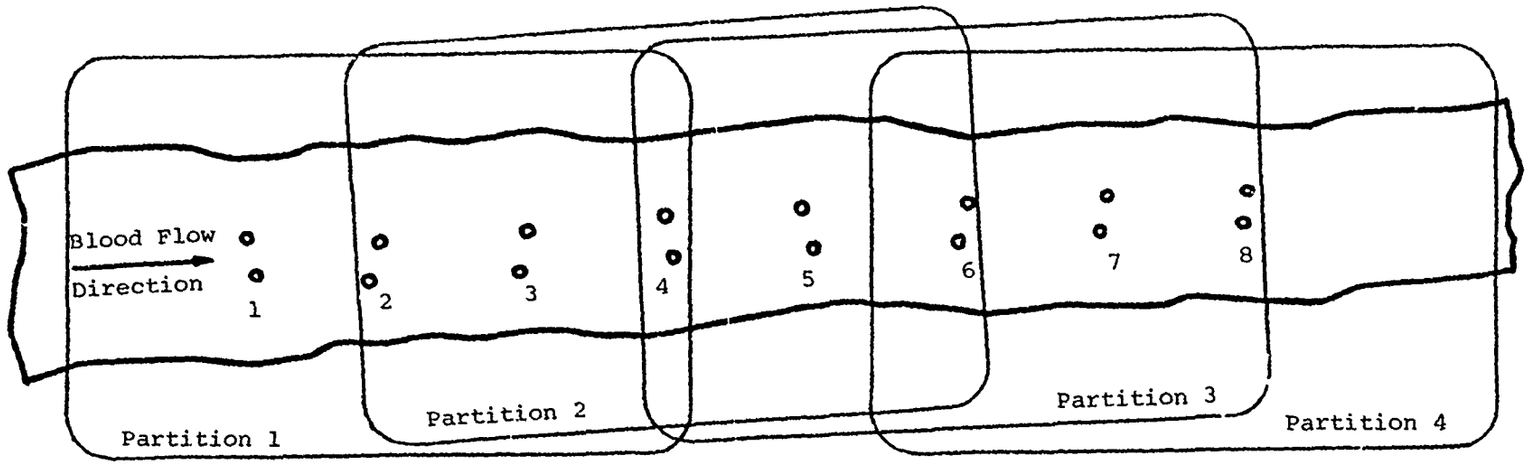

Figure F1. Descending thoracic rabbit aorta, opened along the ventral aspect and flattened, showing the typical regions to be enclosed in the camera viewfinder by each of four photographic partitions. The intercostal ostia are numbered from 1, caudally through 8.

Note: All partitions must be photographed at the same magnification (which will result from adherence to the Protocol).

Partition 1 must include ostial pairs 1, 2, and 3; Partition 2 must include 3, 4, and 5; Partition 3 must include 5, 6, and 7; and Partition 4 must include 7 and 8. The required ostial pairs should be centered in each partition. Partition overlap in this figure is typical; though, for example, the fourth ostial pair need not be included in Partition 1, each partition must enclose ample areas proximal to its first required ostial pair and distal to its last required ostial pair.

Of course, DO NOT include partition or ostial labels in the photographs.

Change magnification to accomodate largest partition. Repeat calibration photographs and continue as follows:

5. 18% reflectance neutral grey test card

6. White reference patch on 18% reflectance neutral grey background

7. Partition 1

8. Partition 2

9. Partition 3

10. Partition 4

Process and submit slides.